



NUCLEAR WASTE SOCIÉTÉ DE GESTION  
MANAGEMENT DES DÉCHETS  
ORGANIZATION NUCLÉAIRES

## Phase 2 Geoscientific Preliminary Assessment, Acquisition, Processing and Interpretation of High- Resolution Airborne Geophysical Data

TOWNSHIP OF IGNACE, ONTARIO



**APM-REP-06145-0002**

**FEBRUARY 2015**

*This report has been prepared under contract to the NWMO. The report has been reviewed by the NWMO, but the views and conclusions are those of the authors and do not necessarily represent those of the NWMO.*

*All copyright and intellectual property rights belong to the NWMO.*

*For more information, please contact:*

**Nuclear Waste Management Organization**

22 St. Clair Avenue East, Sixth Floor

Toronto, Ontario M4T 2S3 Canada

Tel 416.934.9814

Toll Free 1.866.249.6966

Email [contactus@nwmo.ca](mailto:contactus@nwmo.ca)

[www.nwmo.ca](http://www.nwmo.ca)

 <b>Sander Geophysics</b>	Airborne Geophysics Acquisition and Interpretation	Issue Date:	February 2015
--	--	-------------	---------------

## **PHASE 2 GEOSCIENTIFIC PRELIMINARY ASSESSMENT**

# **ACQUISITION, PROCESSING AND INTERPRETATION OF HIGH-RESOLUTION AIRBORNE GEOPHYSICAL DATA**

## **TOWNSHIP OF IGNACE, ONTARIO**

**Prepared for:**

**Nuclear Waste Management Organization (NWMO)**

**by:**

**Sander Geophysics Limited (SGL)**

**NWMO REPORT NUMBER:**

**APM-REP-06145-0002**

# Signatures

Martin Bates, Ph.D.



Martin Mushayandebvu, Ph.D.

M. M. L. Feb. 20. 2015

## Executive Summary

This technical report documents the results of the acquisition, processing and interpretation of high-resolution airborne geophysical data conducted as part of the Phase 2 Geoscientific Preliminary Assessment, to further assess the suitability of the Ignace area to safely host a deep geological repository (Golder, 2015). This study followed the successful completion of a Phase 1 Geoscientific Desktop Preliminary Assessment (NWMO, 2013; Golder, 2013). The desktop study identified four potentially suitable areas warranting further studies such as high-resolution surveys and geological mapping.

The purpose of the Phase 2 acquisition, processing and interpretation of geophysical data was to provide an updated interpretation of the geological characteristics of the potentially suitable bedrock units identified in Phase 1 and to provide additional information to further assess the geology of the Ignace area. Both magnetic and gravimetric data were acquired during the surveys in order to provide data that can be used to interpret the geometry and thickness of the potentially suitable bedrock units; the nature of geological contacts; bedrock lithologies; the degree of geological heterogeneities and the nature of intrusive phases within the batholiths in the area; as well as the nature of structural features such as faults, shears zones, and alteration zones.

The grids of the acquired magnetic and gravimetric data and associated processed grids (first, second and horizontal derivatives, total gradient amplitude, trend analysis solutions and tilt angle) were analyzed and interpreted together with the mapped bedrock geology and other available geological information (e.g. magnetic susceptibility and rock density). The geophysical data and derivative products were used to estimate the locations of geological boundaries related to magnetic susceptibility and density changes, reveal regions of different geophysical character giving insight into variations in composition of the batholiths, and provide additional insight into the presence of potential faults, dykes, and other heterogeneities within and surrounding the batholiths.

In general, the Revell batholith has a low and quiet magnetic character, with two distinct exceptions. One exception occurs in the northern portion of the batholith, where two linear east-southeast trending magnetic highs are observed and are associated with Wabigoon mafic dykes. The other exception is an oval shaped area of high magnetic activity in the centre of the batholith. A broad area of consistent magnetic character encompasses the Basket Lake batholith, along with the surrounding foliated and gneissic tonalite units, and continues southeast into the western portion of the Indian Lake batholith. The broad pattern of consistent character encompasses all of the Basket Lake batholith and the northwestern portion of the Indian Lake batholith.

The report provides results of preliminary forward modelling completed on five profile lines that transect the Revell, Basket Lake and Indian Lake batholiths to estimate the shape, depth, thickness and the distribution of geological units within the geophysical survey area.



<b>1</b>	<b>Introduction.....</b>	<b>1</b>
1.1	<i>Study Objective.....</i>	1
1.2	<i>Geophysical Survey Area.....</i>	1
<b>2</b>	<b>Summary of Geology .....</b>	<b>3</b>
2.1	<i>Geologic Setting.....</i>	3
2.2	<i>Bedrock Geology.....</i>	3
2.2.1	<i>Intrusive Rocks.....</i>	3
2.2.2	<i>Greenstone Belts.....</i>	5
2.2.3	<i>Mafic Dykes.....</i>	5
2.3	<i>Structural History and Mapped Structures.....</i>	6
2.4	<i>Metamorphism.....</i>	7
2.5	<i>Quaternary Geology.....</i>	8
<b>3</b>	<b>Data Source Acquisition and Quality .....</b>	<b>9</b>
3.1	<i>Magnetic Data.....</i>	10
3.2	<i>Gravity Data.....</i>	11
3.3	<i>Digital Elevation Data.....</i>	11
3.4	<i>Additional Data Sources.....</i>	12
3.4.1	<i>OGS Mapped Bedrock Geology.....</i>	12
3.4.2	<i>OGS Detailed Bedrock Mapping of Ignace Area.....</i>	12
3.4.3	<i>OGS PETROCH Lithogeochemical Database.....</i>	12
3.4.4	<i>OGS Precambrian Bedrock Magnetic Susceptibility Database.....</i>	12
3.4.5	<i>Other Density Measurements.....</i>	13
<b>4</b>	<b>Geophysical Data Processing Methods.....</b>	<b>14</b>
4.1	<i>Gravity Data Processing.....</i>	14
4.1.1	<i>Bouguer Correction.....</i>	15
4.1.2	<i>Static and Level Corrections.....</i>	15
4.1.3	<i>Gridding and Filtering.....</i>	16
4.2	<i>Magnetic Data Processing.....</i>	16
4.2.1	<i>Levelling.....</i>	17
4.2.2	<i>Micro-Levelling.....</i>	17
4.2.3	<i>Gridding.....</i>	17
4.3	<i>Gravity and Magnetic Derivative Products.....</i>	18
4.3.1	<i>Total Magnetic Intensity Reduced to Pole.....</i>	18
4.3.2	<i>Vertical Derivatives of Total Magnetic Intensity and Bouguer Gravity.....</i>	18
4.3.3	<i>Total Horizontal Gradient of Total Magnetic Intensity and Bouguer Gravity.....</i>	19
4.3.4	<i>Total Gradient Amplitude of Total Magnetic Intensity.....</i>	19
4.3.5	<i>Tilt Angle.....</i>	20
4.3.6	<i>Trend Analysis Method.....</i>	20
<b>5</b>	<b>Geophysical Interpretation.....</b>	<b>22</b>
5.1	<i>Results of Qualitative Analysis.....</i>	22
5.1.1	<i>Revell Batholith.....</i>	22
5.1.2	<i>Basket Lake Batholith and Surrounding Tonalitic Units.....</i>	23
5.1.3	<i>Indian Lake Batholith.....</i>	25
5.2	<i>Preliminary 2.5D Modeling.....</i>	25

5.2.1	Model Descriptions .....	26
5.2.1	Model Results.....	29
<b>6</b>	<b>Summary of Results.....</b>	<b>36</b>
<b>7</b>	<b>REFERENCES .....</b>	<b>39</b>
<b>8</b>	<b>FIGURES.....</b>	<b>44</b>

# 1 Introduction

This technical report documents the results of the acquisition and interpretation of high-resolution airborne geophysical data (gravity and magnetic) conducted as part of the Phase 2 Geoscientific Preliminary Assessment, to further assess the suitability of the Ignace area to safely host a deep geological repository (Golder, 2015). This study followed the successful completion of a Phase 1 Geoscientific Desktop Preliminary Assessment (NWMO, 2013; Golder, 2013). The desktop study identified four potentially suitable areas warranting further studies such as high-resolution surveys and geological mapping.

## 1.1 Study Objective

The main purposes of the interpretation of the acquired magnetic and gravity data are as follows:

- Acquire high-resolution airborne magnetic and gravimetric data within a geophysical survey area that encompasses the general potentially suitable areas identified in the Phase 1 Geoscientific Desktop Preliminary Assessment (Golder, 2013; NWMO, 2013).
- Characterize the geophysical response of the bedrock units (e.g. bedrock contacts, intrusive phases, potential for natural resources, etc).
- Characterize the extent of bedrock heterogeneity (e.g. ductile fabric, complexity, etc).
- Interpret the geophysical character of potential structures (faults, dykes, joints, etc).
- Develop initial models of bedrock units at depth (2.5D forward modelling).

## 1.2 Geophysical Survey Area

The Township of Ignace is located in Northwestern Ontario, approximately 250 km northwest of Thunder Bay and 110 km southeast of Dryden. The Township encompasses approximately 100 km<sup>2</sup>. The geophysical survey area covers two blocks, one located approximately 6 km west of the Township of Ignace and the other approximately 13 km north-east of the Township. The two survey areas cover a total area of approximately 1,780 km<sup>2</sup>. The location of the geophysical survey area is shown in Figure 1.1, and the full set of survey lines are shown in Figure 1.2. The survey lines that were flown in an east-west direction link the two survey areas together. The two survey areas are bounded by the coordinates presented in Table 1.1 (NAD83 datum, UTM zone 15N).

Table 1.1: Coordinates of the survey area

Easting (m)	Northing (m)
Western Block	
548510	5482367
548510	5491394
559342	5498074
569362	5515676

<b>Easting (m)</b>	<b>Northing (m)</b>
591000	5502226
591000	5468900
567600	5468900
557000	5468900
548510	5482367
Eastern Block	
608800	5497600
627000	5497600
627000	5478950
608800	5478950
608800	5497600

## **2 Summary of Geology**

Details of the geology of the Ignace area were described in the Phase 1 Geoscientific Desktop Preliminary Assessment (Golder, 2013). The following sub-sections provide a brief description of the geologic setting, bedrock geology, structural history and mapped structures, metamorphism and Quaternary geology is provided in the following subsections, with a focus on the areas identified during Phase 1 as being potentially suitable (Revell, Indian Lake and Basket Lake batholiths), their surrounding bedrock units and important structural features.

### **2.1 Geologic Setting**

The Ignace area is located in the central portion of the Archean Wabigoon Subprovince of the Superior Province. The Wabigoon Subprovince is further subdivided into three lithotectonic terranes: the granitoid Marmion terrane, the predominantly volcanic Western Wabigoon terrane, and the plutonic Winnipeg River terrane. The Ignace area includes portions of all three terranes. The boundaries between lithotectonic terranes are not sharply defined due to the emplacement of younger plutonic rocks at places along the inferred terrane boundaries (Stone, 2010a).

### **2.2 Bedrock Geology**

The geology of the Ignace area is dominated by large granitic intrusions and associated tonalitic units, including the Indian Lake, Revell, and Basket Lake batholiths, where the four general potentially suitable areas were identified in Phase 1 Geoscientific Desktop Preliminary Assessment (Figure 1.1; Golder, 2013). These intrusions were emplaced into the older Raleigh Lake and Bending Lake greenstone belts. These bedrock units exhibit evidence of both ductile and brittle deformation and are transected by at least two suites of undeformed diabase dykes. A description of these three granitic batholiths, associated tonalitic units, and surrounding greenstone belts and dykes is provided in the following subsections.

#### **2.2.1 Intrusive Rocks**

##### **2.2.1.1 Revell Batholith**

The Revell batholith is the oldest granitoid intrusion in the Ignace area. It is roughly rectangular in shape, trends northwest, is approximately 40 km in length, and it covers an area of approximately 455 km<sup>2</sup> (Figure 1.1). Szewczyk and West (1976) interpreted this batholith to be a sheet-like intrusion approximately 1.6 km thick.

Three different intrusive phases are currently recognized in the Revell batholith (Stone et al., 2010). The oldest phase corresponds to an approximately 2.734 billion years old, medium-grained, foliated, mesocratic biotite tonalite (Stone et al., 2010) exposed primarily along the western margin of the batholith and in its southern portion. A younger 2.732 billion years old phase (Stone et al., 2010) consisting of coarse-grained mesocratic gneissic hornblende tonalite is also found along the western margin of the batholith. The youngest phase, approximately 2.694 billion years old (Buse et al., 2010), consists of mesocratic to leucocratic feldspar megacrystic biotite granodiorite to granite; this phase extends over most of the remaining surface extent of the batholith. A distinctive oval-shaped, K-feldspar megacrystic lithofacies of this younger phase that is approximately 47 km<sup>2</sup> in areal extent is

identified on the central-east portion of the batholith based on previous mapping and interpretation of existing geophysical data (Stone et al., 2011a, 2011b; Stone et al., 2007; PGW, 2013).

### **2.2.1.2 Basket Lake Batholith**

The Basket Lake batholith is exposed in the northwestern part of the Ignace area (Figure 1.1). The batholith is approximately 10 to 15 km in width and 35 km in length, in which almost half of this batholith extends beyond the Ignace survey area to the northwest. Szewczyk and West (1976) estimated the thickness of the northern part of the Basket Lake batholith to be at least 8 km and thinning progressively to 0.5 km to the southeast, forming a tongue-like extension of the main batholith body.

Detailed mapping of the eastern portion of the Basket Lake batholith describes the lithology as hornblende-biotite quartz-diorite to tonalite (Sage et al., 1974). The western-northwestern portion of the batholith consists mainly of leucocratic biotite-rich granodiorite, which varies to granite with subordinate tonalite, quartz monzonite, quartz diorite and a mixed hybrid zone locally developed near the contact with the Raleigh Lake greenstone belt (Berger, 1988). The contact zone contains white tonalite dykes which cross-cut the granite and granodiorite facies of the intrusion, as well as the adjacent metavolcanics. These dykes are interpreted to be a late phase of the Basket Lake batholith (Berger, 1988).

Bedrock of the Basket Lake batholith is commonly foliated, with foliation being weak and mostly defined by alignment of biotite and a fine- to medium-grained character. This suggests that this batholith experienced some degree of ductile deformation (Szewczyk and West, 1976), and that it predates the intrusion of the Indian Lake batholith, as well as the youngest phase of the Revell batholith.

A small swarm of Wabigoon dykes cut across the southern margin of the batholith while two mapped Kenora-Fort Frances dykes occur immediately to the southeast (Figure 1.1).

### **2.2.1.3 Indian Lake Batholith**

The approximately 2,671 million years old Indian Lake batholith (Tomlinson et al., 2004) covers a total surface area of about 1,366 km<sup>2</sup>, with 563 km<sup>2</sup> within the two blocks where geophysical data were acquired during the Phase 2 Preliminary Assessment (Figure 1.1). This batholith has previously been estimated to be a sheet-like intrusion up to 2 km thick (Szewczyk and West, 1976; Everitt, 1999).

The Indian Lake batholith is composed of light grey-white to pale pink biotite granite, typically medium- to coarse-grained, inequigranular, leucocratic, and is massive to weakly foliated. It usually contains a small percentage of biotite (3-5%), and subequal proportions of quartz, plagioclase and potassium feldspar (Stone et al., 1998). Non-tectonic foliation present in the batholith is defined by the alignment of igneous minerals that delineate concentric patterns in the granite (Stone et al., 1998).

An enclave of biotite-hornblende tonalite to granite, approximately 35 km<sup>2</sup> in area is mapped within the Indian Lake batholith, extending from the southern portion of the Township of Ignace southward beyond its boundaries (OGS, 2011). This enclave is usually coarse, granular and mesocratic and, when hornblende granite is present, it is characterized by large potassium feldspar megacrystals that are 1 to 5 cm in size (Stone et al., 1998). It is not known whether this tonalitic body is a separate intrusive body, the product of different phases of magmatic injection, or compositional zoning.

#### **2.2.1.4 Tonalitic Units**

The region in the northeastern Ignace area, surrounding the Basket Lake and Indian Lake batholiths, has been mapped as compositionally heterogeneous tonalitic gneiss and biotite tonalite (Figure 1.1). The Biotite Tonalite Suite is typically white to grey, medium grained, and variably massive to foliated. Weakly gneissic biotite tonalite to granodiorite is the principal type of rock within this suite. The Biotite Tonalite Suite grades into the Tonalite Gneiss Suite largely through progressive development of a gneissic texture. Intrusions of the Biotite Tonalite Suite show considerable variation in age, ranging from approximately 2,994 to 2,688 million years (Stone, 2010a).

The Tonalite Gneiss Suite comprises older gneissic, foliated, migmatized tonalite-granodiorite, intruded by younger granitoid batholiths. The Tonalite Gneiss Suite is layered with individual gneissic layers varying compositionally from leucocratic tonalite and granodiorite through mesocratic tonalite and granodiorite to diorite and amphibolite. They range substantially in age from approximately 3,009 to 2,673 million years old, similar to the variation in age shown by the Biotite Tonalite Suite (Stone, 2010a). The gneiss commonly shows strongly foliated to mylonitic textures and belts of gneiss are spatially associated with zones of high ductile strain such as the margins of large batholiths (Stone, 2010a). Locally, the tonalitic gneiss is gradational in composition to amphibolitic gneiss of volcanic or migmatized sedimentary rock origin, whereas the more felsic phases are gradational to biotite tonalite (Stone, 2010a).

#### **2.2.2 Greenstone Belts**

The Raleigh Lake and Bending Lake greenstone belts surround the Revell batholith and the area adjacent to the Indian Lake and Basket Lake batholiths (Figure 1.1). These greenstone belts are composed of alternating units of mafic pillowed metavolcanic rocks and intermediate fragmental metavolcanic rocks, both metamorphosed to amphibolite facies.

The northwest-trending Raleigh Lake greenstone belt occurs north of the Revell batholith and extends over a length of 50 km. The Raleigh Lake greenstone belt is dominated by mafic metavolcanic rocks, and contains approximately 30 % intermediate to felsic fragmental metavolcanic rocks (Stone, 2010a). The greenstone belt is intruded by oval, smaller felsic to intermediate plutons such as the Raleigh Lake intrusions, which consist of three epizonal granitic stocks hosted in the metavolcanic rocks of the Raleigh Lake greenstone belt (Figure 1.1). These small bodies are compositionally similar to the larger granodioritic to granitic batholiths that dominate the Ignace area.

The northwest-trending Bending Lake greenstone belt occurs southwest of the Revell batholith. It is composed of mafic metavolcanic rocks, with subordinate gabbro, intermediate metavolcanic rocks, and clastic metasedimentary rocks (wacke and argillite; Stone, 2010b).

#### **2.2.3 Mafic Dykes**

Mafic dykes in the Ignace area include the Kenora-Fort Frances and Wabigoon swarms, emplaced between approximately 2.20 and 1.96 billion years (Osmani, 1991). The Wabigoon dyke swarm constitutes the most prominent dyke generation and extends in a northwest orientation for at least 70 km from Ignace to Lac des Mille Lacs without offsets along any terrane boundaries. Within the Ignace area, the Wabigoon dykes are typically 100 to 200 m in width. Fahrig and West (1986) obtained a K/Ar age of approximately 1.9 billion years for the Wabigoon dykes.

The Kenora-Fort Frances dyke swarm contains hundreds of northwest-trending dykes up to 100 km long and 120 m wide, covering an area of approximately 90,000 km<sup>2</sup> (Osmani, 1991). The Kenora-Fort Frances dykes form clusters in the Melgund Lake area to the northwest of the Revell batholith, and in the Mameigwess Lake area between the Basket and Indian Lake batholiths. The Kenora-Fort Frances dykes are composed of variable amounts of plagioclase, pyroxene, quartz, hornblende, as well as varying degrees of alteration minerals. Southwick and Halls (1987) reported a Rb-Sr age of approximately 2.120 billion years old for these dykes.

### **2.3 Structural History and Mapped Structures**

Information on the structural history of the Ignace area and surrounding region is limited. This summary was built using information available for the Wabigoon Subprovince and is largely based on Percival et al. (2004), Bethune et al. (2006), Sanborn-Barrie and Skulski (2006), and Stone (2010a). Five episodes of penetrative strain (D<sub>1</sub> to D<sub>5</sub>) affected the central Wabigoon Subprovince (Percival et al. 2004). Gneissic tonalitic rocks (Tonalite Gneiss Suite) commonly show D<sub>1</sub> and D<sub>2</sub> fabrics, overprinted by pervasive, regional D<sub>3</sub> to D<sub>5</sub> fabrics or structures.

The S<sub>1</sub> foliation is a gneissic layering that was folded during the D<sub>2</sub> deformation event into tight to isoclinal F<sub>2</sub> folds. The geometric and kinematic character of the D<sub>1</sub> and D<sub>2</sub> deformation events is cryptic as a result of magmatic and structural (D<sub>3</sub>-D<sub>5</sub>) overprinting (Percival et al. 2004). D<sub>1</sub> and D<sub>2</sub> deformation fabrics are confined to gneissic rocks in the central Wabigoon Subprovince. The best constraints on the age of the early (D<sub>1</sub>-D<sub>2</sub>) events are approximately 2,725 to 2,713 million years (Percival et al. 2004).

Two episodes of penetrative strain (D<sub>3</sub> and D<sub>4</sub> of Percival et al. 2004; D<sub>1</sub>, D<sub>2</sub> of Sanborn-Barrie and Skulski, 2006), hereby termed D<sub>3</sub> and D<sub>4</sub> affected the supracrustal rocks of the central Wabigoon Subprovince. D<sub>3</sub> and D<sub>4</sub> deformation events are interpreted to have occurred prior to 2,698 million years (Percival et al. 2004). The earliest penetrative deformation (D<sub>3</sub>) resulted in northwest-trending F<sub>3</sub> folds and development of an associated S<sub>3</sub> axial planar cleavage. These fabrics are well exposed in the nearby Savant-Sturgeon Lake greenstone belt to the northeast of the area of Ignace where they have been correlated with a northwest-striking foliation (locally known as F<sub>1</sub> and S<sub>1</sub>) within the Lewis Lake biotite-tonalite (2,735 to 2,730 Ma; Sanborn-Barrie and Skulski, 2006). In the Raleigh Lake and Bending Lake greenstone belts, within the Ignace area, D<sub>3</sub> structures dominate as shown in the strong north-west grain observed in the supracrustal rocks. East- to northeast-striking D<sub>4</sub> structures locally overprint the northwest-striking S<sub>3</sub> foliation. The S<sub>4</sub> foliation occurs as a moderately to strongly developed schistosity that is characterized by a uniformly steep dip. The S<sub>4</sub> foliation is commonly axial planar to 050-070° trending, steeply plunging F<sub>4</sub> folds (locally known as F<sub>2</sub>; Sanborn-Barrie and Skulski, 2006).

Percival et al. (2004) attributed sinistral shear zone development in plutonic and gneissic rocks to a D<sub>5</sub> deformation event in the central Wabigoon Subprovince, bracketed between about 2,690 million years (Davis, 1989) and 2,678 million years (Brown, 2002). These shear zones are associated with significant sinistral strike-slip displacement along the Miniss River fault zone and dextral strike-slip motion along the Sydney-Lake St. Joseph fault zone 150 km north of the area of Ignace (Bethune et al., 2006). Regional differential uplift associated with movement along these shear zone systems continued until ca. 2,400 Ma (Hanes and Achibald, 1998) indicating a protracted D<sub>5</sub> fault history.

The subsequent emplacement of the Kenora-Fort Frances and Wabigoon dykes was followed by pulses of brittle deformation and fault reactivation during the Penokean Orogeny approximately 1.8 billion years ago. Following these deformation stages, late dyke emplacement and presumably fault-joint reactivation associated with the Midcontinent Rift magmatism occurred at approximately 1.150 to 1.130 billion years (Easton et al., 2007).

There are three mapped faults within the area shown on Figure 1.1, none of which is within the four potentially suitable areas. One, the Washeibemaga fault, trends east and is located to the west of the Revell batholith. An unnamed fault is located in the northwestern corner of the Ignace area and trends northeast close to Minnitaki Lake.

The northeast-trending Finlayson-Marmion fault is located approximately 30 km south of the eastern survey block in the Ignace area (Figure 1.1), and extends northeast from Steep Rock Lake where it intersects and is thought to represent a splay of the east-west-trending Quetico Fault. The Finlayson-Marmion fault crosscuts the White Otter Lake and Indian Lake batholiths and is interpreted to represent a D<sub>5</sub> shear zone. The Finlayson-Marmion fault caused the mylonitization and brittle deformation of the granitoid rocks within the White Otter Lake and Indian Lake batholiths (Schwerdtner et al., 1979; Stone, 2010a). To the south, close to the Quetico fault, the Finlayson-Marmion fault broadens to a complex braided zone of fault segments, some of which are mineralized with gold (Stone, 2010a). The latest known movement along the associated Quetico fault, and therefore potentially the D<sub>5</sub> Marmion Fault, occurred at approximately 1.947 billion years with the development of pseudotachylite (Peterman and Day, 1989). In the southeast corner of the Ignace area, a Wabigoon dyke (1,900 Ma; Buchan and Ernst, 2004) crosscuts the Finlayson-Marmion fault, which indicates that only limited movement could have occurred along the Finlayson-Marmion fault since the intrusion of the Wabigoon dyke swarm.

## 2.4 Metamorphism

Metamorphism in the Central Wabigoon region occurred in late Neoproterozoic time, from approximately 2,722 to 2,657 million years ago (Stone, 2010a) and peaked at approximately 2,701 million years ago (Easton, 2000). The collision of the Western Wabigoon terrane with the Winnipeg River-Marmion terrane at approximately 2.7 billion years (Percival et al., 2006) may have been the cause of this strain and regional metamorphism. Metamorphism in the Central Wabigoon region is generally restricted to greenschist facies, and increases locally to middle amphibolite facies in parts of the greenstone belts (Sage et al., 1974; Blackburn et al., 1991; Easton, 2000; Sanborn-Barrie and Skulski, 2006). Very high grade (i.e., granulite facies) and very low grade (e.g., zeolite facies) metamorphism is largely absent in the central Wabigoon (Stone, 2010b).

A low to medium metamorphic grade overprint is recognized within the rocks of the Ignace area, mainly within the Raleigh Lake and Bending Lake greenstone belts and within marginal zones of the Revell batholith. High metamorphic grade occurs in the Ignace area in tonalite adjacent to plutons and greenstone belts and is accompanied by widespread migmatization of the rocks.

In the Raleigh Lake greenstone belt, greenschist facies metamorphism grades into amphibolite facies. In the Bending Lake greenstone belt, mineral assemblages are indicative of variable metamorphic grade, up to amphibolite facies. Rocks at the margins and in narrow extensions of the greenstone

belts exhibit higher metamorphic grade than rocks in the core of the belt, implying a degree of contact metamorphism adjacent to the surrounding intrusive bodies (Stone, 2010a).

## **2.5 Quaternary Geology**

Information on Quaternary geology in the Ignace area was described in detail as part of the terrain study carried out during Phase 1 Preliminary Assessment (JDMA, 2013), and is summarized here.

Quaternary deposits in the Ignace area accumulated during and after the Wisconsinan Glaciation. Advancement of the Laurentide Ice Sheet from the northeast across the area deposited a veneer of till throughout the areas, with thicker accumulations of till mapped as morainal terrain. During the retreat of the Laurentide Ice Sheet, significant deposition of glaciofluvial outwash and glaciolacustrine plains occurred, with two major end moraines—Lac Seul and Hartman moraines—extending through the Ignace area recording the progressive retreat of the ice sheet.

The Hartman moraine is a significant Quaternary landform in the Ignace area that divides the area into distinct zones based on the thickness of Quaternary deposits. Thicker till, glaciofluvial outwash, and deep-water glaciolacustrine deposits occur north of this moraine, whereas surficial deposits are generally thinner to the south. Areas mapped as bedrock terrain to the north of the Hartman moraine represent a spattering of islands within a proglacial lake known as Glacial Lake Agassiz that subsequently contracted into a set of large modern lakes.

Recorded depths to bedrock from water well records and diamond drill holes in the Ignace area range from 0 to 80 m, with an average depth of about 7 to 10 m. The thickness of the Quaternary deposits southwest of the highway in the periphery of the Township of Ignace is typically less than 5 m. The thickest overburden is inferred to occur along the axes of the Hartman and Lac Seul moraines.

### 3 Data Source Acquisition and Quality

Sander Geophysics Limited (SGL) completed a fixed-wing high-resolution airborne magnetic and gravity survey in the Ignace area between April 3 and May 5, 2014. The survey area comprised two survey blocks located to the west and north-east of the Township of Ignace (Figure 1.1). These survey blocks were designed to cover the four general potentially suitable areas identified in the Phase 1 Preliminary Assessment, and to cover relevant geological features in the area.

The airborne survey in the Ignace area included a total of 24,453 km of flight lines covering a surface area of approximately 1,780 km<sup>2</sup> (Figure 1.2). Flight operations were conducted out of the Dryden Regional Airport, Dryden, Ontario using two of SGL's Cessna 208 Grand Caravans. Data were acquired along traverse lines flown in a north-south direction spaced at 100 m, and control lines flown east-west spaced at 500 m. The survey was flown at an altitude of 80 m above ground level, with an average ground speed of 100 knots (approximately 185 km/h or 50 m/s). Airborne magnetic and gravity data were acquired along the flight lines using equipment on board the plane that have very high sensitivity and accuracy. The airborne magnetic data were recorded using a single magnetometer sensor mounted in a fibreglass stinger extending from the tail of each of the aircraft. The airborne gravity data were recorded using a gravimeter, which includes three orthogonal accelerometers that are mounted on a stabilized platform inside the cabin of the aircraft. Table 3.1 gives a quick reference of the details of the survey.

Table 3.1: Survey Details

Survey Particulars	
Survey Start Date:	April 3, 2014
Survey End Date:	May 5, 2014
Field Office Location:	Dryden, Ontario
Airport Used:	Dryden Regional Airport
Aircraft Type:	Cessna Grand Caravan
Total line kilometers:	24,453
Traverse Line numbers:	4000 - 4789
Traverse Line direction:	North-South
Traverse Line spacing:	100 m
Control Line numbers:	400-494
Control Line direction:	East-West
Control Line spacing:	500 m
Survey Altitude:	Smoothed drape with target height of 80 m above ground.
Digital Terrain Source:	SRTM
Number of Flights (numbers):	38 (1001 to 1018 and 2001 to 2020)
Aircraft Target Ground Speed:	100 knots
Magnetic Field Reference location	598392mE 5488376mN (NAD83):UTM 15N
Magnetic Field Inclination (+ve down):	74.94° at reference station
Magnetic Field Declination (+ve east):	-1.88° at reference station

Approximate total field value:	57,200 nT
Magnetic Reference Field Model:	International Magnetic Reference Field (IGRF 2010-2015), interpolated to date and location of acquisition
Fundamental Gravity Network Ties:	Tied to the SGL Ottawa office gravity station. Procedure described in Section 5.1.2.
Survey Base Gravity Value:	980916.37 mGal at centre of gravimeter when aircraft parked on the ramp at Dryden Regional Airport.
Survey Base Parking Location (NAD83):	C-GSGV: 518116.36mE 5519803.03mN UTM 15N Height: 380.71 m (location of gravimeter centre, 1.09 m above the ground.) C-GSGW: 518138.81mE 5519792.70mN UTM 15N Height: 380.61 m (location of gravimeter centre, 1.11 m above the ground.)
Base Station Locations (NAD83):	REF1: 518027.37mE 5519744.66mN UTM 15N Height: 377.736 m REF2: 513259.58mE 5514997.26mN UTM 15N Height: 341.470 m
Field Acquisition Datum:	WGS-84
UTM Projection:	UTM 15N

### 3.1 Magnetic Data

Total magnetic field measurements were recorded with a single cesium magnetometer mounted in a fiberglass stinger extending from the tail of the survey aircraft. SGL's hardware and software system, AIRComp, was used to remove the effects of the aircraft and its manoeuvres from the recorded magnetic data. The data were recorded for post-processing. Coefficients to be used for compensation were derived by processing the calibration flight data, based on principles presented by Leliak (1961). The compensation coefficients were applied to data recorded during normal survey operations to produce compensated magnetic data.

Low-pass filtered reference station diurnal was subtracted from the airborne data on a reading by reading basis. If more than one reference station is used, the reference station value could be interpolated, based on the relative distance of the reading from each reference station.

Both the ground and airborne systems used the Geometrics G-822A cesium magnetic sensor. Total magnetic field measurements were recorded at 160 Hz in the aircraft, and then later down sampled to 10 Hz in the processing. The ground systems recorded magnetic data at 11 Hz.

A pre-planned drape surface was prepared for the survey to guide the aircraft over the topography in a consistent manner, as close to the minimum clearance as possible. The drape surface was prepared with digital elevation model (DEM) data obtained from the Shuttle Radar Topography Mission (SRTM) (<http://srtm.usgs.gov/>) for the area. The DEM included an extension beyond the survey boundary to allow the aircraft to achieve the drape clearance before coming on line.

Details of the processing of the magnetic data are provided in Section 4.2 of this report.

### **3.2 Gravity Data**

Gravity data were acquired with SGL's propriety AIRGrav (Airborne Inertially Referenced Gravimeter) system, which uses a Schuler tuned inertial platform supporting three orthogonal accelerometers, which remain fixed in inertial space, independent of the manoeuvres of the aircraft, allowing precise isolation from the effects of the movement of the aircraft. The gravity sensor used in AIRGrav is a very accurate accelerometer with a wide dynamic range. The system is not affected by the strong vertical motions of the aircraft, allowing the final gravity data to be almost completely unaffected by in-flight conditions classified as "moderate turbulence" or better. The instrument is also considered to be an inertial navigator, and as such the platform levelling was essentially unaffected by horizontal accelerations.

In typical survey flying, accelerations in an aircraft can reach 0.1 G, equivalent to 100,000 milligal (mGal). Data processing must extract gravity data from this very noisy environment. This was achieved by modelling the gravity due to movements of the aircraft in flight as measured by extremely accurate Global Positioning System (GPS) measurement. These measurements are affected by noisy conditions in the ionosphere, and by the variable conditions (e.g. temperature, pressure and humidity) within the troposphere. SGL has developed a full suite of programs to carry out all the necessary corrections.

The GPS data are extracted from the airborne and reference station acquisition system and reformatted. Differential corrections to correct the airborne ranges for variations calculated from the base station GPS data were performed. Each recorded position was recalculated based on these ranges. The original reference system for all GPS data is the WGS-84 datum. Positions were then converted to the local datum, reference system and desired projection. Each line was then checked for data continuity and quality.

An extremely accurate location of the base station GPS receiver was determined using an IGS permanent GPS Reference Station to apply differential corrections (<http://igs.org/network>). This technique provides a final base station receiver location with an accuracy of better than a few decimetres. The entire airborne data set was then reprocessed differentially using the recalculated base station location.

Gravity data were recorded at 128 Hz. Accelerations were filtered and resampled to 10 Hz to match the GPS, using specially designed filters to avoid biasing the data. Gravity was calculated by subtracting the GPS derived accelerations from the inertial accelerations. The calculated gravity was corrected for the Eötvös effect and normal gravity, and the sample interval was then reduced to 2 Hz. These operations were all performed by SGL's proprietary GravGPS software. A detailed description of gravity processing is provided in Section 4.1 of this report.

### **3.3 Digital Elevation Data**

Digital elevation data were collected using a TRT radar altimeter mounted to the base of the aircraft. Elevation data were sampled at a rate of 10 Hz, which is consistent with a sample roughly every 6m. The radar altimeter data were filtered to remove high-frequency noise using a 67-point low pass filter.

A digital elevation model (DEM) was derived by subtracting the radar altimeter data from the differentially corrected DGPS altitude with respect to the Canadian Geodetic Vertical Datum 2013 (CGVD2013). The DEM reflects the presence of vegetation (for example trees) and buildings and thus is not considered to be a digital terrain model (DTM).

The digital elevation data were gridded to form a DEM grid using a cell size of 25 m over the Ignace survey area. The 25 m gridding cell was applied to present the highest resolution of the digital elevation model within the boundaries of the two survey blocks comprising the principal survey area (Figure 3.1).

### **3.4 Additional Data Sources**

In addition to the acquired data, a number of other publically available data sources were used. These are detailed below.

#### **3.4.1 OGS Mapped Bedrock Geology**

The Precambrian Geoscience Section of the Ontario Geological Survey has compiled a 1:250,000 scale map of the bedrock geology of Ontario (OGS, 2011). These maps were recently revised and issued as 'Miscellaneous Release – Data 126 – Revision 1'. The data are publicly available as a seamless GIS data set and includes such details as bedrock units, major faults, dyke swarms, iron formations and kimberlites. This resource was of fundamental importance in assisting with the geophysical interpretation of the acquired potential field data. The mapped bedrock geology was used for both qualitative and quantitative aspects of the interpretation. In the case of the qualitative interpretation the mapped bedrock geology gave the overall context for the magnetic and gravity data. For the 2.5D modelling, the mapped bedrock geology provided initial surface constraints.

#### **3.4.2 OGS Detailed Bedrock Mapping of Ignace Area**

Detailed bedrock mapping is available for portions of the Ignace area, including the south-central portion of the Revell batholith, and parts of the Indian Lake batholith (e.g., Stone et al., 1998; 2007a,b; Stone and Halle, 1999; Stone, 2009a; Stone, 2010a; and Stone et al., 2011a; 2011b; 2011c). This detailed mapping was undertaken between 1998 and 2011, and supplements the level of detail provided in the OGS Data 126-Rev 1 release (OGS, 2011). Detailed mapping for portions of the Ignace area are publicly available as GIS data sets.

#### **3.4.3 OGS PETROCH Lithochemical Database**

The Ontario Geological Survey has a publicly available PETROCH Lithochemical Database (Haus and Pauk, 2010). The database contains detailed rock chemical data collected by OGS geoscientists, which includes information about rock type, chemical composition, age, stratigraphy, major oxide values, sample location, and specific gravity. A few dozen of these data points occur in the south and west of the survey area. This information was used in the interpretation to: 1) obtain further information on the composition of major mapped rock units where samples have been taken; and 2) constrain the density of rock units used in the 2.5D modeling.

#### **3.4.4 OGS Precambrian Bedrock Magnetic Susceptibility Database**

The Ontario Geological Survey has compiled a database of magnetic susceptibilities from several Precambrian bedrock regions across Ontario (Muir, 2013). The database contains a collection of near

29,000 magnetic susceptibility outcrop readings were obtained from 2001 to 2012. Although no measurements were obtained in the Ignace area, this information was used as a guide to constrain the magnetic susceptibilities values of similar bedrock units used in the 2.5D modeling.

#### ***3.4.5 Other Density Measurements***

An earlier study of land gravity data acquired in the Ignace area (Szewczyk and West, 1976) refers to a series of density measurements that were made from rock samples in the area. Although individual density measurements are not provided in this paper, average density values across various rock units are provided, along with histograms of the density variation within these rock units. This information was enormously helpful in assigning rock densities in the 2.5D modeling.

## 4 Geophysical Data Processing Methods

Filters may be applied to the data to enhance different wavelength information that arises from different sources. In many cases, filtering is best achieved by transforming the data from the space domain to the frequency domain by Fourier Transform, since frequency characteristics of the filter to be applied are more precisely defined in the frequency domain. For this report, filtering was applied in two dimensions on the gridded data. The filtered derivatives created to assist with interpretation are described below.

### 4.1 Gravity Data Processing

Advanced gravity processing allows for the generation of high-resolution gravity data. These advances involve the use of GPS phase angle corrections, the integration of GPS processing with inertial data from the gravimeter and the advanced analysis of system states and uncertainties. This processing helps reduce system noise and allows for the generation of high quality, low noise raw gravity data through a wider range of survey conditions than was previously possible. The following standard corrections were applied to the gravity data (Telford et al., 1990; Blakely, 1996):

a. Eötvös correction,

$$\delta g_{Eötvös} = - \frac{v_x^2}{\frac{r}{(1 - e_2 \sin^2 \Phi)^{1/2}} + h} - 2 W_s v_x \cos \Phi - \frac{v_y^2}{\frac{r(1 - e_2)}{(1 - e_2 \sin^2 \Phi)^{3/2}} + h}$$

where  $\Phi$  is the latitude of the aircraft,  $v_x$  and  $v_y$  are the velocities of the aircraft in the  $x$  (east) and  $y$  (north) direction,  $r$  is the Earth's radius at the equator (6,378,137 m),  $e_2$  is a correction for Earth's flattening towards the poles ( $6.69437999013 \times 10^{-3}$ ),  $W_s$  is the angular velocity of Earth's rotation ( $7.2921158553 \times 10^{-5}$  rad/s), and  $h$  is the altitude of the plane above the WGS84 datum;

b. Normal gravity,

$$g_{Normal} = \frac{9.7803267714 (1 + 0.00193185138639 \sin^2 \Phi)}{\sqrt{1 - 0.00669437999013 \sin^2 \Phi}}$$

where  $\Phi$  is the latitude of the aircraft;

c. Free air correction,

$$g_{fa} = - (0.3087691 - 0.0004398 \sin^2 \Phi) h + 7.2125 \times 10^{-8} h^2$$

where  $h$  is the height of the aircraft in metres above the WGS84 datum

d. Bouguer Slab,

$$g_{sb} = 2 \pi \gamma \rho h = 0.041925 \rho h$$

where  $\gamma$  is the Universal Gravity constant,  $\rho$  is the average density for the project in  $\text{g/cm}^3$ , and  $h$  is height of the surface of land or sea in metres above the WGS84 datum;

e. Curvature of the Earth,

$$g_{ec} = \frac{\rho}{2.67} [1.464 h - 0.3533 h^2 + 0.000045 h^3]$$

where  $h$  is height of the surface of land or sea in kilometres above the WGS84 datum and  $\rho$  is the

density for the project.

- f. Full Bouguer correction,  $g_b$ . See below in subsection 4.1.1 for a description of the Bouguer correction technique;
- g. Static correction,  $g_{sc}$ , based on static ground recordings and repeat lines;
- h. Level Correction,  $g_{lc}$ , based on line intersections. See below in subsection 4.1.2 for a more detailed description of the Static correction ( $g_{sc}$ ) and Level correction ( $g_{lc}$ ) techniques.

The final Bouguer anomaly equals  $G - g_{fa} - g_b - g_{sc} - g_{lc}$ , where  $G$  is the calculated gravity that is adjusted for Eötvös effect and normal gravity.

#### **4.1.1 Bouguer Correction**

Shuttle Radar Terrain Mission (SRTM) digital elevation model data were used to calculate the Bouguer corrections for gravity processing. The SRTM data contains information in a grid with a 3 arcsecond spacing, approximately equal to 100 m cell spacing, which has a higher density than the line spacing for this survey, and therefore provides terrain data at a better resolution between the survey lines. Coverage up to 160 km from the survey block was kept for accurate regional corrections.

Terrain corrections were computed using software developed by SGL. The algorithm calculates the topographic attraction of the terrain using a mass prism model with a constant density. The difference between the topographic attraction and the simple Bouguer correction is the terrain correction. The terrain and Bouguer corrections were calculated for the bedrock at the height of the aircraft using densities of 2.67 and 2.40 g/cm<sup>3</sup>.

Terrain corrections were filtered to match the degree of filtering applied to the gravity data, as described below.

#### **4.1.2 Static and Level Corrections**

The gravimetric data were levelled to compensate for instrument variations in two steps. A single constant shift determined from ground static recordings was applied on a flight-by-flight basis. The pre- and post-flight readings were averaged for each flight and the difference between the average value and the local gravity value was removed. This acts as a simple, but effective, coarse levelling of the data.

Intersection statistics were then used to adjust individual survey lines. Unlike magnetic levelling, individual intersections were not used to make corrections. Instead, intersection differences from whole lines were averaged and a single adjustment was applied to each survey line and each control line. Minor adjustments were calculated for sections of each line based on statistics from groups of intersections. The adjustments were smoothed and applied to line data that was filtered as described below. Grids of adjusted data were inspected to determine that the adjustments were appropriate.

### **4.1.3 Gridding and Filtering**

Statistical noise in the data was reduced by applying a cosine tapered low pass filter to the time series line data. For this survey, a 20 second (1,000 m) half wavelength filter was employed. The data were gridded using a minimum curvature algorithm, which averages all values within any given grid cell and interpolates the data between survey lines to produce a smooth grid. The algorithm produces a smooth grid by iteratively solving a set of difference equations by minimizing the total second horizontal derivative while attempting to honour the input data (Briggs, 1974). Grids were generated using a 25 m grid cell size.

Low-pass spatial filtering was applied to the grid to achieve better noise reduction than by simply increasing the degree of line filtering. A range of grid filters were used and evaluated for their effectiveness in removing noise from the data, and highlighting signal content. The final data were filtered with a 1.0 km half-wavelength grid filter.

The gravity data were gridded using a cell size of 25 m and 250 m over the Ignace area. The 25 m gridding cell was applied to present the highest resolution of the data within the boundaries of the two survey blocks comprising the principal survey area. The 250 m gridding cell was applied to include the extensions of the flight lines beyond the extent of the survey blocks comprising the extended survey area. The Bouguer gravity with a terrain correction of  $2.67 \text{ g/cm}^3$  is displayed in Figures 4.1 (principal survey area, grid cell size of 25 m) and Figure 4.2 (extended survey area, grid cell size of 250 m). The Free Air gravity is displayed in Figure 4.3 (principal survey area, grid cell size of 25 m) and Figure 4.4 (extended survey area, grid cell size of 250 m).

## **4.2 Magnetic Data Processing**

The airborne magnetometer data were recorded at 160 Hz, and down sampled to 10 Hz for processing. A second order Butterworth 0.9 Hz low pass filter was utilized in the process for compensation and anti-aliasing. All magnetic data were plotted and checked for any spikes or noise. A 0.244 second static lag correction due to signal processing, plus a dynamic lag correction, was determined on a by-line basis for each aircraft. The aircraft speed dependent dynamic lag was calculated using SGL's Dynlag software.

Ground magnetometer data were inspected for cultural interference and edited where necessary. All reference station magnetometer data were filtered using a 121 point low-pass filter to remove any high-frequency noise, but retain the low-frequency diurnal variations. For non-technical reasons, the ground magnetometer was changed to a different location during the survey.

A correction for the International Geomagnetic Reference Field (IGRF) year 2010 model was applied to all ground magnetometer data using the fixed ground station location and the recorded date for each flight. The mean residual value of the reference station was calculated (398.172 nT for the first magnetometer position, and 404.673 nT for the second magnetometer position) and subtracted to remove any bias from the local anomalous field. Diurnal variations in the airborne magnetometer data were removed by subtracting the corrected reference station data.

The airborne magnetometer data were corrected for the IGRF using the location, altitude, and date of each point. IGRF values were calculated using the year 2010 IGRF model. The altitude data used for the IGRF corrections are DGPS heights above the WGS84 datum.

#### **4.2.1 Levelling**

Intersections between control and traverse lines were determined by a program which extracts the magnetic, altitude, and x and y values of the traverse and control lines at each intersection point. Each control line was adjusted by a constant value to minimize the intersection differences, calculated as follows:

$$\sum |i - a| \text{ summed over all traverse lines, where:}$$

i	=	(individual intersection difference)
a	=	(average intersection difference for that traverse line)

Adjusted control lines were further corrected locally to minimize any residual differences. Traverse line levelling was carried out by a program called CLEVEL that interpolates and extrapolates levelling values for each point based on the two closest differences at intersections. After traverse lines were levelled, the control lines were matched to them. This ensured that all intersections tied perfectly, and permitted the use of all data in the final products.

CLEVEL provided a curved correction using a function similar to spline interpolation. A third degree polynomial was used to interpolate between two intersections and the two values and two derivatives were chosen to determine the polynomial. CLEVEL is an improved method, as it allows intersection points to be preserved with no mismatch and interpolation is smooth with the first derivative continuously approaching the same value from both sides of the intersection points.

The levelling procedure was verified through inspection of the magnetic anomaly and vertical derivative grids by plotting profiles of corrections along lines, and examination of levelling statistics to check for steep correction gradients.

#### **4.2.2 Micro-Levelling**

Micro-levelling was applied to remove any residual diurnal effects from the data, and was achieved by using directional filters to identify and remove artifacts that are long wavelength parallel to survey lines and short wavelengths perpendicular to survey lines. A limit of +/-0.20 nT was set for all micro-levelling corrections.

#### **4.2.3 Gridding**

The grid of the total magnetic intensity was made using a minimum curvature algorithm to create a two-dimensional grid equally sampled in the x and y directions following Briggs (1974). The final grids of the magnetic data were created with 25 m grid cell size appropriate for survey lines spaced at 100 m. Grids were also made that included the 1,000 m spaced lines that extend out from the main block area. These were gridded with a cell size of 250 m.

The magnetic data were gridded using a cell size of 25 m and 250 m over the Ignace area. The 25 m gridding cell was applied to present the highest resolution of the data within the boundaries of the two survey blocks comprising the principal survey area. The 250 m gridding cell was applied to include the extensions of the flight lines beyond the extent of the survey blocks comprising the extended survey area. The total magnetic intensity (or more precisely, the magnetic anomaly) is displayed in Figure 4.5 (principal survey area, grid cell size of 25 m) and Figure 4.6 (extended survey area, grid cell size of 250 m).

### 4.3 Gravity and Magnetic Derivative Products

Filters may be applied to the data to enhance different wavelength information that arises from different sources. In many cases, filtering is best achieved by transforming the data from the space domain to the frequency domain by Fourier transform, since frequency characteristics of the filter to be applied are more precisely defined in the frequency domain. The filtered derivatives created to assist with interpretation are described below.

#### 4.3.1 Total Magnetic Intensity Reduced to Pole

Reduction to the pole (RTP) transforms anomalies as if they were at the north magnetic pole. The basic assumption is that magnetic anomalies arise from induced magnetization. This assumption may not always be true where significant magnetic remanence occurs. The method allows direct comparison of anomaly shapes from different magnetic latitudes, and if the assumptions hold true the anomaly will be symmetrically disposed about the causative body. Reduction to pole is essentially a phase shift filter applied in the frequency domain, and is described by Baranov and Naudy (1964):

$$F(k_x, k_y) = \frac{1}{[\sin I + i \cos I \cos(D - \theta)]^2}$$

where

- $\theta$  is the angle in the  $k_x, k_y$  plane
- $I$  is the local magnetic inclination
- $D$  is the local magnetic declination

For ease of calculation, this transformation was performed through filtering in the frequency domain using a constant (average/central) inclination and declination which was considered valid throughout the entire grid. The inclination used was  $74.94^\circ$ , and the corresponding declination used was  $-1.55^\circ$ , representing a station approximately at the centre of the survey. The total magnetic intensity reduced to the pole is shown in Figure 4.7 (principal survey area, grid cell size of 25 m) and Figure 4.8 (extended survey area, grid cell size of 250 m).

#### 4.3.2 Vertical Derivatives of Total Magnetic Intensity and Bouguer Gravity

If  $k_x$  and  $k_y$  are the wave numbers of the potential field in the two dimensional frequency domain, the  $n$ th vertical derivative of the a potential field is easily derived in the Fourier domain by applying the following filter:

$$F(k_x, k_y) = (-k)^n \quad \text{where } k = \sqrt{(k_x^2 + k_y^2)}$$

Vertical derivatives act as high-pass filters that enhance high frequency data and suppress low frequency data. The first vertical derivative (n=1) enhances the rapid changes in gravity or magnetic field at the edges of anomalies and is therefore useful for delimiting the extents of causative bodies. The second vertical derivative (n=2) enhances high frequency signal variations even more, such that textural variations in the character or the potential field (especially for magnetic data) can be used to delimit domains of a specific geophysical response.

First vertical derivative of the reduced to pole total magnetic intensity is shown in Figure 4.9 (principal survey area, grid cell size of 25 m) and Figure 4.10 (extended survey area, grid cell size of 250 m). The first vertical derivative of the Bouguer gravity with a terrain correction using a density of 2.67 g/cm<sup>3</sup> is shown in Figure 4.11 (principal survey area, grid cell size of 25 m) and Figure 4.12 (extended survey area, grid cell size of 250m). The first vertical derivative of the Free Air gravity is shown in Figure 4.13 (principal survey area, grid cell size of 25 m) and Figure 4.14 (extended survey area, grid cell size of 250 m). The second vertical derivative of the reduced to pole total magnetic intensity is shown in Figure 4.15 (principal survey area, grid cell size of 25 m) and Figure 4.16 (extended survey area, grid cell size of 250 m). The gravity data does not contain high frequency information to render its second vertical derivative useful for interpretation.

#### **4.3.3 Total Horizontal Gradient of Total Magnetic Intensity and Bouguer Gravity**

Horizontal gradients are most conveniently calculated in the space domain. Total horizontal gradient of a potential field “T” is from the gradients in the horizontal x and y plane as follows:

$$\text{Total horizontal derivative} = \sqrt{(\partial T/\partial x)^2 + (\partial T/\partial y)^2}$$

Horizontal gradient grids are used primarily for edge detection of causative bodies (contacts, faults with large vertical displacement), and the data may also be employed for trend analysis and depth to source calculations.

Total horizontal derivatives of the reduced to pole total magnetic intensity, Bouguer gravity (2.67 g/cm<sup>3</sup> terrain correction) and Free Air gravity are shown in Figures 4.17, 4.19, 4.21 (principal survey area, grid cell size of 25 m) and Figures 4.18, 4.20, 4.22 (extended survey area, grid cell size of 250 m).

#### **4.3.4 Total Gradient Amplitude of Total Magnetic Intensity**

The total gradient amplitude, otherwise known as the 3D analytic signal amplitude, of a potential field (T) is defined as (Nabighian, 1972):

$$|A(x, y)| = \sqrt{(\partial T/\partial x)^2 + (\partial T/\partial y)^2 + (\partial T/\partial z)^2}$$

|A(x, y)| is the amplitude of the analytic signal and T is the magnetic intensity at a point (x, y). The horizontal derivatives are easily calculated in the space domain, whilst the vertical derivative ( $\partial T/\partial z$ ) is calculated using space and frequency domains. Analytic signal is independent of field direction and

direction of magnetization, and is independent of the type of magnetization (induced or remanent). This means that all similar bodies have similar analytic signal response, and that peaks in the analytic signal are symmetric and centred over the middle of narrow bodies and the edges of wide bodies. The amplitude, however, is affected by the strike of a body such that north-south oriented bodies at low latitudes are relatively weak for magnetic data. It highlights areas where the field varies quickly in any direction, such as for contacts, and high or low anomalies.

The total gradient amplitude (analytic signal) of the total magnetic intensity is shown in Figure 4.23 (principal survey area, grid cell size of 25 m) and Figure 4.24 (extended survey area, grid cell size of 250 m).

#### 4.3.5 Tilt Angle

The tilt angle can be applied to the pole reduced total magnetic intensity to preferentially enhance the weaker magnetic signals. This is particularly useful for mapping texture, structure, and edge contacts of weakly magnetic sources. The arctan operator restricts the tilt angle to within the range of  $-90^\circ$  to  $+90^\circ$ , irrespective of the amplitude and wavelength of the field and enhances weak anomalies compared to the stronger anomalies. The tilt angle ( $\theta$ ) is defined as (Miller and Singh, 1994; Verduzco et al., 2004; and Salem et al. 2007):

$$\theta = \tan^{-1} \frac{\text{vertical component of gradient}}{\text{horizontal component of gradient}} = \tan^{-1} \left[ \frac{\partial T / \partial z}{\sqrt{(\partial T / \partial x)^2 + (\partial T / \partial y)^2}} \right]$$

The vertical and horizontal gradients of the reduced to pole total magnetic intensity calculations are described above in subsections 4.3.2 and 4.3.3. The tilt angle grid of the reduced to pole total magnetic intensity is displayed in Figure 4.25 (principal survey area, grid cell size of 25 m) and Figure 4.26 (extended survey area, grid cell size of 250 m).

#### 4.3.6 Trend Analysis Method

Depth trend as implemented by Phillips (1997) can be utilized for the depth estimation using the horizontal gradient grid (HG). It uses the horizontal gradient of the reduced to pole total magnetic intensity and gravity grids to estimate strikes of and depths to thick and thin edges, respectively (Phillips, 2000). The method relies on the general principle that shallow sources produce anomalies with steep gradients, whereas deep sources produce anomalies with broad gradients. Depth estimates from the RTP magnetic and gravity data estimate the minimum and maximum depths to the top edge of the layer, respectively (Phillips, 2000).

The program uses a 5 by 5 window to both locate the crests of maxima and determine their strike direction. Once a crest is located and the strike direction is known, data within the window and within a belt perpendicular to the strike can be used to determine the depth of the contact by performing a least squares fit to the theoretical shape of the *HG* over a contact. If "*h*" is the horizontal distance to the contact, "*d*" is the depth to the top of the contact and "*K*" is a constant, then the theoretical curve is given by (Roest and Pilkington, 1993):

$$HG(h) = K / (h^2 + d^2)$$

The least squares fit gives an estimate of both the depth and its standard error, which can be expressed as a percentage of the depth. Typically only depth estimates with standard errors of 15% or better are retained in the final interpretation.

Due to the assumption of thick sources, the depth estimates obtained using the above procedure represent minimum depths. It is also possible to assume very thin sources and use a standard pseudogravity transformation instead of reduction to the pole (Roest and Pilkington, 1993). In this case the same analysis could be done on the HG of the pseudogravity field, and the depth estimates represent maximum depths.

Figures 4.27 and 4.28 show the depth results from the trend analysis solutions for the Bouguer gravity and the reduced to pole total magnetic intensity.

## 5 Geophysical Interpretation

The geophysical interpretation of the acquired gravity and magnetic data in the Ignace area involved qualitative analysis of the various products derived from the magnetic and gravity grids (described in Section 4), and preliminary 2.5D forward modelling of the gravitational and magnetic data along five profile lines covering the principle features of the Revell, Basket Lake and Indian Lake batholiths within the survey area.

### 5.1 Results of Qualitative Analysis

Qualitative analysis of the gravity derivative products was used to provide general indications about the location and dip of the batholiths' edges, the variation in depth across the batholiths, the internal variations in density within the batholiths, and the presence of major or deep seated structures. Qualitative analysis of the magnetic derivative products was used to identify the presence of potential features within the batholiths, such as faults and dykes (documented in SRK, 2015), and evaluate variation in the magnetic character within the batholiths that may indicate changing composition of the rock or other potential heterogeneities.

For the qualitative geophysical interpretation, the horizontal derivative of the Bouguer gravity (Figure 5.1), as well as the reduced to pole magnetic intensity (Figure 5.3) and its first vertical and horizontal derivative grids (Figures 5.2 and 5.4), were useful. In addition, the total gradient amplitude was particularly useful for interpretation of magnetic data (Figure 4.23 and 4.24) because (a) it has maxima over magnetic contacts, (b) this is true regardless of the direction of magnetization, and (c) the reduced to pole magnetic intensity requires the assumption of only induced magnetization with the result that anomalies from remanently and anisotropically magnetized bodies can be severely distorted. Unlike the reduced to pole, the total gradient amplitude will produce maxima over the edges of vertical magnetic contacts regardless of the presence of remanent magnetism (MacLeod, 1993). The horizontal derivative of the Bouguer gravity (Figure 5.1) produces highs directly over major density contrasts representing potential geological contacts between rock units.

The following qualitative observations were made about the portions of the Revell, Basket Lake and Indian Lake batholiths contained within the Ignace survey area.

#### 5.1.1 Revell Batholith

- The boundaries of the Revell batholith are clearly defined by distinct highs in the horizontal derivative of the Bouguer gravity, and agree very closely with the mapped boundaries as presented by OGS (2011) and Stone et al. (2011a, b) (Figure 5.1, outline of area A1). This is primarily due to the fact that the Revell batholith is bounded by the much denser rocks of the Raleigh Lake and Bending Lake greenstone belts. In the northwest of the intrusion, the peaks in the horizontal gradient coincide with the mapped edges, which are asymmetric and taper towards the interior of the batholith. This suggests that in this part of the batholith, the edges are vertical close to the surface but dip inwards at greater depth.
- A high in the horizontal derivative of the Bouguer gravity within the Revell batholith coincides with a unit mapped by Stone et al. (2011a, b) as hornblende tonalite to granite (Figure 5.1, feature F1). More importantly the feature marks the transition from granite-granodiorite to the

east with a lower associated gravity anomaly, to tonalite-granodiorite with an associated gravity high anomaly to the west. This suggests that other such intra-batholith features in the horizontal derivative of the Bouguer gravity also may be attributable to internal variations in composition and density. Within the Revell batholith several linear gravitational highs may also provide indications of internal lithological variations (Figure 5.1, features 1-8, area A2). Some of these features tend to either be aligned parallel or represent continuations of lithological changes indicated by the mapping of Stone et al. (2011a, b).

- In general, the shape of the gravity anomaly across the Revell batholith implies that the depth of the intrusion is relatively uniform, being deepest in the south east. Modelling presented in Section 5.2 across two profile lines through the Revell batholith provides additional insight into the batholith geometry and depth.
- The reduced to pole magnetic field across the Revell batholith has a uniformly smooth and low character, with the distinct exception of an oval-shaped area in the centre with a magnetic high (Figure 5.2 and 5.3, area A8). The northern, eastern, and southwestern edges of this magnetic anomaly (Figure 5.3, area A8) precisely follow the edges of a distinct feldspar megacrystic phase identified by Stone et al. (2011a); although the area of the anomaly is not distinguished as being a separate element from the main body of the batholith. The interpreted contact associated with oval-shaped area is highlighted in the magnetic trend analysis solutions (Figure 4.27) as being near vertical. Despite the megacrystic phase showing a strong magnetic anomaly, there is no correlation with the gravity data apparent. This suggests that this area must represent a distinct phase within the biotite granodiorite to granite of the Revell batholith, predominantly with higher magnetite content. Although, immediately south of area A8 is a subtle circular anomaly shown in the horizontal derivative of the Bouguer gravity data (Figure 5.1, area A2).
- A similar pattern in the first vertical derivative of the reduced to pole magnetic data can be seen (Figure 5.2) to the south of the oval-shaped magnetic anomaly, although the amplitude is diminished. This could be an indication of another phase within the Revell batholith that has not been observed during previous mapping (e.g., OGS, 2011; Stone et al., 2011 a, b), or which may exist at depth.
- Two west-northwest oriented linear magnetic highs occur in the northwest of the batholith (Figure 5.2, features F24 and F25). These coincide with mapped Kenora-Fort Francis dykes (Figure 1.1). A detailed lineament interpretation, including interpretation of dyke lineaments, within the Revell batholith is presented in SRK (2015).

### **5.1.2 Basket Lake Batholith and Surrounding Tonalitic Units**

- A clear southeast-trending linear peak in the horizontal derivative of the Bouguer gravity generally coincides with the mapped boundary between the tonalitic units south of the Basket Lake batholith and the Raleigh Lake greenstone belt (Figure 5.1, feature F15). This linear peak highlights the big density difference between the greenstones of the Raleigh Lake greenstone belt and the tonalities to the north. The peak of the horizontal derivative is shifted

to the south of the mapped contact (Figure 1.1), indicating a boundary between the units to the south. This would imply that the contact dips to the south, with the greenstones overlying the tonalites.

- There are a number of other linear features in the horizontal derivative of the Bouguer gravity in the tonalitic units south of the Basket Lake batholith in the northwest of the survey area that imply either density or depth changes (Figure 5.1, features F16 through F23). One of these linear features seems to partially follow the mapped boundary between the tonalitic units and the granodiorite of the Basket Lake batholith (F18).
- Although uncertain, other linear features are identified in the horizontal derivative of the Bouguer gravity (Figure 5.1, features 9, 13, 18, 19) throughout the Basket Lake batholith, and may indicate the presence of some internal density variations within the rock unit. Alternatively, despite the terrain correction being applied, many of these linear features throughout the batholith also tend to coincide relatively well with the distribution of larger water bodies. The terrain correction did not incorporate bathymetry for the lakes, thus small anomalies associated with water bodies would be noted. Edges of the larger water bodies would be highlighted by the horizontal derivatives. Despite the presence of these features, overall the horizontal derivative of the Bouguer gravity is relatively uniform across the Basket Lake batholith.
- The gravity data suggest that the Basket Lake batholith is deeper than the surrounding tonalitic units – even taking into account the slight density difference between the tonalite and granodiorite. Modelling presented in Section 5.2 across two profile lines through the Basket Lake batholith provides additional insight into the batholith geometry and depth.
- The first vertical derivative of the reduced to pole magnetic field data (Figure 5.2) across the Basket Lake batholith has a pattern of uniform frequency and amplitude, which is interspersed with a network of linear magnetic lows, indicative of a potential systematic fracture pattern in the area. Detailed interpretations of these linear magnetic features are presented in SRK (2015). The uniformity of the magnetic character and the lack of any major features in the horizontal gradient of the Bouguer gravity (other than between the Basket Lake granite/granodiorite and the tonalite to its south) suggests a near consistent bedrock density and magnetic susceptibility. It is possible that some of the separately mapped units in this broad area experience a smooth and gradual transition in composition rather than a sudden discontinuity in rock type at the mapped boundaries.
- The only exception to this regular pattern is an area of high magnetic variability in the northwestern most part of the Basket Lake batholith (Figure 5.2, features A9, A13, A14). This magnetic anomaly also coincides well with a peak in the horizontal derivative of the Bouguer gravity, which curves around the magnetic anomaly in this area (Figure 5.1, area A4). The source of these anomalies could be either a sliver of greenstone belt or perhaps mafic-ultramafic metavolcanic rocks, similar to the ones mapped in the western edge of the Basket Lake batholith outside the geophysical survey area (Figure 1.1, mapped geological unit 10). Although the modelling also includes its presence, it is unclear whether this sliver penetrates

all the way to the surface. Available bedrock mapping does not identify the presence of greenstone slivers in this area (OGS, 2011).

### **5.1.3 Indian Lake Batholith**

- The broad and diffuse gravity low associated with the Indian Lake batholith is smaller in size and amplitude than that associated with the Basket Lake batholith, which indicates that the Indian Lake batholith is shallower than the Basket Lake batholith - assuming the batholiths are of comparable density (Szewczyk and West, 1976), and that there are no significant changes in the Indian Lake batholith density with depth (Figure 4.3).
- The overall character of the reduced to pole magnetic field shows no clear distinction between the western portion of the Indian Lake batholith and the Basket Lake batholith (Figure 5.3), and one would not be able to determine the boundary between them from any indication given by the magnetic data alone. The broad pattern of consistent character encompasses all of the Basket Lake batholith and the northwestern portion of the Indian Lake batholith.
- In addition, there are no obvious anomalies observed in the horizontal derivative of the Bouguer gravity between the Indian Lake and Basket Lake batholiths, which suggests that they may be part of the same overall structure (Figure 5.1).
- The overall distribution of the Bouguer gravity anomaly indicates that the shallowest portion of the Indian Lake batholith may be located at the centre of the broad gravity high that occurs between the two principle survey areas. This interpretation is based on the assumption of the uniform distribution of bedrock density for the batholith and underlying basement rock.
- To the north of the Indian Lake batholith, the gravity rises steadily, peaking at an exposed sliver of greenstone, which is also seen as a linear peak in the horizontal gradient of the Bouguer gravity (Figure 5.1, area A5). This may imply that the batholith shallows steadily towards the north up to the point where the greenstone is exposed. This linear high continues to the southwest beyond the mapped extent of the greenstone (Figure 5.1, feature F10), suggesting that the sliver of greenstone may continue beneath the surface of the batholith. Elsewhere in the Indian Lake batholith areas A6 and A7 may indicate the presence of some internal density variations within the bedrock unit. Similar to the Basket Lake batholith, these areas tend to coincide relatively well with the distribution of larger water bodies. The terrain correction did not incorporate bathymetry for the lakes; as such their edges may be highlighted by the horizontal derivatives.

## **5.2 Preliminary 2.5D Modeling**

The purpose of the 2.5D modelling is to develop an idea of the relatively deep and relatively shallow parts of the batholith and rough approximation of the depth to the bottom of different parts of the batholiths. The preliminary 2.5D modelling used the gravity, magnetic and terrain data sets, accompanied with constraints from the qualitative interpretation of the geophysical data and the mapped bedrock geology to provide a preliminary image of the subsurface along the five profile lines

shown on Figures 5.5 and 5.6.

For the purpose of this initial modelling attempt, density and magnetic susceptibility values were assigned to the bedrock units mapped on the surface and to the bedrock units at depth based on readily available information (Figure 1.1). In the Ignace area, several surface bedrock density and magnetic susceptibility values have been compiled from available literature (data sources discussed in Section 3) and incorporated as constraints into the models. These assumed density and magnetic susceptibility values should be considered as approximate values, as site-specific information on the bedrock at depth is not available (i.e. data from borehole drilling).

In order to assess the influence of the assumed density and magnetic susceptibilities on the modelled geometry and depth of the batholiths, a series of alternative models were also considered by varying the physical bedrock properties, in particular the bedrock density, for the bedrock units at depth. As we have an idea of the range of likely density values, the resulting 2.5D models can give an idea of the upper and lower bounds on the depth of the batholith.

It is important to emphasize that the accuracy of these preliminary models is limited at this early stage of the assessment due to limited availability of bedrock densities and magnetic susceptibilities that are key for constraining the model. It is anticipated that the preliminary 2.5D models would be revised and refined if more field data is collected in the future.

### 5.2.1 Model Descriptions

The preliminary 2.5D forward modelling of gravity and magnetic data carried out using GMSYS-2D Software (Northwest Geophysical Associates Inc.) running under Geosoft Oasis Montaj (Geosoft, 2012). The modelling considered three profile lines. The locations of the profile lines are shown in Figure 5.5 superimposed on the reduced to pole magnetic field, and in Figure 5.6 superimposed on the free air gravity. The start and end points of the co-ordinates are listed in Table 5.1.

Table 5.1: Coordinates of Model Profiles (UTM 15N, NAD83)

Profile Line	Start		End	
	UTM X	UTM Y	UTM X	UTM Y
1	548381	5474037	577603	5515917
2	556452	5464754	588713	5510990
3	586310	5463390	542857	5493709
4	562040	5513265	596832	5488989
5	617800	5473488	617800	5503312

The process for constructing the models was as follows:

- Lines were chosen to reflect the features of most interest in the general potentially suitable areas within the batholiths. In the case of line 5, the location was chosen to run directly along

the survey line which transects the Indian Lake batholith within the eastern survey block, and extends outside the main survey area.

- The profile lines were modelled using the free air gravity and the reduced to pole total magnetic intensity data. The choice of free air gravity, rather than Bouguer gravity, allowed terrain effects of variable density to be included in the model, by including the topography in the profile.
- Generally speaking, the gravity was modelled first to determine the geometry of the large-scale geological features, and the magnetic data were used to refine the model and include features such as interpreted faults and dykes, and to help model the overall shape of smaller bedrock units.
- Bedrock densities within the greenstone belts, batholiths and other geologic units were assumed to be uniform throughout, unless there were any data that suggested the contrary (well logs, density measurements, etc). This assumption was only otherwise violated if it was impossible to model the gravity using uniform densities. This can be restated by saying that gravity anomalies were generally accounted for by varying the shapes of the rock units after initial density assumptions were made, rather than by varying the densities within the bedrock units. Depth trend solutions of the Bouguer gravity were used as a guide in determining locations and dips of faults/contacts.
- Available geologic mapping (OGS, 2011; Stone et al., 2011a, b) and qualitative interpretation of the geophysical data were used to determine the location of the points at which geological boundaries occurred along the surface of the models.
- Density information was obtained from Szewczyk and West (1976), who performed 2D and 3D modelling of land-based gravity data in an area which significantly overlaps the current survey area. Density data points are also available in certain parts of the survey area from the OGS Petroch database (Haus and Pauk, 2010). The densities and magnetic susceptibility ranges used in the models are listed in Table 5.2.
- In determining the magnetic susceptibilities for modelling the magnetic data, initial values of magnetic susceptibility were chosen that were (a) best able to match the amplitude of the short wavelength magnetic variations that were obviously associated with terrain, and (b) best able to reproduce the overall long wavelength trend associated with the larger rock units. This approach was employed due to the uncertainties of the magnetic susceptibilities used, since no measured susceptibility data were available in the area, and published magnetic susceptibility values for given rock types can vary over several orders of magnitude over short distances.
- In seeking to model magnetic variations within individual rock units, vertical boundaries were generally used in the absence of other indications. Indicators that were used included the presence of faults and dykes as determined by the presence of linear features in the magnetic derivative grids. Trend analysis solutions for the reduced to pole total magnetic intensity data

were also used as a guide in setting the dip of magnetic contacts. Trend analysis solutions are shown in the 2.5D model figures as x and + symbols on the profile lines for gravity and magnetic data, respectively.

- The overburden was not included in the modelling. It is deemed to be sufficiently shallow that its effect on the gravity and magnetic anomaly will be negligible for modelling purposes.
- Density variations within the mapped greenstone belts were generally limited to a depth of approximately 4.0 km, as there is no information on the depth to which these variations would continue to.
- Where the 2.5D model lines intersect, the geological boundaries, densities, and magnetic susceptibilities have been made to coincide at the model intersection points. These intersection points are displayed in the model figures.

*Table 5.2: Densities and magnetic susceptibilities used in the 2.5D models*

<b>Layer</b>	<b>Density (g/cm<sup>3</sup>)</b>	<b>Magnetic Susceptibility (S. I.)</b>
<i>Revell Batholith</i>	<i>2.60</i>	<i>0.0070-0.0230</i>
<i>Basket Lake Batholith</i>	<i>2.61</i>	<i>0.0120-0.0168</i>
<i>Indian Lake Batholith</i>	<i>2.61</i>	<i>0.0134-0.0204</i>
<i>Tonalite</i>	<i>2.61-2.65</i>	<i>0.0035-0.0123</i>
<i>Felsic metavolcanic</i>	<i>2.75</i>	<i>0.0011</i>
<i>Coarse clastics</i>	<i>2.50</i>	<i>0.0011</i>
<i>Mafic-ultramafic rocks</i>	<i>2.77</i>	<i>0.0209-0.0241</i>
<i>Dykes</i>	<i>2.75</i>	<i>0.0056-0.054</i>
<i>Greenstone</i>	<i>2.87-2.92</i>	<i>0.0013-0.0373</i>
<i>Wacke, siltstone, iron formation</i>	<i>3.00-3.10</i>	<i>0.033-0.303</i>
<i>Hornblende tonalite suite</i>	<i>2.69</i>	<i>0.0180</i>
<i>Mafic metavolcanics</i>	<i>2.86-2.87</i>	<i>0.0053-0.0360</i>
<i>Gabbro</i>	<i>2.83</i>	<i>0.0250</i>
<i>Intermediate metavolcanics</i>	<i>2.77-2.87</i>	<i>0.0100-0.0200</i>
<i>Gneissic tonalite.</i>	<i>2.65</i>	<i>0.0100-0.0124</i>
<i>Felsic to intermediate metavolcanics</i>	<i>2.75-2.87</i>	<i>0.00178</i>
<i>Ultramafic metavolcanic rock</i>	<i>2.87</i>	<i>0.0350</i>

### **5.2.1 Model Results**

This section discussed the results of the 2.5D modelling for each of the five profile lines considered. The results are first discusses for the initial models assuming the batholiths are completely surrounded by a bedrock unit with a uniform density (equivalent to the value assigned to the greenstone belt units), and for the alternative models assuming the batholiths are underlain by bedrock units with a density equivalent to gneissic units.

The 2.5D modelling results for Ignace are shown on Figures 5.7 to 5.17. The figures show a plan view along the profile line (e.g. top panel Figure 5.7) in order to show the distribution of bedrock rock units that are included in the model calculations that are perpendicular to the strike of the profile line. The gravity view (e.g. second panel Figure 5.7) shows the observed gravity data along the profile line, as well at the calculated gravity data, and the RMS error (i.e. root mean square error) (e.g. third panel Figure 5.7). The RMS error is used as a measure of the difference between the observed gravity data and the modelled gravity results. The lower portion of the gravity view shows the assignment of the rock density values to each of the bedrock units in the model. The magnetic view (e.g. fourth panel Figure 5.7) shows a similar set of profile data, with the observed and calculated magnetic data, as well as the RMS error between the two data sets. The lower portion of the magnetic view (e.g. fifth panel Figure 5.7) shows the assignment of the magnetic susceptibility values to each of the bedrock units in the model. The structural view provides the overall interpretation of the modelled results, which are coloured based on geological unit (e.g. sixth panel on Figure 5.7). Each of these model views shows the depth on the y-axis in kilometres depth below mean sea level (MSL).

Several alternative models are presented to assess the influence of changing the physical bedrock properties and its impact on the geometry and thickness of the batholith units. These alternative models show only a subset of the profile data discussed above.

#### **5.2.1.1 Results for Profile Line 1**

##### ***Initial Model 1.6 (Figure 5.7)***

As shown in Figure 5.5, Line 1 cuts across both the Revell and Basket Lake batholiths, and the Raleigh Lake and Bending Lake greenstone belts. The orientation of the line is directly perpendicular to the overall orientation of the batholiths and greenstone belts, and the magnetic and gravitational features associated with them.

- The Revell batholith is modelled as having a maximum depth of approximately 3.0 km, with its deepest portion in the southwest, gradually shallowing for a distance of 8 km to the northeast to a depth of approximately 2.5 km. At this point the depth of the intrusion is interpreted to shallow quickly towards the north east.
- Two dykes cross cut the Revell batholith, and are shown within the model line as sharp peaks in the magnetic data.
- Aside from the interpreted dykes, the Revell batholith has a relatively uniform and low magnetic susceptibility. The model suggests that the susceptibility may be slightly higher in the

southwestern portion of the batholith. It seems plausible that any change in the Revell batholith susceptibility across the model line would be small, gradual and uniform.

- The Basket Lake batholith is modelled as being part of a larger structure that includes both the mapped tonalite and granodiorite to granite units. The overall geometry of these units has a relatively flat bottom that varies in depth from approximately 4.0 km to 5.0 km, being at its deepest in the southwest. The shallowest section occurs in the granodiorite to granite section in the centre of the structure.
- Within the granodiorite-granite section of the Basket Lake batholith there are two areas that are interpreted to comprise a higher magnetic susceptibility (Figure 5.2; areas A9 and A13), which are associated with the two magnetic features which run near parallel to the model line. These features are cross-cut by model Line 4, and are modelled as a sliver of dense rock with high susceptibility that cuts into the interior of the batholith. Outside of this section the granite-granodiorite section has a more consistent magnetic character.
- The Raleigh Lake greenstone belt shows considerable magnetic activity. This greenstone belt consists of bands of mafic metavolcanic, intermediate-mafic metavolcanic and mafic-ultramafic rocks. The banding of rocks with varying degrees of magnetic susceptibility is reflected in the model by a set of vertical magnetic contacts which reproduce the magnetic anomalies within this greenstone belt.
- The Bending Lake greenstone belt is similar to the Raleigh Lake greenstone belt, with the same kind of banding of rocks of various mafic/intermediate/ultramafic grades. The significant magnetic high at the far south of the line is associated with one of these bands as well as with a metasedimentary unit to the south of the greenstone belt.

### ***Alternative Model 1.5 (Figure 5.8)***

In this alternative model for the gravity, a gneissic basement with a density of 2.68 g/cm<sup>3</sup> was included underneath the greenstone belts and batholith units. This was done as a point of comparison with the study of Szewczyk and West (1976), which suggests that the gneissic areas in the region may include parts of an original remobilized basement for the metavolcanic greenstone belt units, and that the gneiss may interconnect at depth. The 2D and 3D forward gravity models undertaken by Szewczyk and West (1976) make this assumption.

The gneissic basement has been added at a depth of approximately 4.5 km. The tonalite and granite-granodioritic units of the Basket Lake batholith have been allowed to extend beneath this depth, although the metavolcanic units have not. With regards to the Revell and Basket Lake batholiths, the following differences are noted:

- The geometry of the Basket Lake batholith has changed considerably, with the bottom of the batholith now having a maximum depth of approximately 7.5 km (compared with a maximum depth of 5.0 km shown in Figure 5.7). The resulting modelled depth of the Basket Lake batholith is consistent with the depth determined by Szewczyk and West (1976).

- The bottom of the Revell batholith displays a similar maximum depth of approximately 3.0 km, as shown in Figure 5.7.

Alternative models have been created for the other four 2.5D profile lines in the Ignace area with the introduction of the same gneissic basement. Where each of the model lines intersects each other, the depths of the geological units, their densities, and magnetic susceptibilities have been made to be consistent.

### **5.2.1.2 Results of Profile Line 2**

#### ***Initial Model 2.3 (Figure 5.9)***

As shown in Figure 5.5, Line 2 runs parallel to Line 1, located approximately 12 km to the east, and likewise cuts across both the Revell and Basket Lake batholiths, and the Raleigh Lake and Bending Lake greenstone belts. The orientation of the line is directly perpendicular to the overall orientation of the batholiths and greenstone belts, and the magnetic and gravitational features associated with them. The line crosses through the middle of magnetic feature (area A8 in Figure 5.3) in the centre of the Revell Batholith.

- The Revell batholith modelled along Line 2 has a flat bottom with a fairly uniform depth of approximately 1.8 km. The northeastern portion of the Revell batholith reaches a maximum depth of approximately 2.0 km. The dip of the northeastern and southwestern batholith contacts is near vertical adjacent to the greenstone units.
- Along the model line, within the portion of the Revell batholith, the magnetic data displays two distinct characters – a quiet and low signal to the southeast and a higher and more active signal for the northeastern two thirds of the batholith (area A8 in Figure 5.3). The more active area can be well modelled by vertical bands of higher magnetic susceptibility. Some of the higher magnetic anomalies tend to be associated with variations in the topography, and may not reflect internal magnetic variations.
- The base of the granodiorite to granite unit of the Basket Lake batholith shows some variability in the geometry with a depth of approximately 2.0 km. The central portion of the granodiorite to granite unit is modelled as being cut by two vertical faults and a dyke based on the response from the magnetic data. The tonalite unit southwest of the Basket Lake batholith have an interpreted depth range of approximately 2.5 km to 3.0 km, which shallows to the surface in contact with the greenstone unit. Within this tonalite section a potential fault has been included in the model based on the magnetic data.
- The magnetic susceptibilities throughout the Basket Lake batholith show significant lateral variations, with vertical to near vertical contacts. The tonalite and gneissic tonalite units are interpreted to have magnetic susceptibilities that are generally lower, compared to the granodiorite-granite units.
- The Raleigh Lake greenstone belt shows less lateral variation in interpreted magnetic susceptibility compared to Line 1, with the notable exception of the Wabigoon dyke that runs

parallel to the Revell batholith within the greenstone belt (Figure 5.3; Feature F25).

- To the south of the interpreted dyke, it is necessary to both increase the density and reduce the magnetic susceptibility of the greenstone units in order to fit the gravitational and magnetic anomalies. This section clearly coincides with a band of mafic metavolcanic rocks within the greenstone belt mapped by Stone et al. (2011a, b).
- The Bending Lake greenstone belt is composed of an alternating series of metasedimentary and metavolcanic bedrock units. The magnetic signature of the whole model line is dominated by a unit of banded iron formation wedged in either side by units of metavolcanic rock. Another small unit mapped as wacke, siltstone, iron formation, only produces a small magnetic anomaly suggesting that the iron content is much smaller in these units. The larger and smaller units of iron formation coincide with significant gravity highs.

### ***Alternative Model 2.5 (Figure 5.10)***

As in model 1.5, a gneissic basement was introduced for model 2.5. The depth of the basement was matched to that for models 3.5 and 4.5 where they intersect. With regards to the Revell and Basket Lake batholiths, the following differences are noted from model 2.3:

- The bottom of the Revell batholith is more convex and the batholith as a whole is deeper, with a maximum depth of approximately 3.0 km. This model presents a depth to the base of the Revell batholith similar to that presented in Figure 5.9.
- The depth to the base of the granite to granodiorite portion of the Basket Lake batholith is approximately 3.0 km. This depth is similarly presented in Figure 5.9; despite the inclusion of a rock density assigned at depth that is consistent with gneissic bedrock. The tonalite and gneissic tonalite units to the northeast and southwest of the granite to granodiorite have increased in thickness, now reaching approximately 6.0 km depth.

### ***5.2.1.3 Results of Profile Line 3***

#### ***Initial Model 3.3.4 (Figure 5.11)***

As shown in Figure 5.5, Line 3 cuts southeastwards across the northern half of the Revell batholith, and the surrounding greenstone belts. Within the batholith, the model line cross-cuts the magnetically active feature (area A8 in Figure 5.3) also transected by Line 2, but in an orthogonal direction.

- The Revell batholith is modelled as having a broad flat bottom, with depths generally ranging between approximately 2.0 km and 2.5 km. The depths taper off at either end of the batholith, although the edges of the batholith are interpreted as near vertical closer to the surface.
- Along this profile line, a block of felsic to intermediate mafic rock has been included in the model occurring within the batholith on its southeastern side.
- The profile line crosses through a potential fault within the magnetically active area (Figure 5.3;

area A8) of the Revell batholith. The fault is modelled as a thin zone of low magnetic susceptibility that passes vertically through the batholith.

- Generally, the magnetic susceptibility within the Revell batholith varies between 0.010-0.015 SI, apart from the more active area where it increases to 0.021-0.023 SI. The susceptibility also drops off to the southeastern end of the batholith adjacent to the greenstone belt units.
- A thin unit of hornblende tonalite to granite occurs immediately to the northwest of the magnetically active feature and marks its boundary.
- To the northwest of the Revell batholith, variation in the magnetic and gravitational anomalies suggests that there may be alternating bedrock units within the greenstone belt. This is incorporated into the model by varying the magnetic susceptibilities and rock densities in the model.
- At the northwestern boundary of the Revell batholith, adjacent to the greenstone units, two interpreted dykes were included in the model based on two prominent peaks within the magnetic data.
- The density variations in the greenstone belt, illustrate that the assumption of a uniform greenstone density beneath the Revell batholith is an approximation that is unlikely to hold true.
- To the southeast of the Revell batholith the greenstone belt is similarly complex, with further evidence of density variations and banding of metavolcanic rocks with varying magnetic susceptibilities.
- A small granodiorite intrusion occurs in the southern portion of the line. This unit is relatively shallow (maximum depth of approximately 700 m), and corresponds exactly with a distinct high in the magnetic data.

### ***Alternative Model 3.5 (Figure 5.12)***

As in model 1.5, a gneissic basement was introduced for model 3.5. The depth of the basement was matched to that for models 1.5 and 2.5 where they intersect. The following differences are noted from model 3.3.4:

- The bottom of the Revell batholith has a slightly more convex geometry, and the batholith as a whole is deeper, with a maximum depth of approximately 3.0 km.

#### ***5.2.1.4 Results for Profile Line 4***

##### ***Initial Model 4.3.3 (Figure 5.13)***

As shown in Figure 5.5, Line 4 cuts across the centre of the Basket Lake batholith along its major-axis, and continues into the northwestern portion of the Indian Lake batholith.

- The Basket Lake batholith has a generally flat bottom along the model line, with a depth ranging between approximately 3.0 km and 4.0 km. The batholith becomes gradually shallower from the northwest towards the southeast.
- A very large and sharp positive magnetic anomaly coincides with the edge of a positive gravity anomaly within the interior of the Basket Lake batholith. A cluster of trend analysis solutions from the Bouguer gravity extended vertically to a significant depth. This has been modelled as a sliver of dense ultramafic metavolcanics spliced within the batholith (area A4 in Figure 5.1 and A9 in Figure 5.3).
- In the model this metavolcanic sliver does not reach the surface. It was modelled this way primarily to be consistent with the mapped surface geology, although it is quite possible that this unit may actually reach the surface.
- The Indian Lake batholith is shallower than the Basket Lake batholith, and along the model line the depth varies from approximately 3.0 km to 2.0 km, potentially becoming shallower towards the southeast.
- It is arguably a matter of convention as to whether the Basket Lake batholith is considered separate from the Indian Lake batholith. These model results indicate that there is continuity in depth with the tonalite and gneissic tonalite units that lie between the granite to granodiorite units of the Indian Lake and Basket Lake batholiths.
- The magnetic susceptibility within both of the batholiths shows some minor variability, but is generally similar.

#### ***Alternative Model 4.5.2 (Figure 5.14)***

As in model 1.5, a gneissic basement was introduced into model 4.5.2. The depth of the basement was matched to that for models 1.5 and 2.5 where they intersect. The following differences are noted from model 4.3.3:

- The results shown on Figure 5.14 indicate that there is a general deepening from the Indian Lake in the southeast to the Basket Lake batholith in the northwest. The depth of the Indian Lake batholith varies between 500 m and 3.0 km, and the depth of the Basket Lake batholith varies from 3.0 km to 9.0 km. These modelled depths are generally consistent with the results from Szewczyk and West, 1976 for both the Basket Lake and Indian Lake batholiths. The deepening of these batholiths compared to model 4.3.3 underlines the importance of the assumptions that are made with regards to the density of the basement in estimating the depths of the batholiths.

#### ***5.2.1.5 Results of Profile Line 5***

##### ***Initial Model 5.2 (Figure 5.15)***

As indicated in Figure 5.5, Line 5 runs north to south through the eastern portion of the Indian Lake

batholith, across almost the entire extent of the granodiorite to granite unit.

- The entire model consists of granite to granodiorite of the Indian Lake batholith which is underlain by greenstone units.
- At the southern end of the profile line the bottom of the batholith bulges out to a depth of approximately 7.5 km, becoming gradually shallower to approximately 4.0 km towards the north.
- The central section of the batholith also bulges downward, but to a lesser extent than the southern section, with depth varying between approximately 4.0 m and 4.5 km.
- In the northernmost portion of the profile line the batholith deepens to approximately 5.0 km.

#### ***Alternative Model 5.3 (Figure 5.16)***

Two positive gravity anomalies to the north of the model line were not accounted for in model 5.2. These two gravity anomalies coincide with sharp negative magnetic anomalies. One way of reconciling both of these features is to incorporate two narrow slivers of greenstone units penetrating the intrusion almost to the surface. Such an interpretation has been incorporated in model 5.3.

#### ***Alternative Model 5.5 (Figure 5.17)***

As in model 1.5, a gneissic basement was introduced for model 5.5 with a density of  $2.68 \text{ g/cm}^3$ . The resulting differences between models 5.5 and 5.2 are:

- The southern end of the Indian Lake batholith is very similar to model 5.2 in terms of both shape and depth - extending to a maximum depth of approximately 8.0 km.
- To the north of this bulge, there is another broader but much shallower bulge in the batholith with a peak depth of approximately 3.2 km that extends from the 8 km mark to the northern end of the model line. The shallowest part of the batholith has a depth of approximately 800 m. This contrasts with model 5.2, which has a generally more flat bottom. In model 5.2 the batholith starts to deepen again in the far north whereas in this model the batholith continues to become shallower.

## 6 Summary of Results

The Ignace survey area covered large portions of the Revell, Basket Lake and Indian Lake batholiths. The main results of the modelling and interpretation of these batholiths are as follows:

### ***Revell Batholith***

- For the greater part, the Revell batholith has a low and quiet magnetic character, with two clear exceptions. One exception occurs in the northern portion of the batholith, where two linear ESE trending magnetic highs are observed and are associated with Wabigoon mafic dykes. The other exception is an oval shaped area of high magnetic activity in the centre of the batholith. The northern, eastern, and southwestern edges of this magnetic anomaly precisely follow a distinct feldspar megacrystic phase identified by Stone et al. (2011a, b), although the area of the anomaly is not distinguished as being a separate element from the main body of the batholith. There is no correlation between the magnetically active area and the gravity anomaly. This suggests that this area probably represents a distinct phase within the biotite granodiorite to granite of the Revell batholith, with higher magnetite content. The magnetic trend analysis solutions help to determine the dip of the boundary associated with this feature and imply that it has vertical contacts, although it is possibly a rounded slightly-dome like structure close to the surface. It is not clear whether this unit extends to the bottom of the batholith or not, as there appears to be no significant density contrast with the rest of the batholith.
- A similar pattern in the first vertical derivative of the reduced to pole magnetic data is identified to the south east of the oval-shaped magnetic anomaly, although the amplitude is not so high. This likely indicates a transitional phase between the active area and the biotite granodiorite of the rest of the batholith.
- The edges of the Revell batholith are clearly defined by distinct highs in the horizontal derivative of the Bouguer gravity, and agree very closely with the mapped boundaries. This indicates that the sides of the batholith are vertical. However, in the northwest of the intrusion, the peaks in the horizontal gradient coincide with the mapped edges, which are asymmetric and taper towards the interior of the batholith. This suggests that in this part of the batholith, the edges are vertical close to the surface but dip inwards at greater depth, so that the north of the batholith is more bowl-shaped.
- The Revell batholith has an elongated and somewhat amorphous shape, and is oriented to the northwest having an approximate mapped dimension of 40 km by 14 km. Based on modelling with a greenstone basement rock, the batholith has a relatively flat bottom (with some shallowing to the north) with approximate depths ranging between 2.5 km and 3.0 km. For the purposes of the modelling, the depth of the greenstone-gneiss boundary is only identifiable in gravity data if it results in lateral density contrasts. As described in section 5, a set of models were created which incorporated a greenstone-gneiss interface at a depth of approximately 4.5 km. The resulting effect of the gneissic basement on the depth of the Revell batholith was negligible.

### ***Basket Lake Batholith***

- A broad area of consistent magnetic character encompasses the Basket Lake batholith, along with the surrounding foliated and gneissic tonalite units, and continues southeast into the western portion of the Indian Lake batholith. The magnetic character of the first vertical derivative of the reduced to pole magnetic anomaly consists of a network of SSE and ESE running linear magnetic lows against a high-frequency, low-amplitude background. The uniformity of the magnetic character and the lack of any major features in the horizontal gradient of the Bouguer gravity (other than perhaps between the Basket Lake granite/granodiorite and the tonalite to its south) implies a consistent structural history, together with a uniform density and susceptibility. It is possible that some of the separately mapped units in this broad area experience a smooth and gradual transition in composition rather than a sudden discontinuity in rock type at the mapped boundaries.
- A very large and sharp positive magnetic anomaly (Figure 5.3; areas A9, and A11) within the interior of the Basket Lake batholith coincides with a positive gravity anomaly (Figure 5.1; area A4). This coincidence has been interpreted and modelled as a sliver of dense ultramafic metavolcanics spliced within the batholith. A similar greenstone unit is geologically mapped parallel to the magnetic and gravity anomalies in the northwestern portion of the batholith beyond the extent of the survey area.
- A couple of other minor linear highs in the horizontal derivative of the Bouguer gravity occur within the Basket Lake batholith. Their significance is not clear and they do not coincide with any mapped boundary or magnetic feature. They are close and parallel to the mapped boundary between the Basket Lake batholith and surrounding tonalite at the southeastern end of the intrusion, and could represent minor density changes within the batholith.
- The Basket Lake batholith is approximately 10 to 15 km in width and 35 km in length. There is a broad and deep gravity low encompassing the Basket Lake batholith and adjacent tonalite units. The preliminary 2.5D modelling implies that the batholith is a symmetric structure along its major axis, and deepens from the southeast to the northwest. On its southeastern margin the batholith is modelled as being approximately 2.5 km to 3.0 km deep, with the depth steadily increasing to the northwest, where it reaches a depth of approximately 4.0 km at the edge of the model line.
- The inclusion of a shallow gneissic basement to a set of alternative 2.5D models resulted in modelled depths of the Basket Lake batholith 30-60% deeper than depths from 2.5D models that did not include a gneissic basement. The shape of the bottom of the batholith also became more convex in the alternative model.

### ***Indian Lake Batholith***

- The survey area covers parts of the western and eastern portions of the Indian Lake batholith, a vast intrusive body bounded by the Raleigh Lake greenstone belt to the southwest and separated from the Basket Lake batholith by a band of tonalite to the northwest.

- The overall character of the reduced to pole magnetic field shows no clear distinction between the western portion of the Indian Lake batholith and the Basket Lake batholith, and one would not be able to determine the boundary between them from any indication given by the magnetic data alone. The broad pattern of consistent character encompasses all of the Basket Lake batholith and the northwestern portion of the Indian Lake batholith.
- The Bouguer gravity anomaly indicates that the shallowest part of the Indian Lake batholith may be located at the centre of the broad gravity high that occurs between the two principle survey areas.
- The western extent of the Indian Lake batholith is shallower than the Basket Lake batholith, and the 2.5D modelling indicates that the batholith shallows from a depth of approximately 3.0 km at its boundary with the tonalite in the northwest, to a depth of approximately 2.0 km where the 2.5D model line ends, at the eastern boundary of the larger of the two survey areas. In the central area of the batholith, another 2.5D model line runs from north to south, and shows that the batholith is significantly deeper here. From north to south, the bottom of the batholith has a depth of approximately 4.0 km. To the south of the model line the depth of the batholith plunges to 7.5 km. The inclusion of a shallow gneissic basement to a set of alternative 2.5D models resulted in modelled depths of the Indian Lake batholith interpreted to be significantly shallower. The shallowest portion of the batholith is modelled along the eastern part of Line 4, with an interpreted thickness of approximately 500 m. Similarly, the bottom of the batholith in the Line 5 has a depth of approximately 800 m in the northernmost part of the profile line. In addition, the southern portion of the Indian Lake batholith, shown on Line 5, is interpreted to have a depth of 8.0 km.

For the modelling results, it is important to emphasize that the accuracy of these preliminary models is limited at this early stage of the assessment due to limited availability of bedrock densities and magnetic susceptibilities that are key for constraining the model. It is anticipated that the preliminary 2.5D models would be revised and refined if more field data is collected in the future.

## 7 REFERENCES

- Baranov, V. and Naudy, H. 1964. Numerical Calculation of the Formula of Reduction to the Magnetic Pole. *Geophysics*, 29, pg. 67-79
- Berger, B.R., 1988. Geology of the Melgund Lake Area, District of Kenora; Ontario Geological Survey, Open File Report 5680, 184p., 24 figures, 10 tables, 9 photographs and maps P.3068, P.3069, and P.3070 in the back pocket.
- Bethune, K.M., H.H. Helmstaedt and V.J. McNicoll, 2006. Structural analysis of the Miniss River and related faults, western Superior Province: post-collisional displacement initiated at terrane boundaries; *Can. J. Earth Sci.* 43:p. 1031–1054
- Blackburn, C.E., Johns, G.W., Ayer, J.W. and Davis, D.W. 1991. Wabigoon Subprovince; in *Geology of Ontario*, Ontario Geological Survey, Special Volume 4, Part 1, 303-382.
- Blakely, R.J. 1996. *Potential Theory in Gravity and Magnetic Applications*. Cambridge University Press. pg 441
- Briggs, I.C., 1974, Machine contouring using minimum curvature, *Geophysics*, v. 39., no. 1, pp. 39-48.
- Brown, J.L. 2002. Neoproterozoic evolution of the western-central Wabigoon boundary zone, Brightsand Forest area, Ontario. Unpublished M.Sc. thesis, University of Ottawa, Ottawa.
- Buchan, K.L. and Ernst, R.E. 2004. Diabase dike swarms and related units in Canada and adjacent regions. Geological Survey of Canada, Map 2022A, scale 1:5,000,000.
- Buse, S., Stone, D., Lewis, D. and Hamilton, M.A., 2010, U/Pb Geochronology Results for the Atikokan Mineral Development Initiative, Ontario Geological Survey, Miscellaneous Release – data 275.
- Davis, D.W., 1989. Final Report for the Ontario Geological Survey on precise U-Pb age constraints on the tectonic evolution of the western Wabigoon subprovince, Superior Province, Ontario. Earth Science Department, Royal Ontario Museum, 30 p.
- Easton, R.M., 2000. Metamorphism of the Canadian Shield, Ontario, Canada. I. The Superior Province: *Canadian Mineralogist*, April 2000, v. 38, p.287-317.
- Easton, R.M., Hart, T.R., Hollings, P., Heaman, L.M., MacDonald, C.A. and Smyk, M., 2007. Further refinement of the timing of Mesoproterozoic magmatism, Lake Nipigon region, Ontario; *Canadian Journal of Earth Sciences*, 44, 1055-1086.
- Everitt, R.A., 1999. Experience gained from the geological characterisation of the Lac du Bonnet batholith, and comparison with other sparsely fractured granite batholiths in the Ontario portion of the Canadian Shield. OPG Report 06819-REP-01200-0069-R00. OPG. Toronto. Canada.
- Fahrig, W.F. and West, T.D. 1986. Diabase dike swarms of the Canadian Shield; Geological Survey of Canada, Map 1627A
- Geosoft, 2012. Oasis montaj geophysical processing system, v 7.5, Geosoft Inc.

- Golder (Golder Associates Ltd.), 2011. Initial Screening for Siting a Deep Geological Repository for Canada's Used Nuclear Fuel. The Corporation of the Township of Ignace, Ontario. Nuclear Waste Management Organization, March 2011.
- Golder (Golder Associates Ltd.), 2013. Phase 1 Desktop Geoscientific Preliminary Assessment of Potential Suitability for Siting a Deep Geological Repository for Canada's Used Nuclear Fuel, Township of Ignace, Ontario. Prepared for Nuclear Waste Management Organization (NWMO). NWMO Report Number: APM-REP-06144-0011
- Golder (Golder Associates Ltd.), 2015. Phase 2 Geoscientific Preliminary Assessment, Findings from Initial Field Studies, Township of Ignace, Ontario. Prepared for the Nuclear Waste Management Organization (NWMO), NWMO Report Number: APM-REP-06145-0001.
- Hanes, J.A. and D.A. Archibald. 1998. Post-orogenic tectonothermal history of the Archean western Superior Province of the Canadian Shield by conventional and laser Ar-Ar dating. Abstracts with programs - Geological Society of America, vol. 30(7), p.110-110.
- Haus, M. and Pauk, T., 2010, Data from the PETROCH Lithogeochemical database, Ontario Geological Survey, Miscellaneous Release – Data 250, ISBN 978-1-4435-3732-2 [CD] ISBN 978-1-4435-3731-5 [zip file].
- JDMA (J. D. Mollard and Associates Ltd.), 2013. Phase 1 Desktop Geoscientific Preliminary Assessment, Terrain and Remote Sensing Study, Township of Ignace, Ontario. Prepared for Nuclear Waste Management Organization (NWMO). NWMO Report Number: APM-REP-06144-0012.
- Leliak, P. (1961). Identification and evaluation of magnetic field sources of magnetic airborne detector equipped aircraft. IRE Transactions on Aerospace and Navigational Electronics, 8(3), 95-105.
- McLeod, I.N., 1993, 3-D Analytic Signal in the Interpretation of Total Magnetic Field Data at Low Magnetic Latitudes, Exploration Geophysics, v. 24, pp. 679-688.
- Miller, H.G., and Singh, V., 1994, Potential field tilt – a new concept for location of potential field sources, Journal of Applied Geophysics, v. 32, pp. 213-217.
- Muir, T. L., 2013, Ontario Precambrian bedrock magnetic susceptibility geodatabase for 2001 to 2012, Ontario Geological Survey, Miscellaneous Release – Data 273 – Revised.
- Nabighian, M.N. 1972. The analytic signal of two-dimensional magnetic bodies with polygonal cross-section: Its properties and use for automated anomaly interpretation. Geophysics, 37, 507-517.
- NWMO, 2010. Moving Forward Together: Process for Selecting a Site for Canada's Deep Geological Repository for Used Nuclear Fuel, Nuclear Waste Management Organization. (Available at [www.nwmo.ca](http://www.nwmo.ca))
- NWMO, 2013. Preliminary Assessment for Siting a Deep Geological Repository for Canada's Used Nuclear Fuel - Township of Ignace, Ontario - Findings from Phase One Studies. NWMO Report Number APM-REP-06144-0009.
- OGS (Ontario Geological Survey), 2011. 1:250 000 scale bedrock geology of Ontario, Miscellaneous

Release Data 126 - Revision 1.

- Osmani, I.A. 1991. Proterozoic mafic dike swarms in the Superior Province of Ontario; in *Geology of Ontario*, Ontario Geological Survey, Special Volume 4, Part 1, 661-681.
- Percival, J.A., McNicoll, V.J., Brown, J.L., and Whalen, J.B. 2004. Convergent margin tectonic, central Wabigoon subprovince, Superior Province, Canada. *Precambrian Research*, vol. 132, p. 213-244.
- Percival, J.A., Sanborn-Barrie M., Skulski, T., Stott, G.M., Helmstaedt, H., and White, D.J., 2006. Tectonic Evolution of the Western Superior Province from NATMAO and Lithoprobe Studies; *Canadian Journal of Earth Sciences*, v. 43, p. 1085-1117.
- Peterman, Z.E. and Day, W. 1989. Early Proterozoic activity on Archean faults in the western Superior Province: Evidence from pseudotachylite. *Geology*, vol. 17, p. 1089-1092
- PGW (Patterson, Grant and Watson Ltd.), 2013. Phase 1 Geoscientific Desktop Preliminary Assessment, Processing and Interpretation of Geophysical Data, Township of Ignace, Ontario. Prepared for Nuclear Waste Management Organization (NWMO). NWMO Report Number: APM-REP-06144-0013.
- Phillips, J.D., 1997, Potential-field geophysical software for the PC, version 2.2, U.S. Geological Survey Open-File Report 97-725.
- Phillips, J.D., 2000, Locating magnetic contacts: a comparison of the horizontal gradient, analytic signal, and local wavenumber methods, *Society of Exploration Geophysics, Expanded Abstracts with Biographies, 2000 Technical Program*, v. 1, pp. 402-405.
- Roest, W., and Pilkington, M., 1993, Identifying Remanent Magnetization Effects in Magnetic Data, *Geophysics*, v. 58, no. 5, pp. 653-659.
- Sage, R. P., Breaks, F.W., Stott, G.M., McWilliams, G.M. and Atkinson, S. 1974. Operation Ignace-Armstrong, Ignace-Graham Sheet, Districts of Thunder Bay, Kenora, and Rainy River; Ontario Division of Mines, Preliminary Map P. 964.
- Salem, A., Williams, S., Fairhead, J. D., Ravat, D., and Smith, R., 2007, Tilt-depth method: A Simple depth estimation method using first-order magnetic derivatives, *The Leading Edge*, 26, pp. 1502-1505.
- Sanborn-Barrie, M., and Skulski, T. 2006. Sedimentary and structural evidence for 2.7 Ga continental arc-oceanic-arc collision in the Savant-Sturgeon greenstone belt, western Superior Province, Canada. *Canadian Journal of Earth Sciences*, vol. 43, p. 995-1030.
- Schwerdtner, W.M., Stone, D., Osadetz, K., Morgan, J. and Stott, G.M. 1979. Granitoid complexes and the Archean tectonic record of the southern part of northwestern Ontario; *Canadian Journal of Earth Sciences*, vol.16, p.1965-1977.
- Southwick, D.L. and Halls, H. 1987. Compositional characteristics of the Kenora- Kabetogama dike swarm (Early Proterozoic), Minnesota and Ontario; *Canadian Journal of Earth Sciences*, 24, 2197-2205.

- SRK (SRK Consulting Inc.), 2015. Phase 2 Geoscientific Preliminary Assessment, Lineament Interpretation, Township of Ignace, Ontario. Prepared for Nuclear Waste Management Organization (NWMO). NWMO Report Number: APM-REP-06145-0003.
- Stone, D. 2009a, The Central Wabigoon Area, Ontario Geological Survey, poster, Northwest Ontario Mines and Minerals Symposium, Thunder Bay, Ontario, April 7-8, 2009.
- Stone, D. 2009b, Geology of the Bending Lake area, Northwestern Ontario, Ontario Geological Survey, poster, Ontario Exploration and Geoscience Symposium, Sudbury, December 15<sup>th</sup> 2009.
- Stone, D. 2010a, Precambrian geology of the central Wabigoon Subprovince area, northwestern Ontario, Ontario Geological Survey, Open File Report 5422, 130p.
- Stone, D., 2010b. Geology of the Stormy Lake Area, Northwestern Ontario, Project Unit 09-003 in Summary of Field Work and Other Activities 2010, Ontario Geological Survey, Open File Report 6260, p.13-1 to 13-12.
- Stone, D. and Hallé, J., 1999, Precambrian geology, Entwine Lake area, Ontario Geological Survey, Preliminary Map P3400, scale 1:50 000.
- Stone, D., B. Hellebrandt and M. Lange, 2011a. Precambrian geology of the Bending Lake area (north sheet); Ontario Geological Survey, Preliminary Map P.3623, scale 1:20 000.
- Stone, D., B. Hellebrandt and M. Lange, 2011b. Precambrian geology of the Bending Lake area (south sheet); Ontario Geological Survey, Preliminary Map P.3624, scale 1:20 000.
- Stone, D., D.W. Davis, M.A. Hamilton and A. Falcon, 2010. Interpretation of 2009 Geochronology in the Central Wabigoon Subprovince and Bending Lake Areas, Northwestern Ontario, Project Unit 09-003. Summary of Field Work and Other Activities 2010, Ontario Geological Survey, Open File Report 6260, p.14-1 to 14-13.
- Stone, D., G. Paju and E. Smyk, 2011c. Precambrian geology of the Stormy Lake area; Ontario Geological Survey, Preliminary Map P.2515, scale 1:20 000
- Stone, D., Hallé, J. and Chaloux, E., 1998, Precambrian geology, Pekagoning Lake area, Ontario Geological Survey, Preliminary Map P3386, scale 1:50 000.
- Stone, D., Hellebrandt, B. and Lange, M., 2011a, Precambrian geology of the Bending Lake area (north sheet), Ontario Geological Survey, Preliminary Map P3623, scale 1:20 000.
- Stone, D., J. Halle, M. Lange, B. Hellebrandt and E. Chaloux, 2007a. Precambrian Geology, Ignace Area; Ontario Geological Survey, Preliminary Map P.3360—Revised, scale 1:50 000
- Stone, D., J. Halle, M. Lange, B. Hellebrandt and E. Chaloux, 2007b. Precambrian Geology, Ignace Area; Ontario Geological Survey, Preliminary Map P.3360—Revised, scale 1:50 000
- Szewczyk, Z.J. and West, G.F. 1976. Gravity study of an Archean granitic area northwest of Ignace, Ontario Canadian Journal of Earth Sciences 13, 1119-1130.

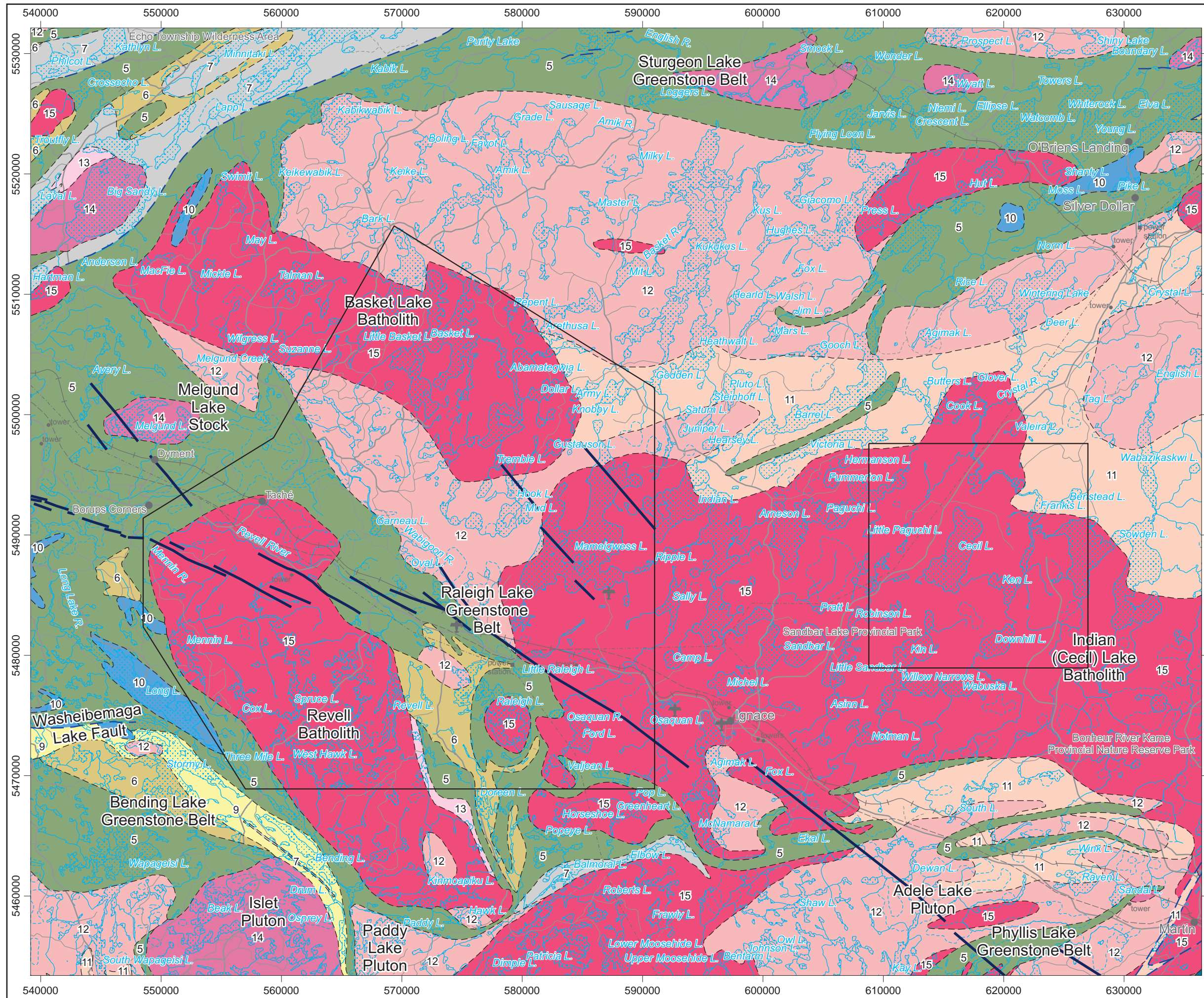
- Telford, W.M.; Geldart, L.P.; Sheriff, R.E. 1990. Applied Geophysics. 2nd edition. Cambridge university press. pg 770
- Tomlinson, K.Y., Stott, G.M., Percival, J.A. and Stone, D. 2004. Basement terrane correlations and crustal recycling in the western Superior Province: Nd isotopic character of granitoid and felsic volcanic rocks in the Wabigoon Subprovince, N. Ontario, Canada; Precambrian Research, vol.132, p. 245-274.
- Verduzco B., Fairhead J.D., Green C.M. and MacKenzie C., (2004), New insights into magnetic derivatives for structural mapping, The Leading Edge, p. 116-119.

## 8 FIGURES

- 1.1 Survey Area
- 1.2 Flight Lines
- 3.1 Digital Elevation Model (25m cell)
- 4.1 Bouguer Gravity (Density:  $2.67\text{g/cm}^3$ ) (25 m cell)
- 4.2 Bouguer Gravity (Density:  $2.67\text{g/cm}^3$ ) (250 m cell)
- 4.3 Free Air Gravity (25 m cell)
- 4.4 Free Air Gravity (250 m cell)
- 4.5 Total Magnetic Intensity (25 m cell)
- 4.6 Total Magnetic Intensity (250 m cell)
- 4.7 Reduction to the Pole of the Total Magnetic Intensity (25 m cell)
- 4.8 Reduction to the Pole of the Total Magnetic Intensity (250 m cell)
- 4.9 First Vertical Derivative of the Reduction to the Pole of the Total Magnetic Intensity (25 m cell)
- 4.10 First Vertical Derivative of the Reduction to the Pole of the Total Magnetic Intensity (250 m cell)
- 4.11 First Vertical Derivative of the Bouguer Gravity (Density:  $2.67\text{g/cm}^3$ ) (25 m cell)
- 4.12 First Vertical Derivative of the Bouguer Gravity (Density:  $2.67\text{g/cm}^3$ ) (250 m cell)
- 4.13 First Vertical Derivative of the Free Air Gravity (25 m cell)
- 4.14 First Vertical Derivative of the Free Air Gravity (250 m cell)
- 4.15 Second Vertical Derivative of the Reduction to the Pole of the Total Magnetic Intensity (25 m cell)
- 4.16 Second Vertical Derivative of the Reduction to the Pole of the Total Magnetic Intensity (250 m cell)
- 4.17 Total Horizontal Derivative of the Reduction to the Pole of the Total Magnetic Intensity (25 m cell)

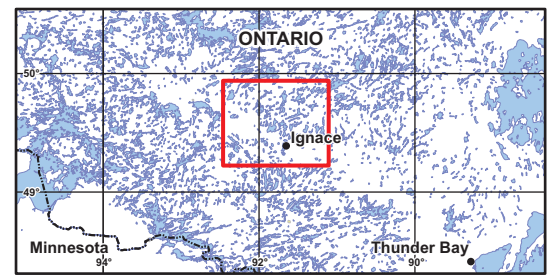
- 4.18 Total Horizontal Derivative of the Reduction to the Pole of the Total Magnetic Intensity (250 m cell)
- 4.19 Total Horizontal Derivative of the Bouguer Gravity (Density: 2.67g/cm<sup>3</sup>) (25 m cell)
- 4.20 Total Horizontal Derivative of the Bouguer Gravity (Density: 2.67g/cm<sup>3</sup>) (250 m cell)
- 4.21 Total Horizontal Derivative of the Free Air Gravity (25 m cell)
- 4.22 Total Horizontal Derivative of the Free Air Gravity (250 m cell)
- 4.23 Analytic Signal of the Total Magnetic Intensity (25 m cell)
- 4.24 Analytic Signal of the Total Magnetic Intensity (250 m cell)
- 4.25 Tilt Angle of the Reduction to the Pole of the Total Magnetic Intensity (25 m cell)
- 4.26 Tilt Angle of the Reduction to the Pole of the Total Magnetic Intensity (250 m cell)
- 4.27 Trend Analysis Solutions of Bouguer Gravity (terrain correction density = 2.67 g/cm<sup>3</sup>)
- 4.28 Trend Analysis Solutions of Reduction to the Pole of the Total Magnetic Intensity
- 5.1 Horizontal Derivative of Bouguer Gravity (terrain correction density = 2.67 g/cm<sup>3</sup>) with Selected Interpreted Features
- 5.2 First Vertical Derivative of the Total Magnetic Intensity with Selected Interpreted Features
- 5.3 Reduction to the Pole of the Total Magnetic Intensity with Selected Interpreted Features
- 5.4 Total Horizontal Derivative of the Reduction to the Pole of the Total Magnetic Intensity with Selected Interpreted Features
- 5.5 Location of 2.5D Model Lines shown with Reduction to the Pole of the Total Magnetic Intensity
- 5.6 Location of 2.5D Model Lines shown with Free Air Gravity
- 5.7 Forward Modeling Results: Line 1, Model 1.6, Ignace Ontario
- 5.8 Forward Modeling Results: Line 1, Model 1.5, Ignace Ontario
- 5.9 Forward Modeling Results: Line 2, Model 2.3, Ignace Ontario
- 5.10 Forward Modeling Results: Line 2, Model 2.5, Ignace Ontario
- 5.11 Forward Modeling Results: Line 3, Model 3.3.4, Ignace Ontario

- 5.12 Forward Modeling Results: Line 3, Model 3.5, Ignace Ontario
- 5.13 Forward Modeling Results: Line 4, Model 4.3.3, Ignace Ontario
- 5.14 Forward Modeling Results: Line 4, Model 4.5.2, Ignace Ontario
- 5.15 Forward Modeling Results: Line 5, Model 5.2, Ignace Ontario
- 5.16 Forward Modeling Results: Line 5, Model 5.3, Ignace Ontario
- 5.17 Forward Modeling Results: Line 5, Model 5.5, Ignace Ontario



- Legend**
- Hydrography
  - Road
  - Railway
- Geology**
- Fault
  - Dyke
- 3: Mafic metavolcanic and metasedimentary rocks
  - 5: Mafic to intermediate metavolcanic rocks
  - 6: Felsic to intermediate metavolcanic rocks
  - 7: Metasedimentary rocks
  - 9: Coarse clastic metasedimentary rocks
  - 10: Mafic and ultramafic rocks
  - 11: Gneissic tonalite suite
  - 12: Foliated tonalite suite
  - 13: Muscovite-bearing granite rock
  - 14: Diorite-monzodiorite-granodiorite suite
  - 15: Massive granodiorite suite
  - 16: Hornblende - nepheline syenite suite

Survey Area Boundary



BASE DATA: National Topographic Database - NRCAN  
 GEOLOGY DATA: OGS Dataset MRD 126-Rev 1  
 DATUM: NAD83  
 PROJECTION: Universal Transverse Mercator (UTM Zone 15N)



**Airborne Geophysics  
 Acquisition and Interpretation**

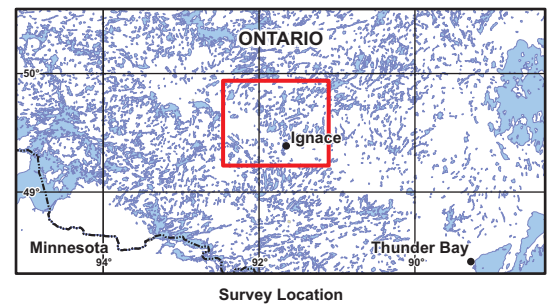
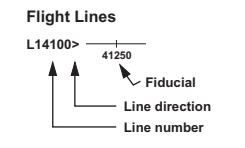
**Ignace Area, Ontario 2014**

**Survey Area**

	DESIGN	JK	29/01/2015	REV. 1.1
	GIS	YC, AP	06/02/2015	<b>FIGURE: 1.1</b>
	DATA	MM, DK	06/02/2015	
	QC	MB	06/02/2015	



- Legend**
- Hydrography
  - Road
  - Railway
- Geology**
- Fault
  - Dyke
- 3: Mafic metavolcanic and metasedimentary rocks
  - 5: Mafic to intermediate metavolcanic rocks
  - 6: Felsic to intermediate metavolcanic rocks
  - 7: Metasedimentary rocks
  - 9: Coarse clastic metasedimentary rocks
  - 10: Mafic and ultramafic rocks
  - 11: Gneissic tonalite suite
  - 12: Foliated tonalite suite
  - 13: Muscovite-bearing granite rock
  - 14: Diorite-monzodiorite-granodiorite suite
  - 15: Massive granodiorite suite
  - 16: Hornblende - nepheline syenite suite



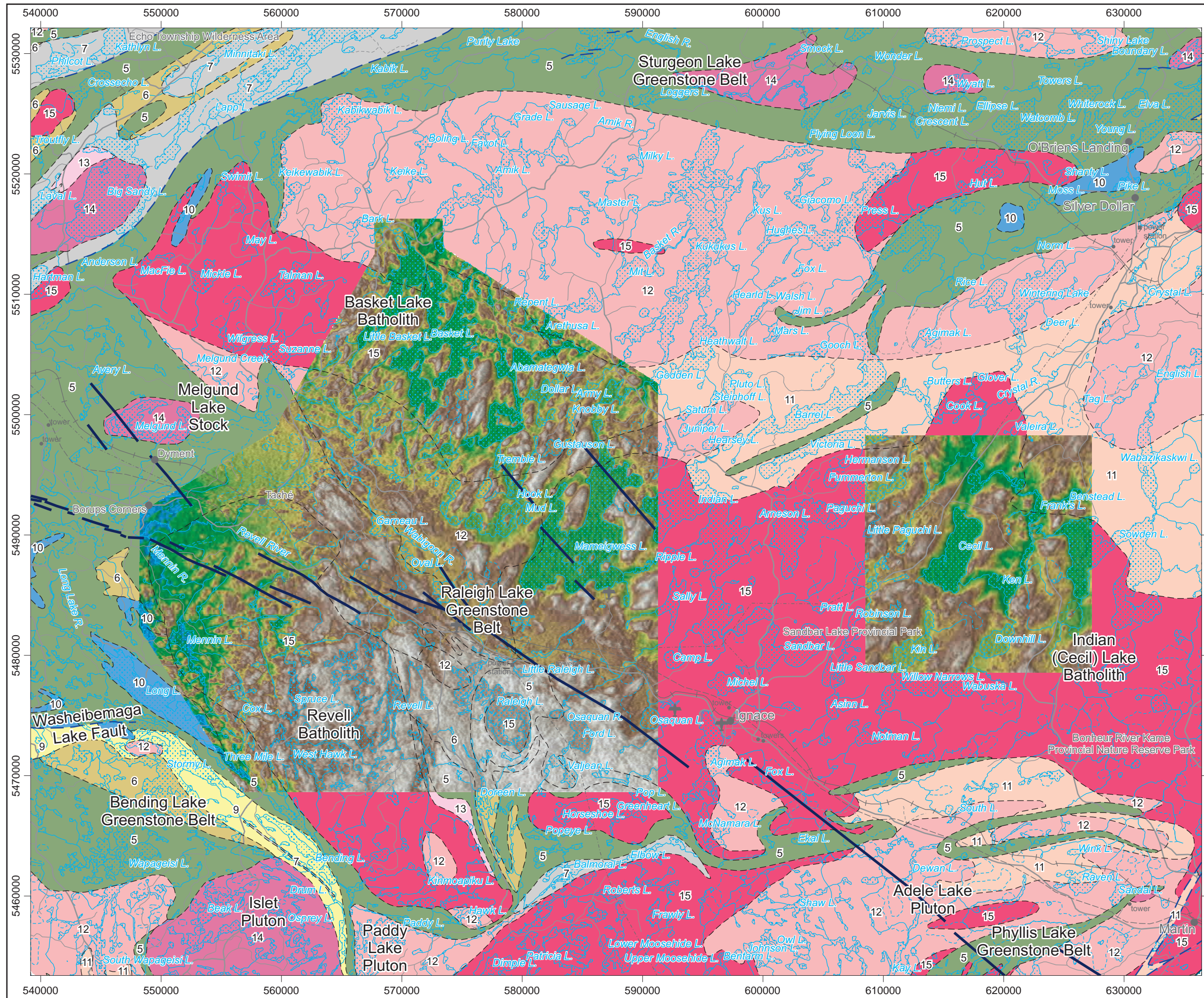
BASE DATA: National Topographic Database - NRCAN  
 GEOLOGY DATA: OGS Dataset MRD 126-Rev 1  
 DATUM: NAD83  
 PROJECTION: Universal Transverse Mercator (UTM Zone 15N)



**Airborne Geophysics  
 Acquisition and Interpretation**  
 Ignace Area, Ontario 2014

**Flight Lines**

	DESIGN	JK	29/01/2015	REV. 1.1
	GIS	YC, AP	06/02/2015	<b>FIGURE: 1.2</b>
	DATA	MM, DK	06/02/2015	
	QC	MB	06/02/2015	



**Legend**

Hydrography .....

Road .....

Railway .....

**Geology**

Fault .....

Dyke .....

**Map Parameters**

Illumination: inclination 50°, declination 270°

**Legend**

3: Mafic metavolcanic and metasedimentary rocks

5: Mafic to intermediate metavolcanic rocks

6: Felsic to intermediate metavolcanic rocks

7: Metasedimentary rocks

9: Coarse clastic metasedimentary rocks

10: Mafic and ultramafic rocks

11: Gneissic tonalite suite

12: Foliated tonalite suite

13: Muscovite-bearing granite rock

14: Diorite-monzodiorite-granodiorite suite

15: Massive granodiorite suite

16: Hornblende - nepheline syenite suite

**Elevation Legend**

533.6

483.3

475.5

469.6

465.0

461.2

457.9

455.2

452.8

451.2

449.4

447.4

445.5

443.9

442.2

440.7

439.2

437.8

436.6

435.3

434.1

433.0

431.9

430.9

429.9

428.9

427.8

426.8

425.7

424.7

423.5

422.2

420.9

419.5

418.2

416.9

415.6

414.7

413.3

411.5

409.9

408.4

406.6

405.4

404.8

404.2

403.5

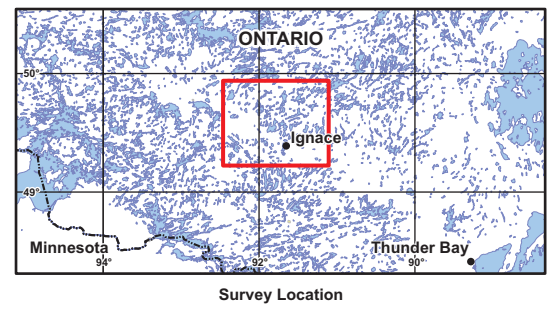
402.0

398.2

392.1

365.3

m



BASE DATA: National Topographic Database - NRCAN  
 GEOLOGY DATA: OGS Dataset MRD 126-Rev 1  
 DATUM: NAD83  
 PROJECTION: Universal Transverse Mercator (UTM Zone 15N)

Scale 1 : 310 000

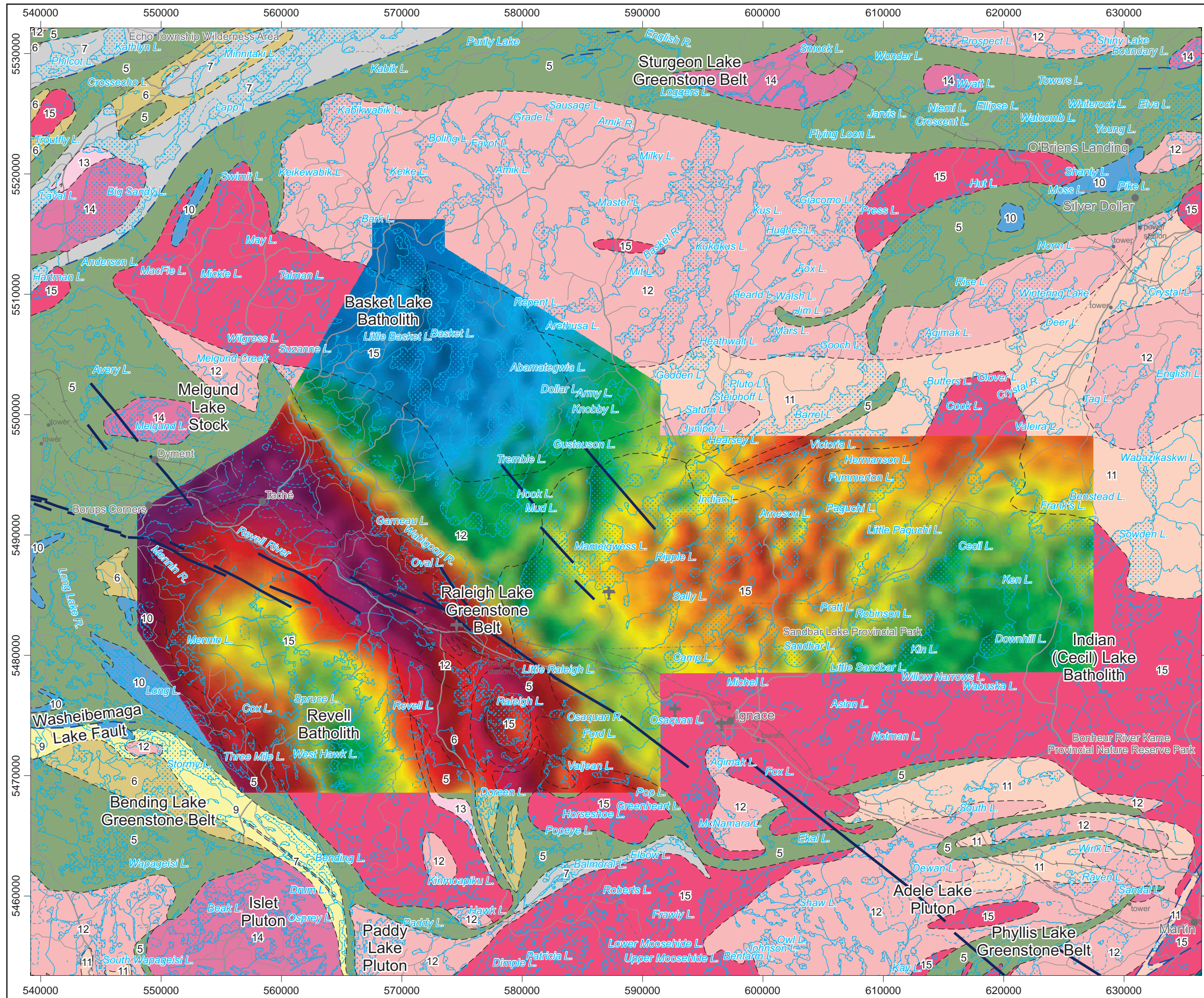
km 5 0 5 10 km

**Airborne Geophysics  
 Acquisition and Interpretation**

**Ignace Area, Ontario 2014**

**Digital Elevation Model (25 m cell)**

	DESIGN	JK	29/01/2015	REV. 1.1
	GIS	YC, AP	06/02/2015	<b>FIGURE: 3.1</b>
	DATA	MM, DK	06/02/2015	
	QC	MB	06/02/2015	



**Legend**

Hydrography .....

Road .....

Railway .....

**Geology**

Fault .....

Dyke .....

3: Mafic metavolcanic and metasedimentary rocks

5: Mafic to intermediate metavolcanic rocks

6: Felsic to intermediate metavolcanic rocks

7: Metasedimentary rocks

9: Coarse clastic metasedimentary rocks

10: Mafic and ultramafic rocks

11: Gneissic tonalite suite

12: Foliated tonalite suite

13: Muscovite-bearing granite rock

14: Diorite-monzodiorite-granodiorite suite

15: Massive granodiorite suite

16: Hornblende - nepheline syenite suite

**Map Parameters**

Illumination: inclination 50°, declination 270°

Spatial Filter (half-wavelength): 1000 m

Bouguer Density: 2.67 g/cm<sup>3</sup>

mGal

-44.0

-51.8

-55.6

-58.1

-60.8

-62.5

-63.8

-64.8

-66.0

-67.2

-68.5

-69.8

-70.8

-71.6

-72.0

-72.4

-72.7

-73.0

-73.2

-73.4

-73.7

-73.9

-74.2

-74.4

-74.7

-74.9

-75.1

-75.3

-75.5

-75.8

-76.0

-76.2

-76.4

-76.6

-76.8

-77.0

-77.1

-77.3

-77.5

-77.8

-78.0

-78.3

-78.6

-79.2

-80.3

-81.4

-83.0

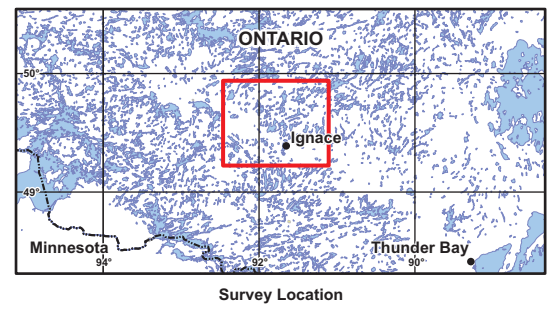
-84.2

-85.2

-86.1

-87.0

-89.2



BASE DATA: National Topographic Database - NRCAN

GEOLOGY DATA: OGS Dataset MRD 126-Rev 1

DATUM: NAD83

PROJECTION: Universal Transverse Mercator (UTM Zone 15N)

Scale 1 : 310 000

km 5 0 5 10 km

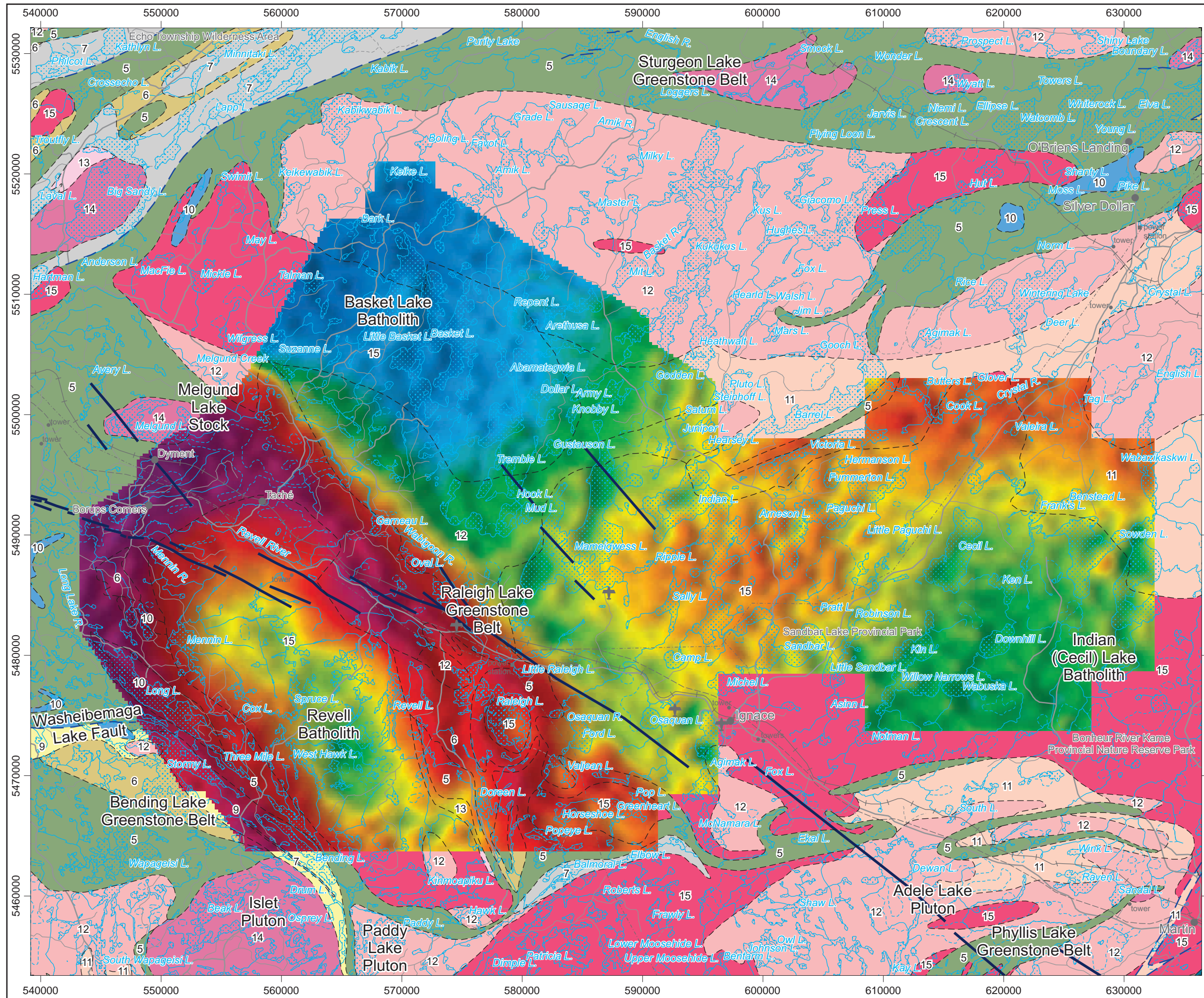
**Airborne Geophysics**

**Acquisition and Interpretation**

**Ignace Area, Ontario 2014**

**Bouguer Gravity (Density: 2.67 g/cm<sup>3</sup>) (25 m cell)**

	DESIGN	JK	29/01/2015	REV. 1.1
	GIS	YC, AP	06/02/2015	<b>FIGURE: 4.1</b>
	DATA	MM, DK	06/02/2015	
	QC	MB	06/02/2015	



**Legend**

Hydrography .....

Road .....

Railway .....

**Geology**

Fault .....

Dyke .....

- 3: Mafic metavolcanic and metasedimentary rocks
- 5: Mafic to intermediate metavolcanic rocks
- 6: Felsic to intermediate metavolcanic rocks
- 7: Metasedimentary rocks
- 9: Coarse clastic metasedimentary rocks
- 10: Mafic and ultramafic rocks
- 11: Gneissic tonalite suite
- 12: Foliated tonalite suite
- 13: Muscovite-bearing granite rock
- 14: Diorite-monzodiorite-granodiorite suite
- 15: Massive granodiorite suite
- 16: Hornblende - nepheline syenite suite

**Map Parameters**

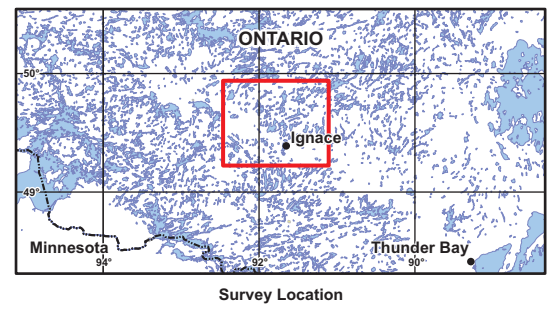
Illumination: inclination 50°, declination 270°

Spatial Filter (half-wavelength): 1000 m

Bouguer Density: 2.67 g/cm<sup>3</sup>

mGal

-38.3  
-47.1  
-50.4  
-54.3  
-56.5  
-58.8  
-61.2  
-63.0  
-64.4  
-65.7  
-67.1  
-68.4  
-69.4  
-70.1  
-70.8  
-71.4  
-71.9  
-72.4  
-72.8  
-73.1  
-73.6  
-73.9  
-74.2  
-74.5  
-74.8  
-75.0  
-75.2  
-75.5  
-75.8  
-76.0  
-76.2  
-76.5  
-76.7  
-77.0  
-77.3  
-77.5  
-77.7  
-78.0  
-78.3  
-78.6  
-79.1  
-79.7  
-80.8  
-82.3  
-83.7  
-84.8  
-85.9  
-86.7  
-87.8  
-90.0



BASE DATA: National Topographic Database - NRCAN  
 GEOLOGY DATA: OGS Dataset MRD 126-Rev 1  
 DATUM: NAD83  
 PROJECTION: Universal Transverse Mercator (UTM Zone 15N)

Scale 1 : 310 000

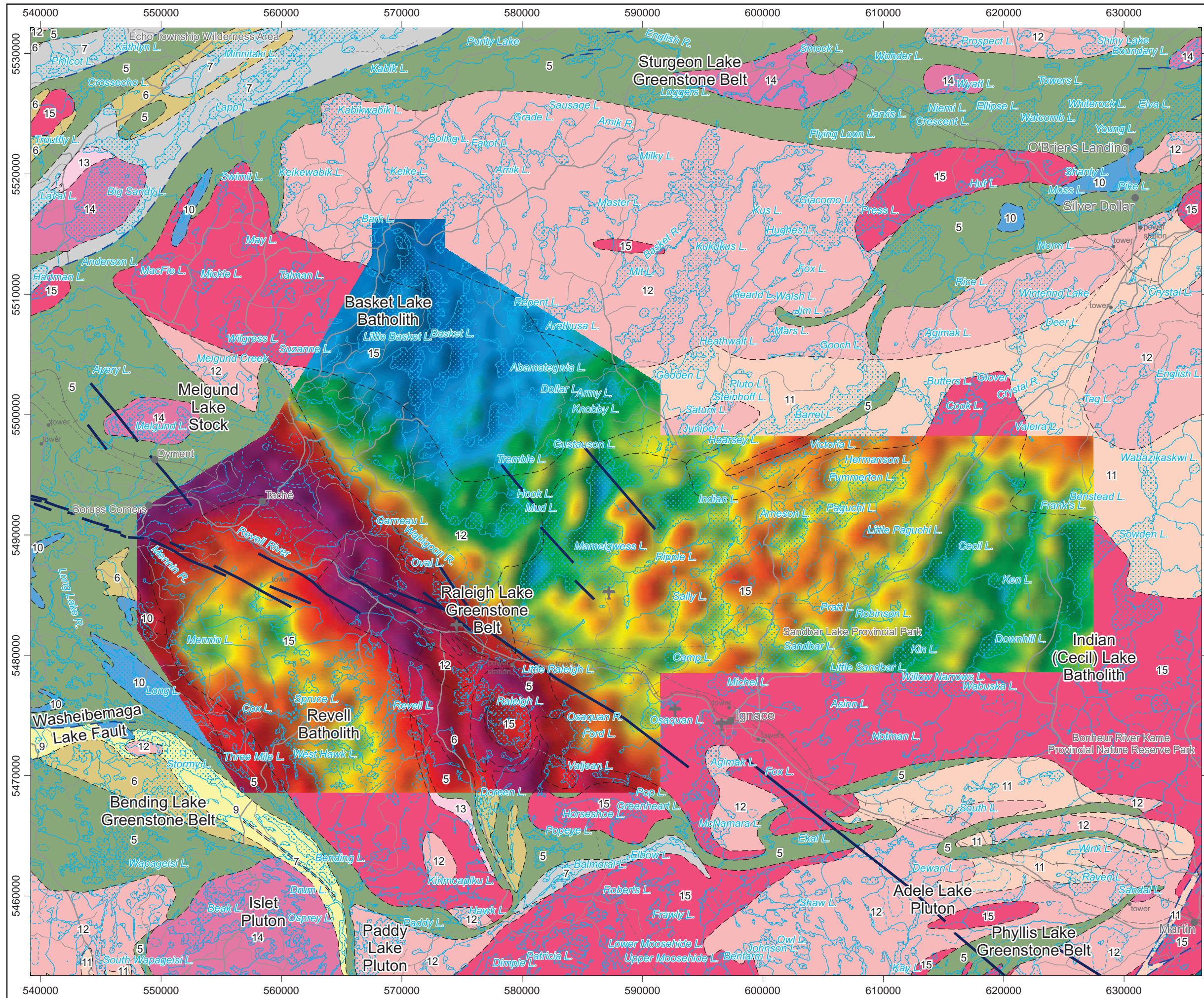
km 5 0 5 10 km

**Airborne Geophysics  
 Acquisition and Interpretation**

**Ignace Area, Ontario 2014**

**Bouguer Gravity (Density: 2.67 g/cm<sup>3</sup>) (250 m cell)**

	DESIGN	JK	29/01/2015	REV. 1.1
	GIS	YC, AP	06/02/2015	<b>FIGURE: 4.2</b>
	DATA	MM, DK	06/02/2015	
	QC	MB	06/02/2015	



**Legend**

Hydrography .....

Road .....

Railway .....

**Geology**

Fault .....

Dyke .....

3: Mafic metavolcanic and metasedimentary rocks

5: Mafic to intermediate metavolcanic rocks

6: Felsic to intermediate metavolcanic rocks

7: Metasedimentary rocks

9: Coarse clastic metasedimentary rocks

10: Mafic and ultramafic rocks

11: Gneissic tonalite suite

12: Foliated tonalite suite

13: Muscovite-bearing granite rock

14: Diorite-monzodiorite-granodiorite suite

15: Massive granodiorite suite

16: Hornblende - nepheline syenite suite

**Map Parameters**

Illumination: inclination 50°, declination 270°

Spatial Filter (half-wavelength): 1000 m

mGal

-3.4

-7.4

-9.0

-11.1

-13.6

-15.0

-16.5

-17.9

-19.5

-20.7

-21.9

-23.3

-24.5

-25.4

-26.0

-26.6

-27.0

-27.4

-27.7

-28.0

-28.2

-28.5

-28.7

-28.9

-29.2

-29.5

-29.7

-29.9

-30.2

-30.4

-30.6

-30.9

-31.2

-31.8

-32.1

-32.5

-32.9

-33.3

-33.7

-34.1

-34.5

-35.1

-35.7

-37.0

-38.6

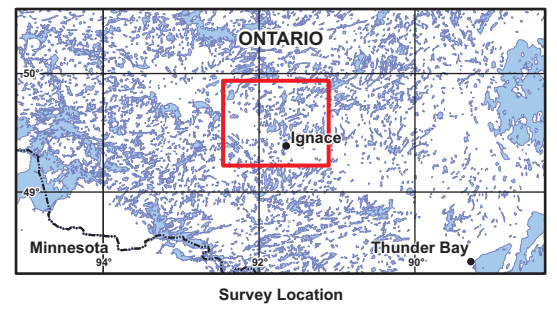
-39.6

-41.0

-42.3

-43.5

-46.6



BASE DATA: National Topographic Database - NRCAN  
 GEOLOGY DATA: OGS Dataset MRD 126-Rev 1  
 DATUM: NAD83  
 PROJECTION: Universal Transverse Mercator (UTM Zone 15N)

Scale 1 : 310 000

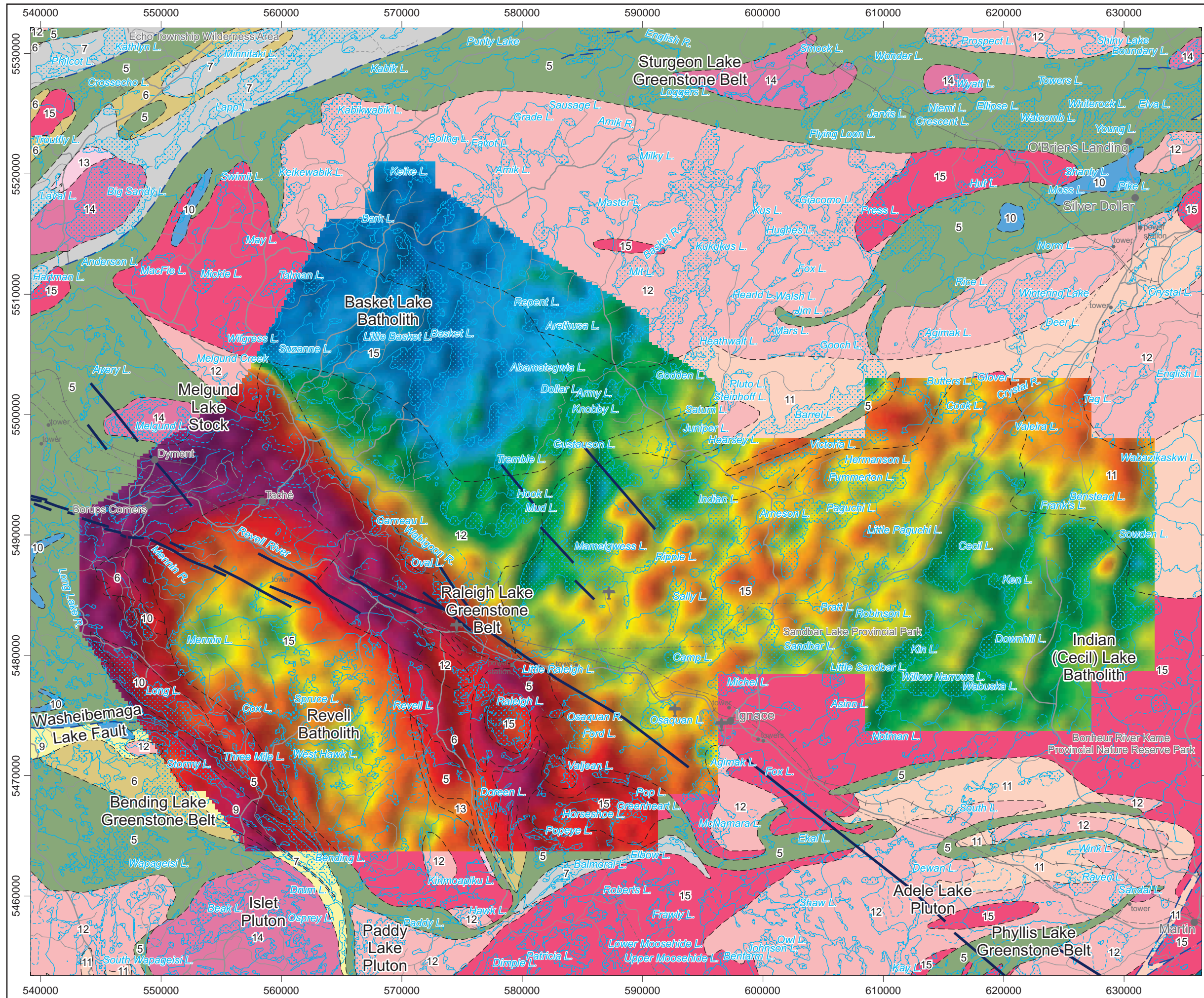
km 5 0 5 10 km

**Airborne Geophysics  
 Acquisition and Interpretation**

**Ignace Area, Ontario 2014**

**Free Air Gravity (25 m cell)**

	DESIGN	JK	29/01/2015	REV. 1.1
	GIS	YC, AP	06/02/2015	<b>FIGURE: 4.3</b>
	DATA	MM, DK	06/02/2015	
	QC	MB	06/02/2015	



**Legend**

Hydrography .....

Road .....

Railway .....

**Geology**

Fault .....

Dyke .....

3: Mafic metavolcanic and metasedimentary rocks

5: Mafic to intermediate metavolcanic rocks

6: Felsic to intermediate metavolcanic rocks

7: Metasedimentary rocks

9: Coarse clastic metasedimentary rocks

10: Mafic and ultramafic rocks

11: Gneissic tonalite suite

12: Foliated tonalite suite

13: Muscovite-bearing granite rock

14: Diorite-monzodiorite-granodiorite suite

15: Massive granodiorite suite

16: Hornblende - nepheline syenite suite

**Map Parameters**

Illumination: inclination 50°, declination 270°

Spatial Filter (half-wavelength): 1000 m

mGal

5.7

-5.1

-7.4

-9.1

-11.0

-13.1

-14.7

-16.0

-17.3

-18.6

-19.9

-21.1

-22.6

-23.9

-24.8

-25.5

-26.1

-26.6

-27.0

-27.4

-27.7

-28.0

-28.2

-28.5

-28.8

-29.1

-29.4

-29.7

-30.0

-30.3

-30.6

-30.9

-31.2

-31.6

-31.9

-32.3

-32.7

-33.1

-33.5

-34.0

-34.4

-34.9

-35.5

-36.6

-38.0

-39.3

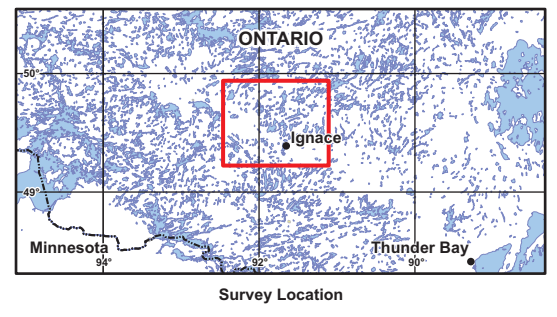
-40.6

-42.0

-43.2

-44.2

-47.7



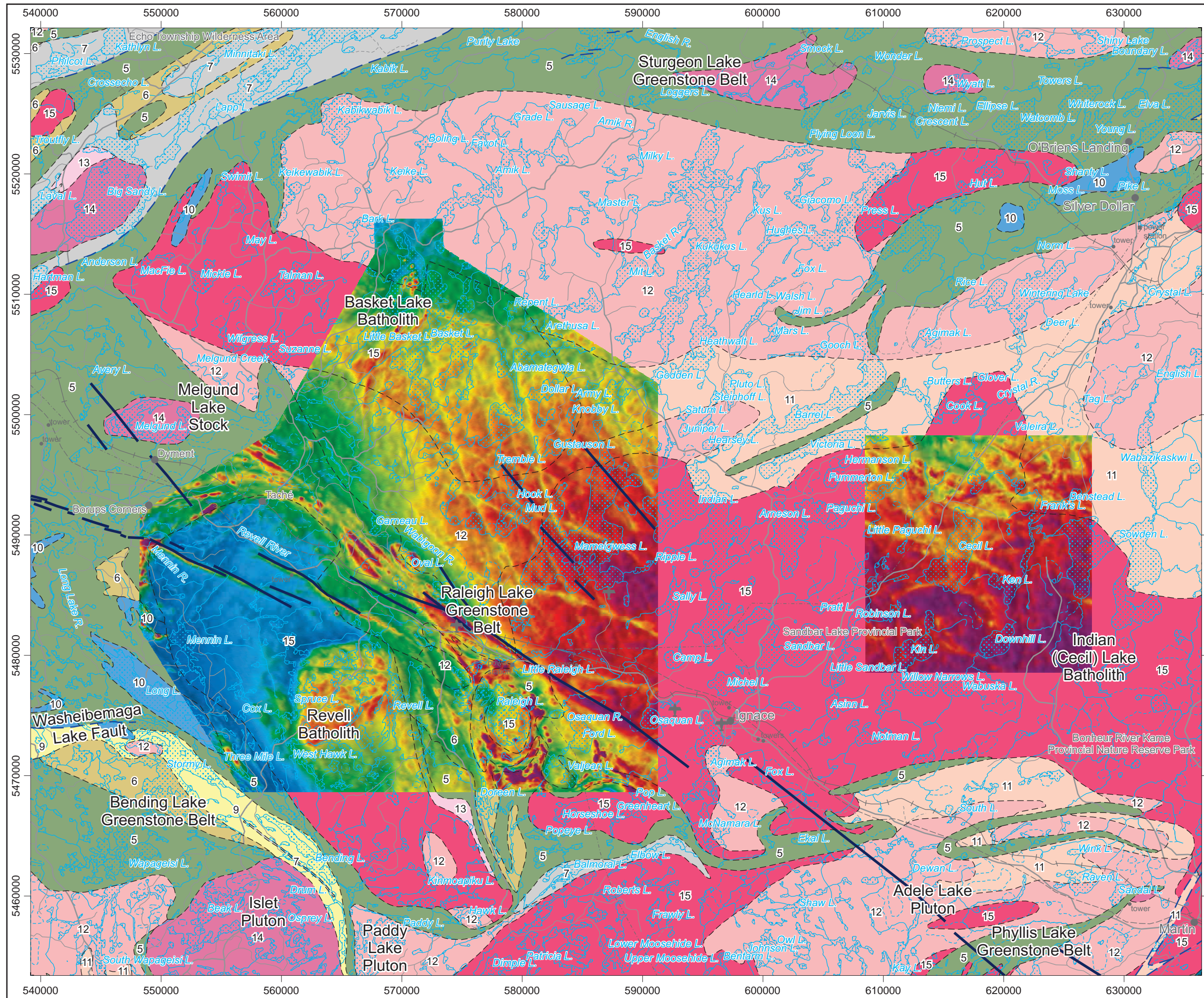
BASE DATA: National Topographic Database - NRCAN  
 GEOLOGY DATA: OGS Dataset MRD 126-Rev 1  
 DATUM: NAD83  
 PROJECTION: Universal Transverse Mercator (UTM Zone 15N)



**Airborne Geophysics**  
**Acquisition and Interpretation**  
 Ignace Area, Ontario 2014

**Free Air Gravity (250 m cell)**

	DESIGN	JK	29/01/2015	REV. 1.1
	GIS	YC, AP	06/02/2015	<b>FIGURE: 4.4</b>
	DATA	MM, DK	06/02/2015	
	QC	MB	06/02/2015	



**Legend**

Hydrography .....

Road .....

Railway .....

**Geology**

Fault .....

Dyke .....

3: Mafic metavolcanic and metasedimentary rocks

5: Mafic to intermediate metavolcanic rocks

6: Felsic to intermediate metavolcanic rocks

7: Metasedimentary rocks

9: Coarse clastic metasedimentary rocks

10: Mafic and ultramafic rocks

11: Gneissic tonalite suite

12: Foliated tonalite suite

13: Muscovite-bearing granite rock

14: Diorite-monzodiorite-granodiorite suite

15: Massive granodiorite suite

16: Hornblende - nepheline syenite suite

**Map Parameters**

Illumination: inclination 50°, declination 270°

nT

2532.4

67.8

36.5

18.8

6.9

-3.4

-12.6

-20.9

-28.3

-35.4

-42.4

-49.3

-55.9

-62.1

-68.3

-74.1

-79.6

-84.8

-90.0

-95.2

-100.1

-104.9

-109.8

-114.5

-119.4

-124.2

-128.8

-133.6

-138.7

-143.9

-149.1

-154.6

-160.3

-166.4

-173.2

-180.3

-187.3

-194.4

-201.9

-210.8

-220.6

-231.0

-242.6

-256.4

-271.9

-288.0

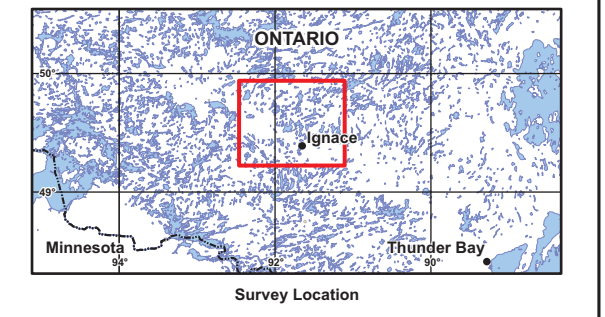
-300.1

-310.0

-319.6

-335.7

-445.0



BASE DATA: National Topographic Database - NRCAN  
 GEOLOGY DATA: OGS Dataset MRD 126-Rev 1  
 DATUM: NAD83  
 PROJECTION: Universal Transverse Mercator (UTM Zone 15N)

Scale 1 : 310 000

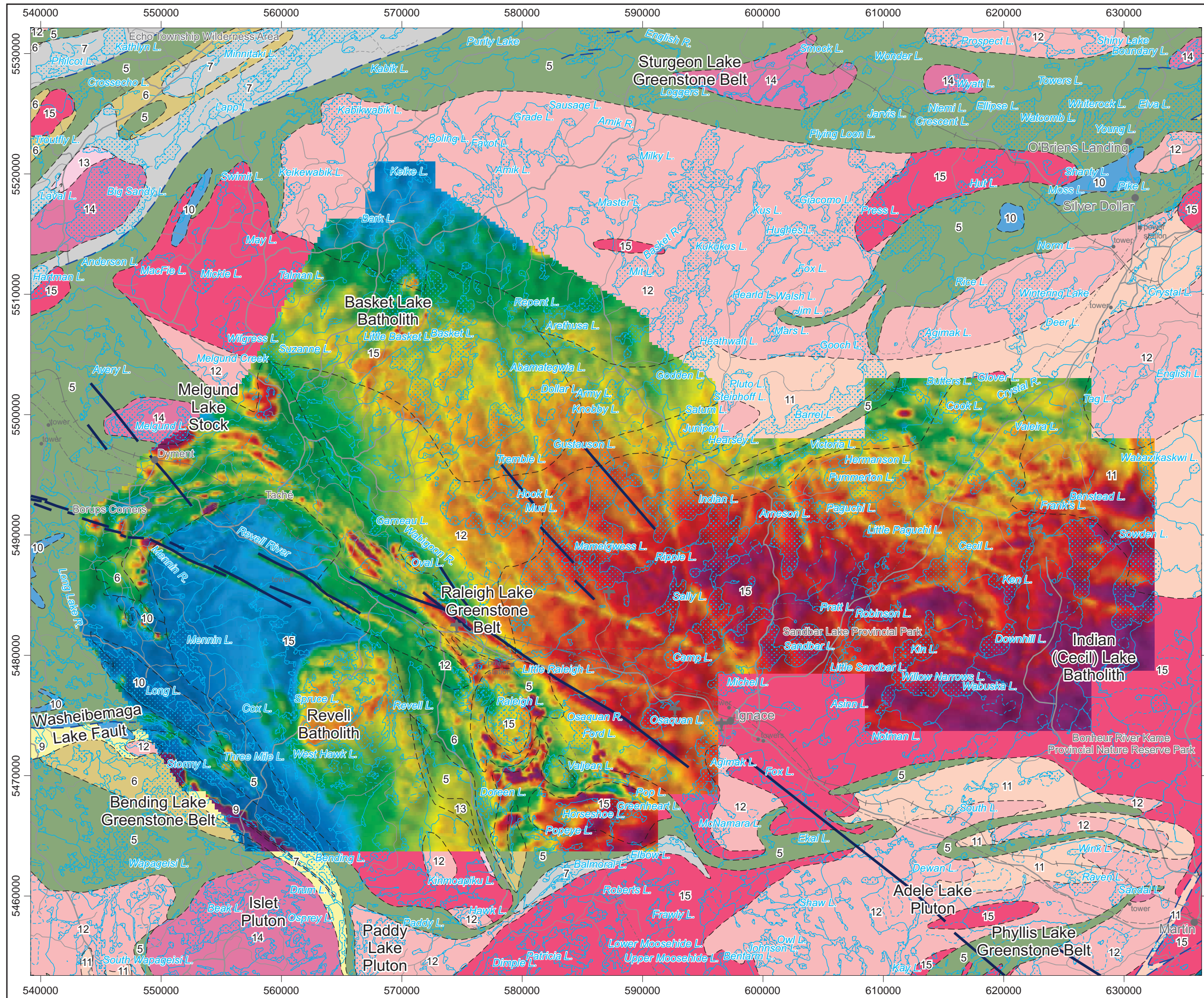
km 5 0 5 10 km

**Airborne Geophysics  
 Acquisition and Interpretation**

**Ignace Area, Ontario 2014**

**Total Magnetic Intensity (25 m cell)**

	DESIGN	JK	29/01/2015	REV. 1.1
	GIS	YC, AP	06/02/2015	<b>FIGURE: 4.5</b>
	DATA	MM, DK	06/02/2015	
	QC	MB	06/02/2015	



**Legend**

Hydrography .....

Road .....

Railway .....

**Geology**

Fault .....

Dyke .....

3: Mafic metavolcanic and metasedimentary rocks

5: Mafic to intermediate metavolcanic rocks

6: Felsic to intermediate metavolcanic rocks

7: Metasedimentary rocks

9: Coarse clastic metasedimentary rocks

10: Mafic and ultramafic rocks

11: Gneissic tonalite suite

12: Foliated tonalite suite

13: Muscovite-bearing granite rock

14: Diorite-monzodiorite-granodiorite suite

15: Massive granodiorite suite

16: Hornblende - nepheline syenite suite

**Map Parameters**

Illumination: inclination 50°, declination 270°

nT

23444.3

132.7

83.8

58.8

41.1

28.4

17.8

8.5

-0.2

-7.9

-15.6

-22.8

-30.1

-37.4

-45.3

-53.3

-60.8

-68.5

-75.8

-82.5

-89.1

-95.7

-101.8

-107.8

-113.4

-119.0

-124.4

-129.7

-135.1

-140.7

-146.0

-151.4

-157.1

-162.8

-169.1

-175.8

-183.3

-190.9

-199.1

-208.8

-219.0

-229.0

-241.1

-254.2

-268.6

-286.0

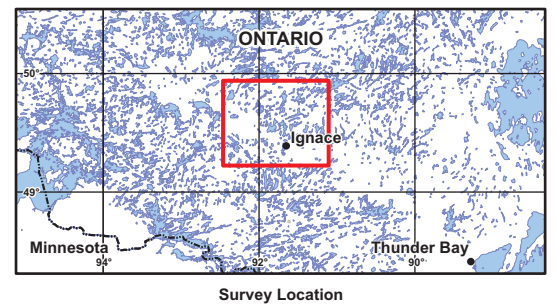
-301.0

-314.0

-329.5

-363.9

-2223.8



BASE DATA: National Topographic Database - NRCAN  
 GEOLOGY DATA: OGS Dataset MRD 126-Rev 1  
 DATUM: NAD83  
 PROJECTION: Universal Transverse Mercator (UTM Zone 15N)

Scale 1 : 310 000

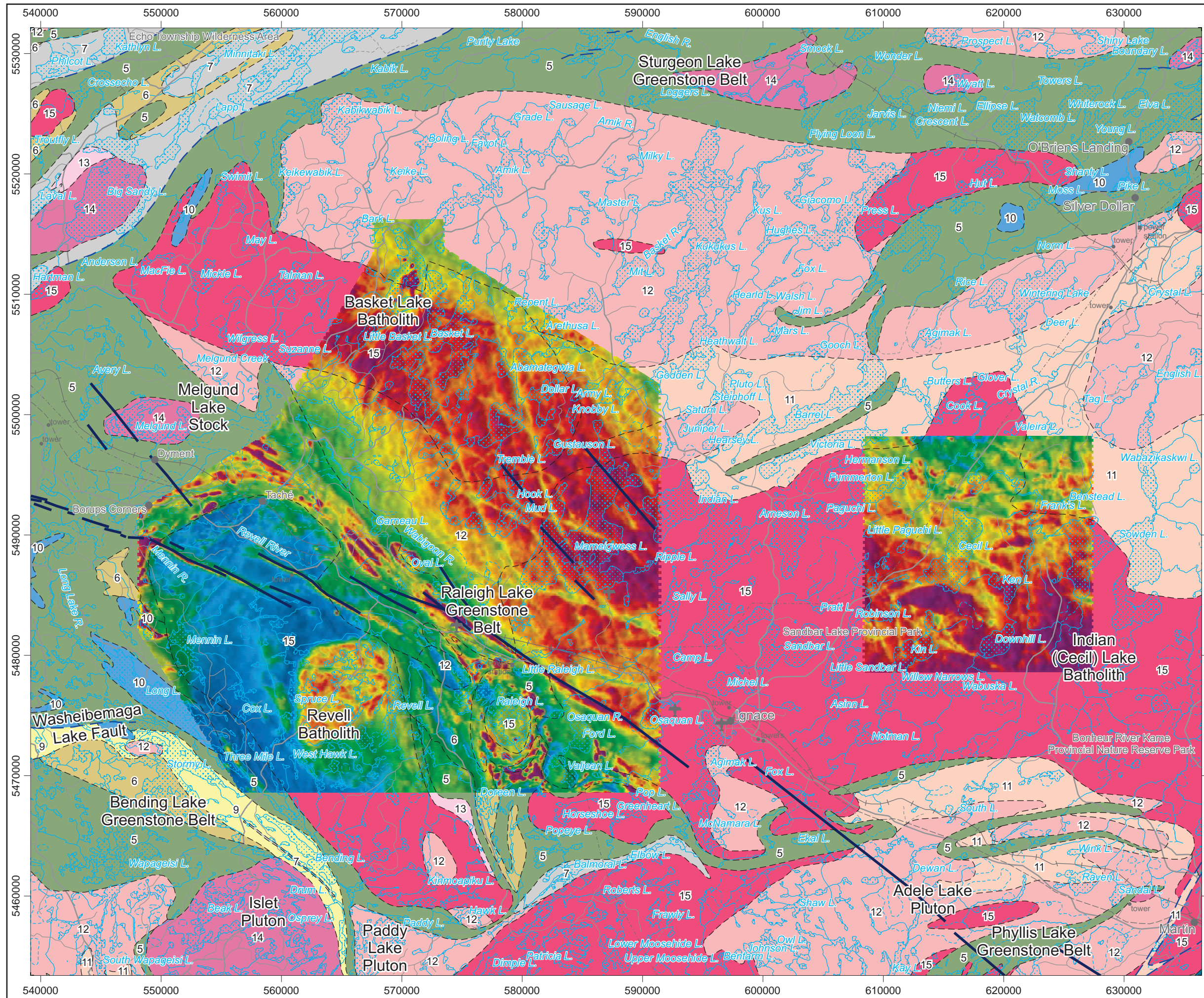
km 5 0 5 10 km

**Airborne Geophysics  
 Acquisition and Interpretation**

**Ignace Area, Ontario 2014**

**Total Magnetic Intensity (250 m cell)**

	DESIGN	JK	29/01/2015	REV. 1.1
	GIS	YC, AP	06/02/2015	<b>FIGURE: 4.6</b>
	DATA	MM, DK	06/02/2015	
	QC	MB	06/02/2015	



**Legend**

Hydrography .....

Road .....

Railway .....

**Geology**

Fault .....

Dyke .....

3: Mafic metavolcanic and metasedimentary rocks

5: Mafic to intermediate metavolcanic rocks

6: Felsic to intermediate metavolcanic rocks

7: Metasedimentary rocks

9: Coarse clastic metasedimentary rocks

10: Mafic and ultramafic rocks

11: Gneissic tonalite suite

12: Foliated tonalite suite

13: Muscovite-bearing granite rock

14: Diorite-monzodiorite-granodiorite suite

15: Massive granodiorite suite

16: Hornblende - nepheline syenite suite

**Map Parameters**

Illumination: inclination 50°, declination 270°

nT

2754.6

145.5

118.8

103.8

95.1

88.6

83.5

80.0

75.0

71.3

67.5

63.9

60.2

56.4

52.6

48.7

44.9

40.9

36.7

32.5

28.2

23.9

19.6

15.2

10.8

6.2

1.2

-9.1

-14.4

-19.9

-25.3

-30.8

-36.3

-42.4

-49.0

-56.0

-63.0

-70.7

-78.7

-87.3

-96.7

-106.4

-114.8

-123.7

-132.1

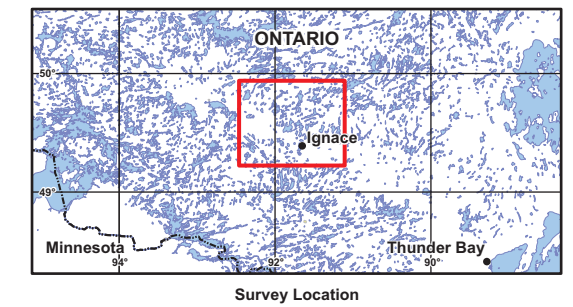
-138.6

-145.2

-155.8

-173.1

-293.2



BASE DATA: National Topographic Database - NRCAN  
 GEOLOGY DATA: OGS Dataset MRD 126-Rev 1  
 DATUM: NAD83  
 PROJECTION: Universal Transverse Mercator (UTM Zone 15N)

Scale 1 : 310 000

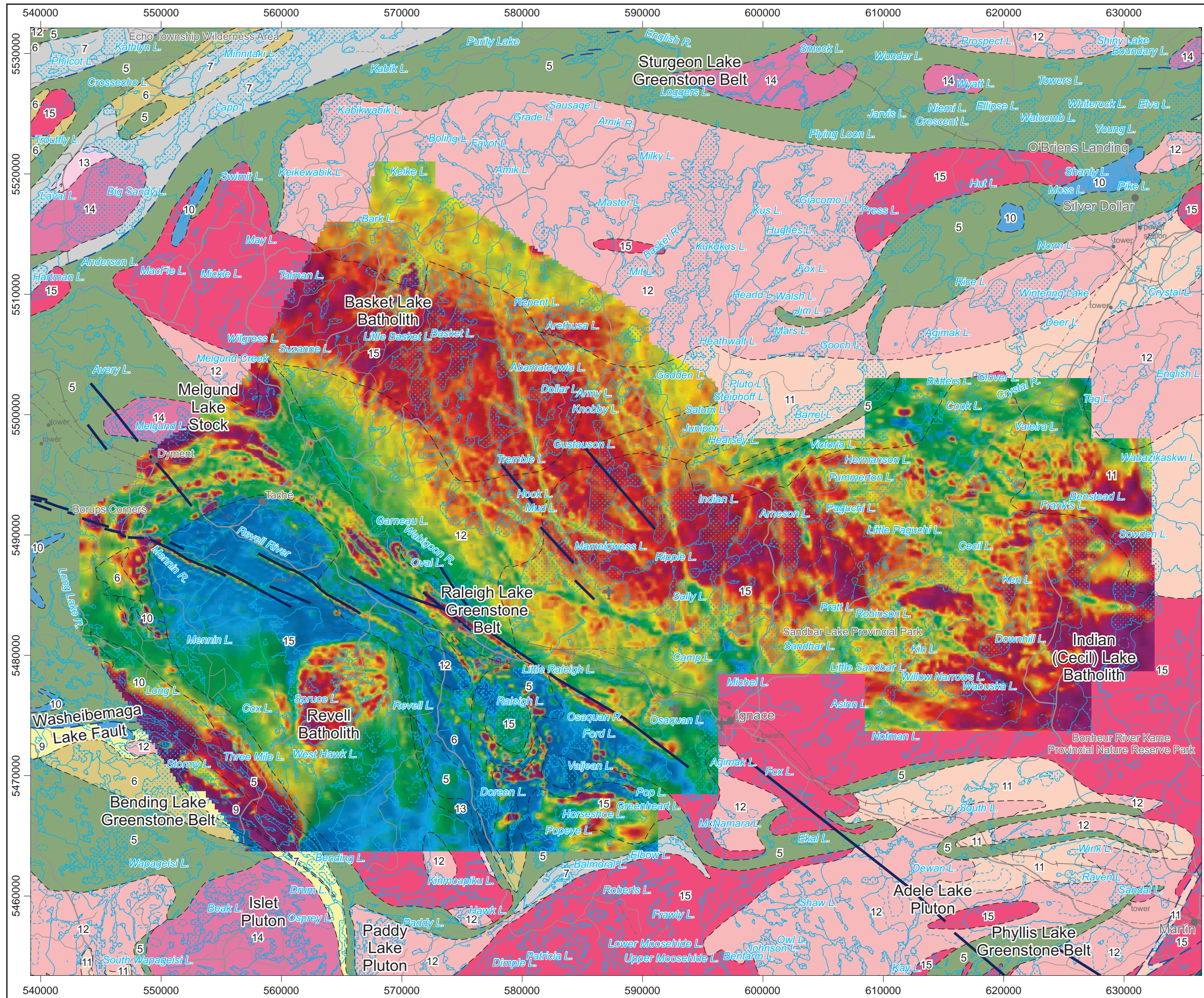
km 5 0 5 10 km

**Airborne Geophysics**  
**Acquisition and Interpretation**

**Ignace Area, Ontario 2014**

**Reduction to the Pole**  
**of the Total Magnetic Intensity (25 m cell)**

	DESIGN	JK	29/01/2015	REV. 1.1
	GIS	YC, AP	06/02/2015	<b>FIGURE: 4.7</b>
	DATA	MM, DK	06/02/2015	
	QC	MB	06/02/2015	



**Legend**

Hydrography .....

Road .....

Railway .....

**Geology**

Fault .....

Dyke .....

3: Mafic metavolcanic and metasedimentary rocks

5: Mafic to intermediate metavolcanic rocks

6: Felsic to intermediate metavolcanic rocks

7: Metasedimentary rocks

9: Coarse clastic metasedimentary rocks

10: Mafic and ultramafic rocks

11: Gneissic tonalite suite

12: Foliated tonalite suite

13: Muscovite-bearing granite rock

14: Diorite-monzodiorite-granodiorite suite

15: Massive granodiorite suite

16: Hornblende - nepheline syenite suite

**Map Parameters**

Illumination: inclination 50°, declination 270°

nT

25487.0

171.1

116.8

94.8

82.1

73.6

67.1

61.4

56.4

51.7

47.2

42.7

38.2

33.6

29.1

24.8

20.6

16.5

12.5

8.6

5.0

1.4

-2.2

-5.7

-9.2

-12.8

-16.2

-19.8

-23.5

-27.5

-31.8

-36.5

-41.4

-46.7

-52.5

-58.3

-64.2

-70.5

-76.9

-83.9

-91.1

-98.8

-107.5

-116.8

-125.8

-133.9

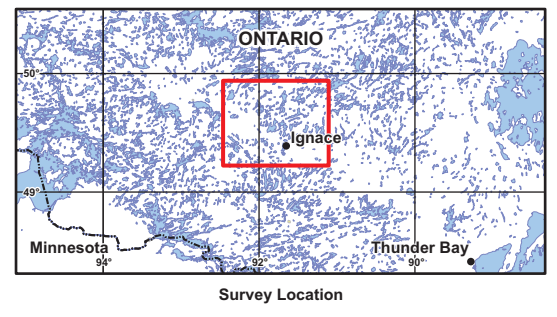
-142.0

-151.6

-163.4

-180.3

-2148.7



BASE DATA: National Topographic Database - NRCAN  
 GEOLOGY DATA: OGS Dataset MRD 126-Rev 1  
 DATUM: NAD83  
 PROJECTION: Universal Transverse Mercator (UTM Zone 15N)

Scale 1 : 310 000

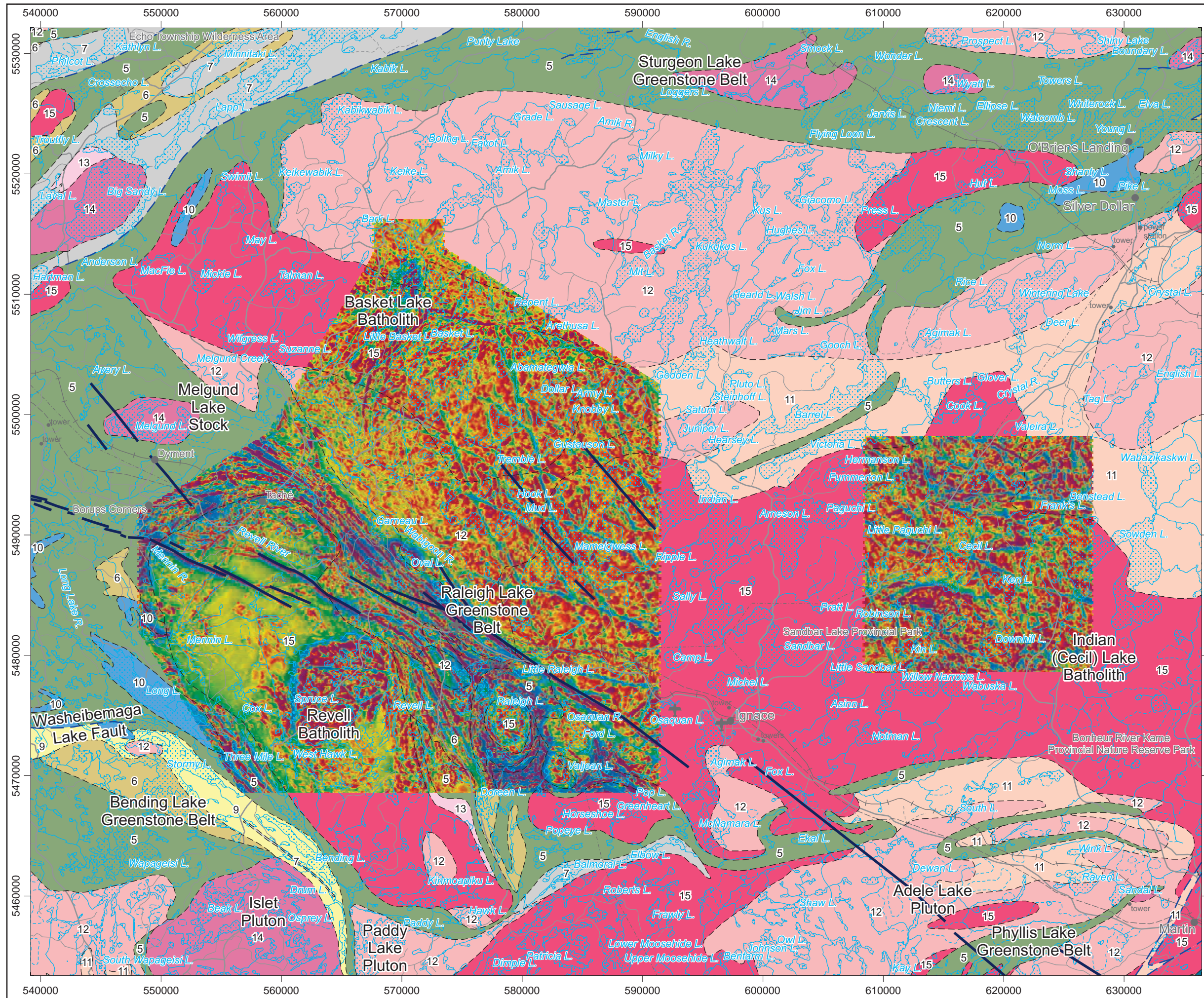
km 5 0 5 10 km

**Airborne Geophysics  
 Acquisition and Interpretation**

**Ignace Area, Ontario 2014**

**Reduction to the Pole  
 of the Total Magnetic Intensity (250 m cell)**

	DESIGN	JK	29/01/2015	REV. 1.1
	GIS	YC, AP	06/02/2015	<b>FIGURE: 4.8</b>
	DATA	MM, DK	06/02/2015	
	QC	MB	06/02/2015	



**Legend**

Hydrography .....

Road .....

Railway .....

**Geology**

Fault .....

Dyke .....

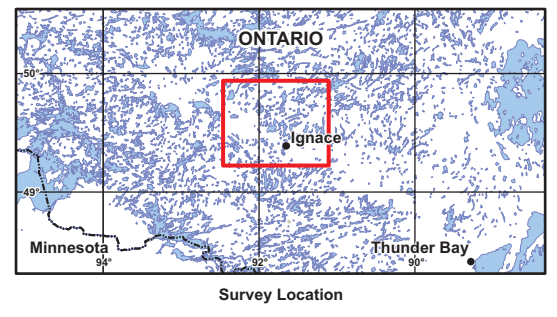
- 3: Mafic metavolcanic and metasedimentary rocks
- 5: Mafic to intermediate metavolcanic rocks
- 6: Felsic to intermediate metavolcanic rocks
- 7: Metasedimentary rocks
- 9: Coarse clastic metasedimentary rocks
- 10: Mafic and ultramafic rocks
- 11: Gneissic tonalite suite
- 12: Foliated tonalite suite
- 13: Muscovite-bearing granite rock
- 14: Diorite-monzodiorite-granodiorite suite
- 15: Massive granodiorite suite
- 16: Hornblende - nepheline syenite suite

**Map Parameters**

Illumination: inclination 50°, declination 270°

nT/km

44586.8  
446.0  
278.9  
212.1  
172.6  
145.8  
125.5  
109.6  
96.2  
85.0  
75.0  
66.0  
57.8  
50.2  
43.0  
36.3  
29.7  
23.5  
17.4  
11.6  
5.8  
0.3  
-5.2  
-10.6  
-16.0  
-21.1  
-26.2  
-30.8  
-35.2  
-39.7  
-44.3  
-49.1  
-54.3  
-59.7  
-65.6  
-71.8  
-78.5  
-85.7  
-93.4  
-102.1  
-111.4  
-122.0  
-134.3  
-148.4  
-165.1  
-184.7  
-209.0  
-241.6  
-289.2  
-379.4  
-4968.1



BASE DATA: National Topographic Database - NRCAN  
 GEOLOGY DATA: OGS Dataset MRD 126-Rev 1  
 DATUM: NAD83  
 PROJECTION: Universal Transverse Mercator (UTM Zone 15N)

Scale 1 : 310 000

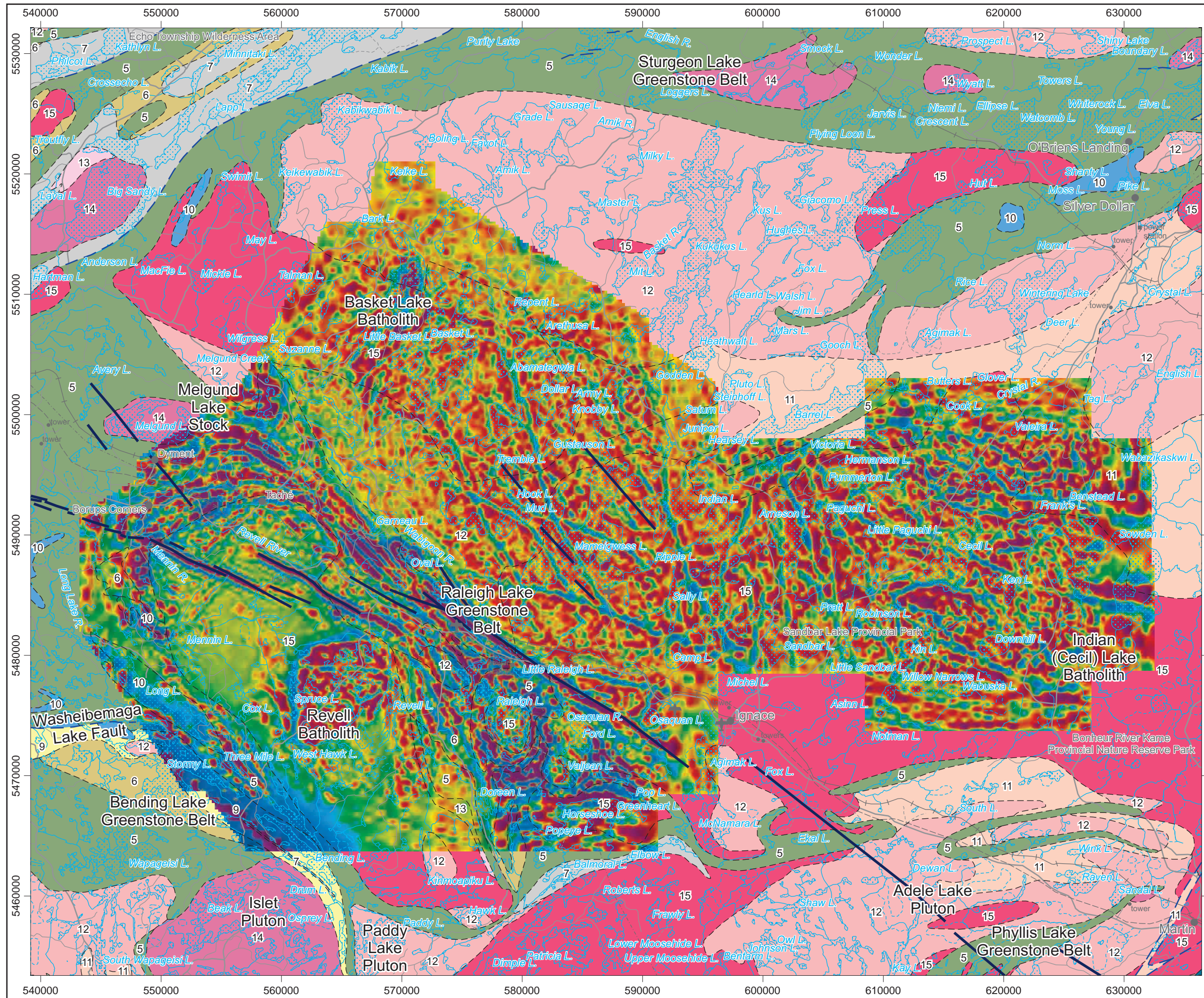
km 5 0 5 10 km

**Airborne Geophysics  
 Acquisition and Interpretation**

**Ignace Area, Ontario 2014**

**First Vertical Derivative of the  
 Reduction to the Pole of the Total Magnetic Intensity  
 (25 m cell)**

	DESIGN	JK	29/01/2015	REV. 1.1
	GIS	YC, AP	06/02/2015	<b>FIGURE: 4.9</b>
	DATA	MM, DK	06/02/2015	
	QC	MB	06/02/2015	



**Legend**

Hydrography .....

Road .....

Railway .....

**Geology**

Fault .....

Dyke .....

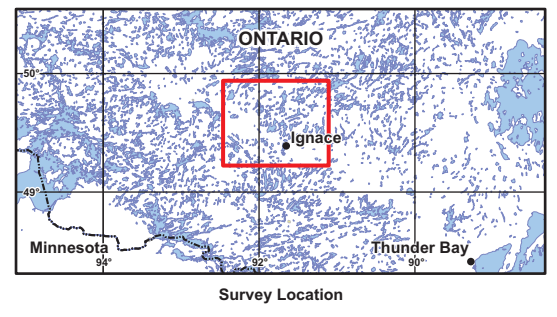
- 3: Mafic metavolcanic and metasedimentary rocks
- 5: Mafic to intermediate metavolcanic rocks
- 6: Felsic to intermediate metavolcanic rocks
- 7: Metasedimentary rocks
- 9: Coarse clastic metasedimentary rocks
- 10: Mafic and ultramafic rocks
- 11: Gneissic tonalite suite
- 12: Foliated tonalite suite
- 13: Muscovite-bearing granite rock
- 14: Diorite-monzodiorite-granodiorite suite
- 15: Massive granodiorite suite
- 16: Hornblende - nepheline syenite suite

**Map Parameters**

Illumination: inclination 50°, declination 270°

nT/km

73681.8  
307.8  
200.0  
155.4  
128.1  
109.2  
94.7  
83.2  
73.4  
64.9  
57.2  
50.4  
44.2  
38.4  
33.0  
27.7  
22.9  
18.2  
13.8  
9.5  
5.4  
1.4  
-2.6  
-6.5  
-10.4  
-14.2  
-18.1  
-22.0  
-25.9  
-29.7  
-33.4  
-37.2  
-41.2  
-45.3  
-49.7  
-54.4  
-59.5  
-65.0  
-71.0  
-77.7  
-85.1  
-93.5  
-103.0  
-113.8  
-126.8  
-142.5  
-161.8  
-188.2  
-230.1  
-338.3



BASE DATA: National Topographic Database - NRCAN  
 GEOLOGY DATA: OGS Dataset MRD 126-Rev 1  
 DATUM: NAD83  
 PROJECTION: Universal Transverse Mercator (UTM Zone 15N)

Scale 1 : 310 000

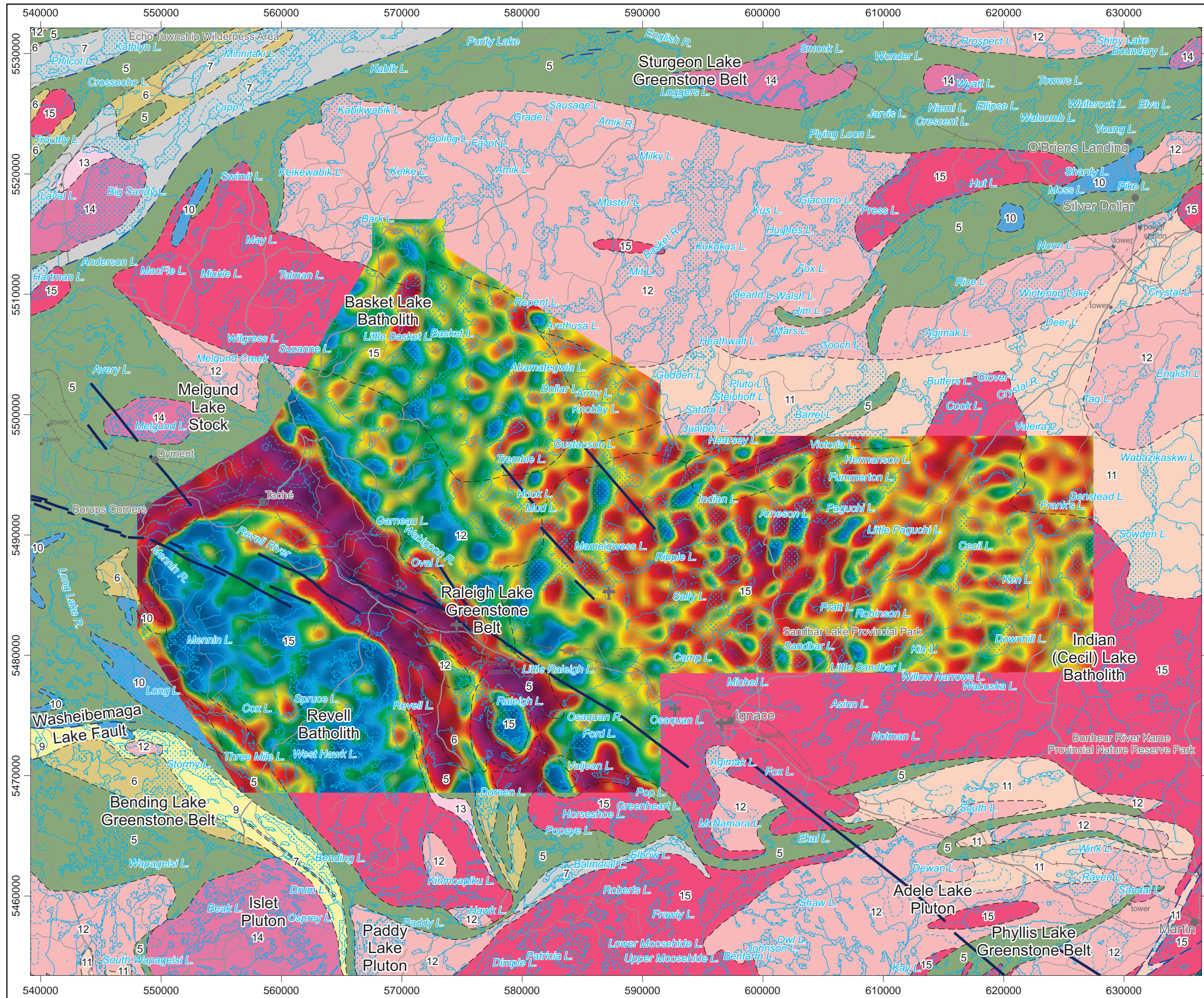
km 5 0 5 10 km

**Airborne Geophysics  
 Acquisition and Interpretation**

**Ignace Area, Ontario 2014**

**First Vertical Derivative of the  
 Reduction to the Pole of the Total Magnetic Intensity  
 (250 m cell)**

	DESIGN	JK	29/01/2015	REV. 1.1
	GIS	YC, AP	06/02/2015	<b>FIGURE: 4.10</b>
	DATA	MM, DK	06/02/2015	
	QC	MB	06/02/2015	



**Legend**

Hydrography .....

Road .....

Railway .....

**Geology**

Fault .....

Dyke .....

3: Mafic metavolcanic and metasedimentary rocks

5: Mafic to intermediate metavolcanic rocks

6: Felsic to intermediate metavolcanic rocks

7: Metasedimentary rocks

9: Coarse clastic metasedimentary rocks

10: Mafic and ultramafic rocks

11: Gneissic tonalite suite

12: Foliated tonalite suite

13: Muscovite-bearing granite rock

14: Diorite-monzodiorite-granodiorite suite

15: Massive granodiorite suite

16: Hornblende - nepheline syenite suite

**Map Parameters**

Illumination: inclination 50°, declination 270°

Spatial Filter (half-wavelength): 1000 m

Bouguer Density: 2.67 g/cm<sup>3</sup>

Eötvös

95.2

57.6

45.6

36.9

30.2

24.9

20.5

16.9

14.1

11.9

10.0

8.3

6.9

5.7

4.6

3.6

2.6

1.7

0.9

0.1

-0.7

-1.5

-2.3

-3.1

-3.8

-4.6

-5.4

-6.2

-6.9

-7.7

-8.5

-9.3

-10.2

-11.1

-12.1

-13.1

-14.1

-15.1

-16.3

-17.4

-18.6

-20.0

-21.4

-22.9

-24.4

-26.2

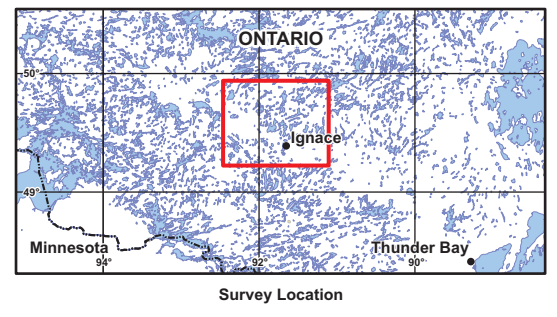
-28.4

-30.8

-33.7

-38.6

-56.8



BASE DATA: National Topographic Database - NRCAN

GEOLOGY DATA: OGS Dataset MRD 126-Rev 1

DATUM: NAD83

PROJECTION: Universal Transverse Mercator (UTM Zone 15N)

Scale 1 : 310 000

km 5 0 5 10 km

**Airborne Geophysics**

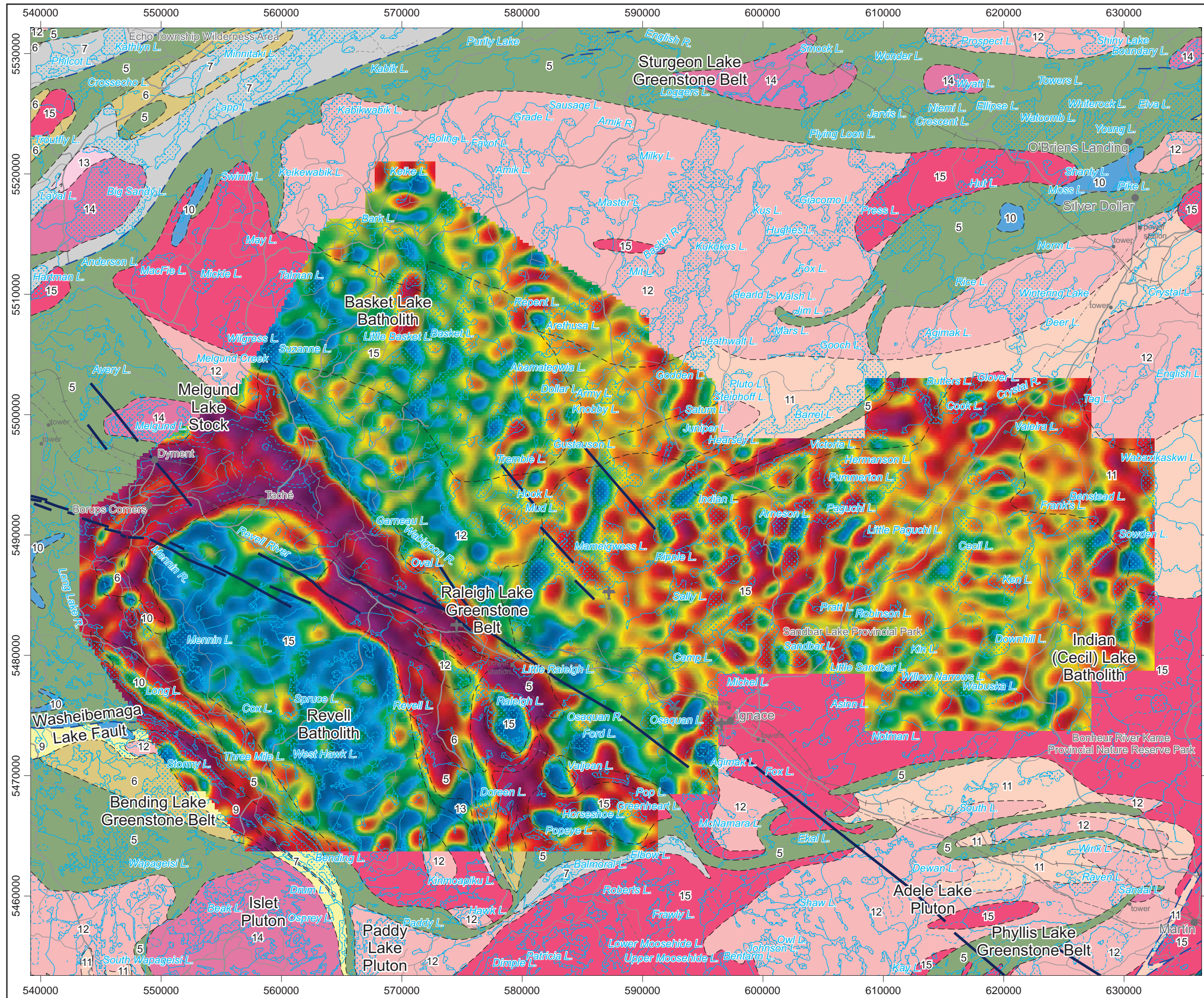
**Acquisition and Interpretation**

**Ignace Area, Ontario 2014**

**First Vertical Derivative of the Bouguer Gravity**

**(Density: 2.67 g/cm<sup>3</sup>) (25 m cell)**

	DESIGN	JK	29/01/2015	REV. 1.1
	GIS	YC, AP	06/02/2015	<b>FIGURE: 4.11</b>
	DATA	MM, DK	06/02/2015	
	QC	MB	06/02/2015	



**Legend**

Hydrography .....

Road .....

Railway .....

**Geology**

Fault .....

Dyke .....

3: Mafic metavolcanic and metasedimentary rocks

5: Mafic to intermediate metavolcanic rocks

6: Felsic to intermediate metavolcanic rocks

7: Metasedimentary rocks

9: Coarse clastic metasedimentary rocks

10: Mafic and ultramafic rocks

11: Gneissic tonalite suite

12: Foliated tonalite suite

13: Muscovite-bearing granite rock

14: Diorite-monzodiorite-granodiorite suite

15: Massive granodiorite suite

16: Hornblende - nepheline syenite suite

**Map Parameters**

Illumination: inclination 50°, declination 270°

Spatial Filter (half-wavelength): 1000 m

Bouguer Density: 2.67 g/cm<sup>3</sup>

Eötvös

97.6

57.5

46.5

38.7

32.8

28.1

24.3

21.0

18.1

15.7

13.6

11.7

10.0

8.5

7.1

5.9

4.7

3.7

2.7

1.7

0.8

-0.0

-1.7

-2.6

-3.4

-4.2

-5.1

-5.9

-6.7

-7.6

-8.4

-9.3

-10.2

-11.2

-12.2

-13.2

-14.3

-15.5

-16.6

-17.9

-19.2

-20.7

-22.3

-24.0

-25.9

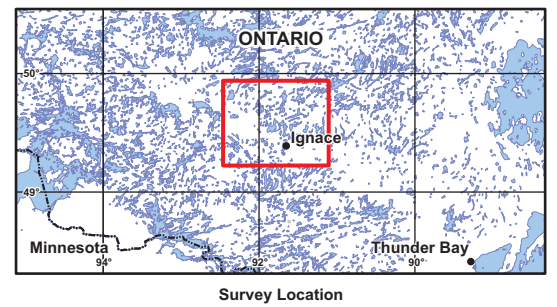
-28.2

-30.8

-34.1

-39.5

-77.2



BASE DATA: National Topographic Database - NRCAN

GEOLOGY DATA: OGS Dataset MRD 126-Rev 1

DATUM: NAD83

PROJECTION: Universal Transverse Mercator (UTM Zone 15N)

Scale 1 : 310 000

km 5 0 5 10 km

**Airborne Geophysics**

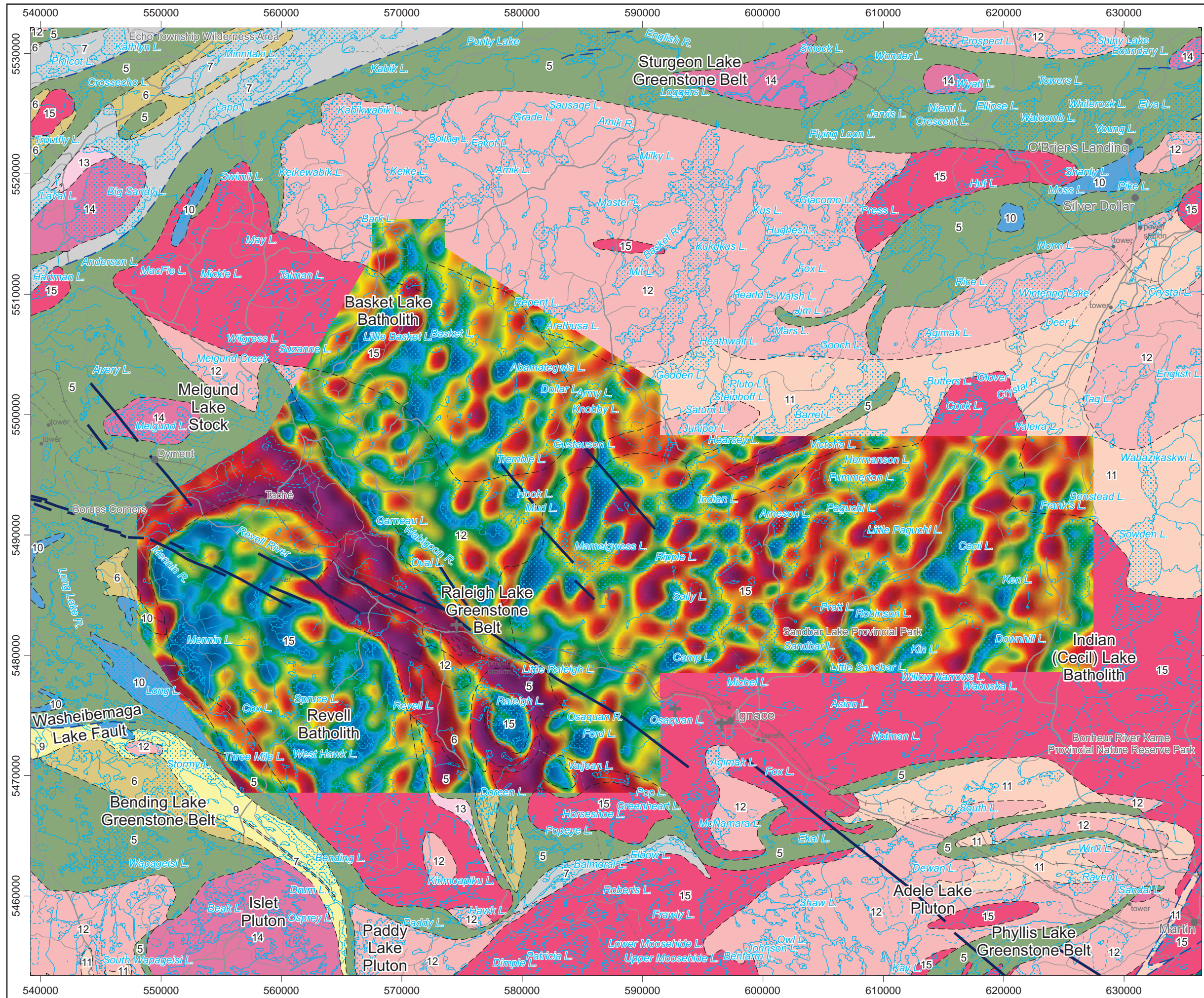
**Acquisition and Interpretation**

**Ignace Area, Ontario 2014**

**First Vertical Derivative of the Bouguer Gravity**

**(Density: 2.67 g/cm<sup>3</sup>) (250 m cell)**

	DESIGN	JK	29/01/2015	REV. 1.1
	GIS	YC, AP	06/02/2015	<b>FIGURE: 4.12</b>
	DATA	MM, DK	06/02/2015	
	QC	MB	06/02/2015	



**Legend**

Hydrography .....

Road .....

Railway .....

**Geology**

Fault .....

Dyke .....

**Map Parameters**

Illumination: inclination 50°, declination 270°

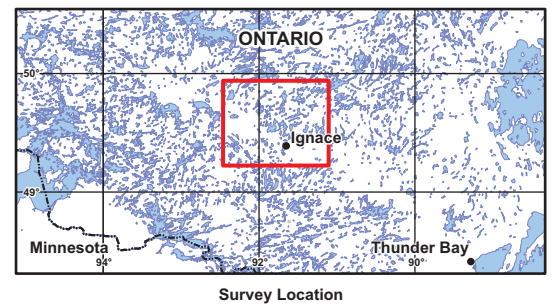
Spatial Filter (half-wavelength): 1000 m

Eötvös

141.4
69.0
57.3
47.3
40.2
35.0
31.0
27.2
23.9
21.0
18.5
16.2
14.1
12.2
10.4
8.8
7.2
4.3
2.9
1.5
0.1
-1.2
-2.5
-3.8
-5.0
-6.2
-7.5
-8.7
-9.9
-11.2
-12.5
-13.8
-15.1
-16.4
-17.7
-19.1
-20.5
-21.9
-23.4
-24.9
-26.5
-28.1
-29.9
-31.9
-34.1
-36.4
-39.3
-43.6
-50.5
-90.6

**Geology**

- 3: Mafic metavolcanic and metasedimentary rocks
- 5: Mafic to intermediate metavolcanic rocks
- 6: Felsic to intermediate metavolcanic rocks
- 7: Metasedimentary rocks
- 9: Coarse clastic metasedimentary rocks
- 10: Mafic and ultramafic rocks
- 11: Gneissic tonalite suite
- 12: Foliated tonalite suite
- 13: Muscovite-bearing granite rock
- 14: Diorite-monzodiorite-granodiorite suite
- 15: Massive granodiorite suite
- 16: Hornblende - nepheline syenite suite



BASE DATA: National Topographic Database - NRCAN  
 GEOLOGY DATA: OGS Dataset MRD 126-Rev 1  
 DATUM: NAD83  
 PROJECTION: Universal Transverse Mercator (UTM Zone 15N)

Scale 1 : 310 000

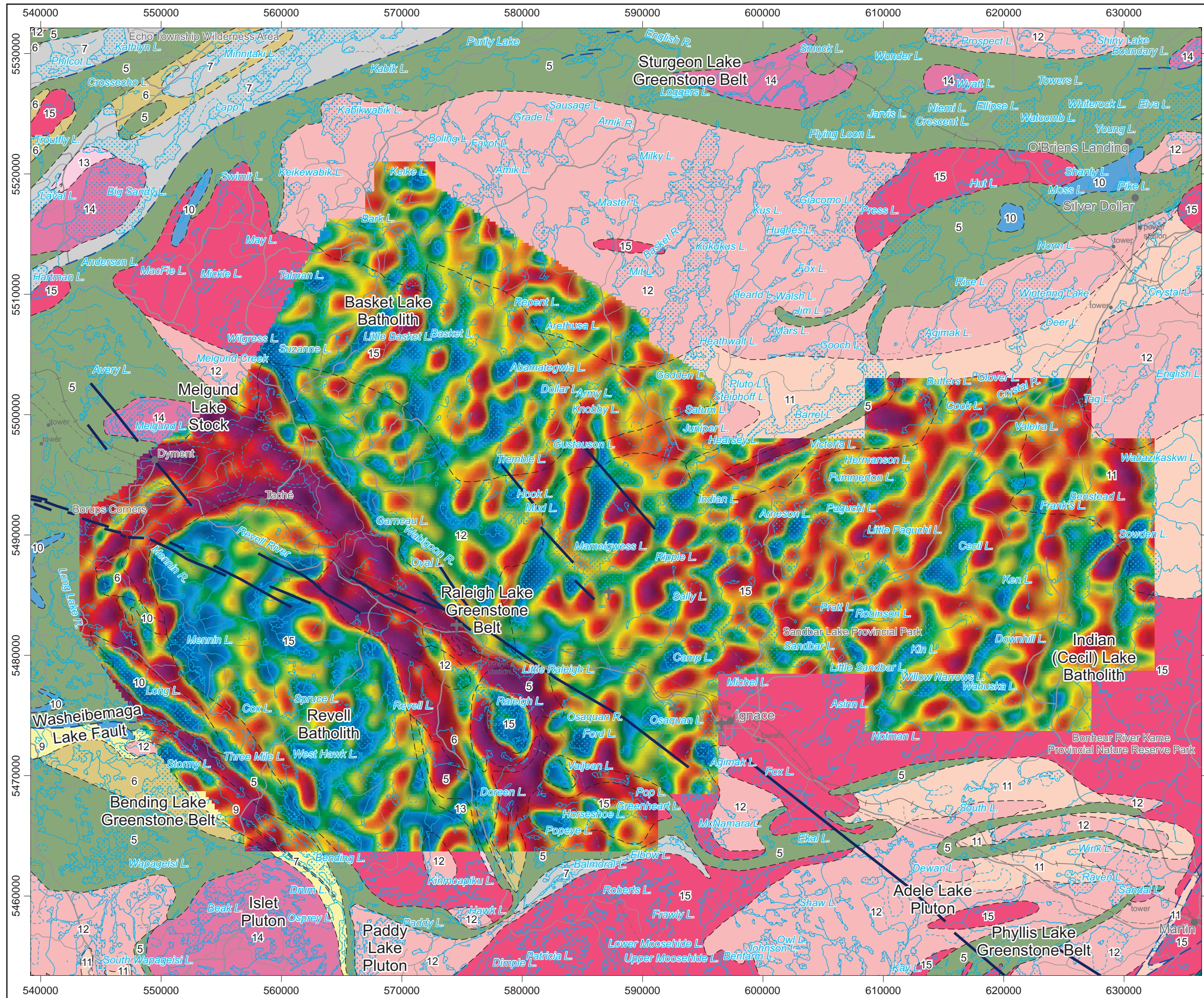
km 5 0 5 10 km

**Airborne Geophysics  
 Acquisition and Interpretation**

**Ignace Area, Ontario 2014**

**First Vertical Derivative  
 of the Free Air Gravity (25 m cell)**

	DESIGN	JK	29/01/2015	REV. 1.1
	GIS	YC, AP	06/02/2015	<b>FIGURE: 4.13</b>
	DATA	MM, DK	06/02/2015	
	QC	MB	06/02/2015	



**Legend**

Hydrography .....

Road .....

Railway .....

**Geology**

Fault .....

Dyke .....

3: Mafic metavolcanic and metasedimentary rocks

5: Mafic to intermediate metavolcanic rocks

6: Felsic to intermediate metavolcanic rocks

7: Metasedimentary rocks

9: Coarse clastic metasedimentary rocks

10: Mafic and ultramafic rocks

11: Gneissic tonalite suite

12: Foliated tonalite suite

13: Muscovite-bearing granite rock

14: Diorite-monzodiorite-granodiorite suite

15: Massive granodiorite suite

16: Hornblende - nepheline syenite suite

**Map Parameters**

Illumination: inclination 50°, declination 270°

Spatial Filter (half-wavelength): 1000 m

Eötvös

141.4

69.1

57.1

47.6

40.9

36.0

32.2

28.8

25.6

22.8

20.3

18.1

16.0

14.1

12.3

10.6

9.1

7.6

6.1

4.6

3.2

1.9

-0.8

-2.1

-3.4

-4.7

-5.9

-7.2

-8.5

-9.8

-11.1

-12.4

-13.8

-15.1

-16.5

-17.9

-19.4

-20.9

-22.4

-24.0

-25.7

-27.4

-29.3

-31.5

-33.8

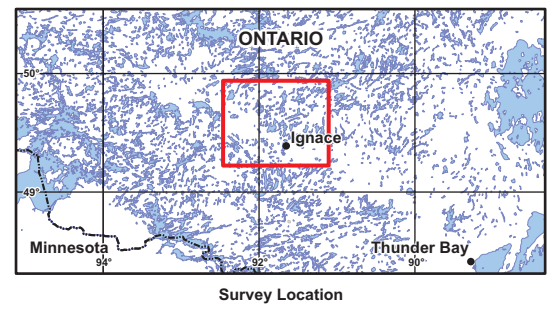
-36.3

-39.5

-44.0

-51.3

-97.5



BASE DATA: National Topographic Database - NRCAN

GEOLOGY DATA: OGS Dataset MRD 126-Rev 1

DATUM: NAD83

PROJECTION: Universal Transverse Mercator (UTM Zone 15N)

Scale 1 : 310 000

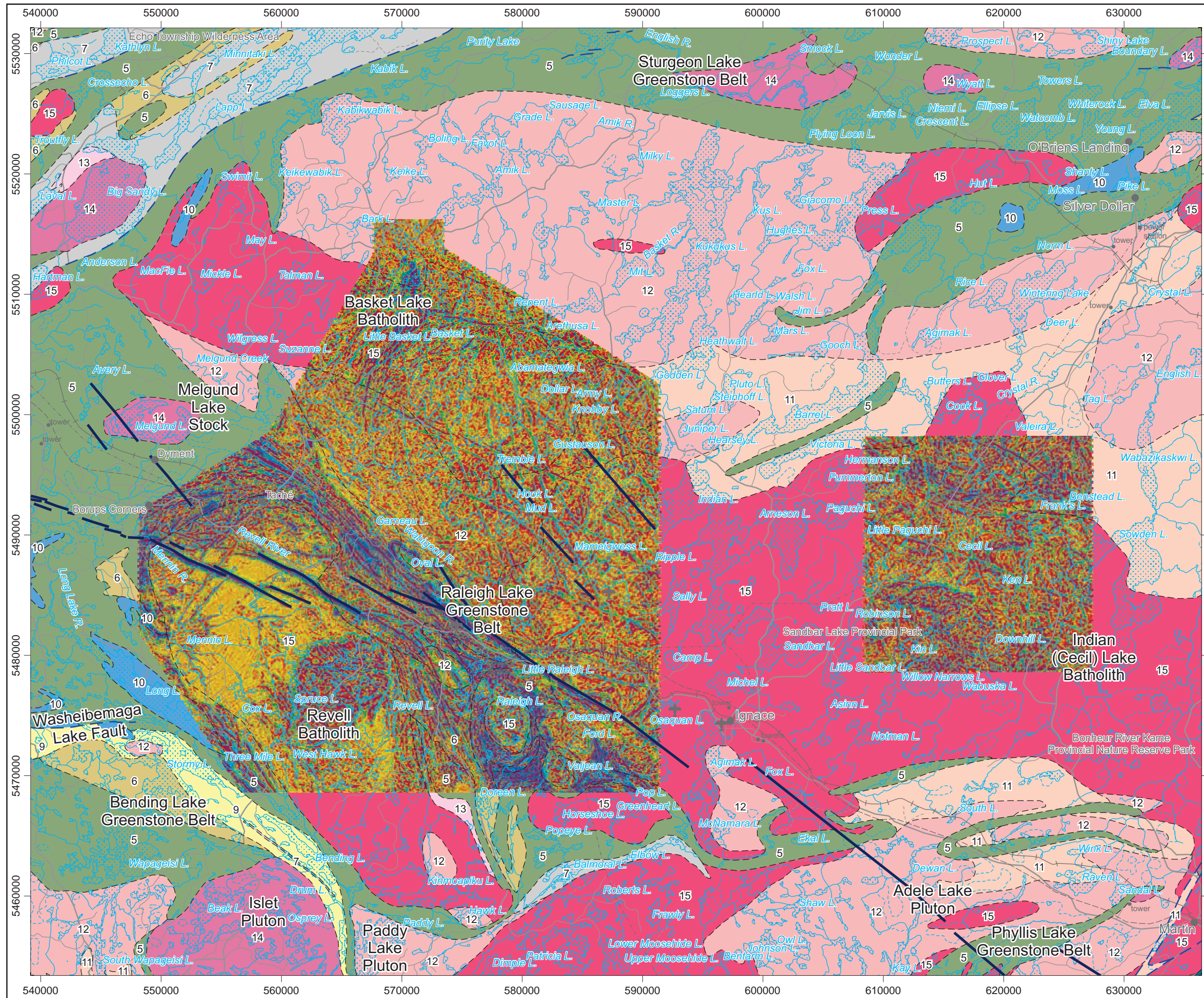
km 5 0 5 10 km

**Airborne Geophysics**  
Acquisition and Interpretation

**Ignace Area, Ontario 2014**

**First Vertical Derivative**  
of the Free Air Gravity (250 m cell)

	DESIGN	JK	29/01/2015	REV. 1.1
	GIS	YC, AP	06/02/2015	<b>FIGURE: 4.14</b>
	DATA	MM, DK	06/02/2015	
	QC	MB	06/02/2015	



**Legend**

Hydrography .....

Road .....

Railway .....

**Geology**

Fault .....

Dyke .....

**Map Parameters**

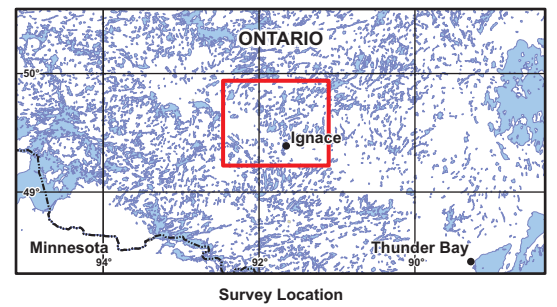
Illumination: inclination 50°, declination 270°

nT/km2

1279681.8
5756.7
3536.0
2627.0
2103.6
1755.0
1495.3
1289.3
1123.3
983.9
863.3
757.0
662.5
577.2
499.5
428.0
361.0
299.0
239.4
183.6
131.0
81.9
37.9
-1.7
-39.6
-78.6
-119.8
-163.8
-210.4
-259.4
-311.6
-366.0
-425.0
-485.0
-554.0
-625.1
-701.8
-785.9
-878.8
-981.3
-1096.2
-1227.7
-1380.6
-1559.3
-1779.3
-2055.3
-2408.6
-2916.0
-3737.6
-5539.6
-306504.3

**Geology**

- 3: Mafic metavolcanic and metasedimentary rocks
- 5: Mafic to intermediate metavolcanic rocks
- 6: Felsic to intermediate metavolcanic rocks
- 7: Metasedimentary rocks
- 9: Coarse clastic metasedimentary rocks
- 10: Mafic and ultramafic rocks
- 11: Gneissic tonalite suite
- 12: Foliated tonalite suite
- 13: Muscovite-bearing granite rock
- 14: Diorite-monzodiorite-granodiorite suite
- 15: Massive granodiorite suite
- 16: Hornblende - nepheline syenite suite



BASE DATA: National Topographic Database - NRCAN  
 GEOLOGY DATA: OGS Dataset MRD 126-Rev 1  
 DATUM: NAD83  
 PROJECTION: Universal Transverse Mercator (UTM Zone 15N)

Scale 1 : 310 000

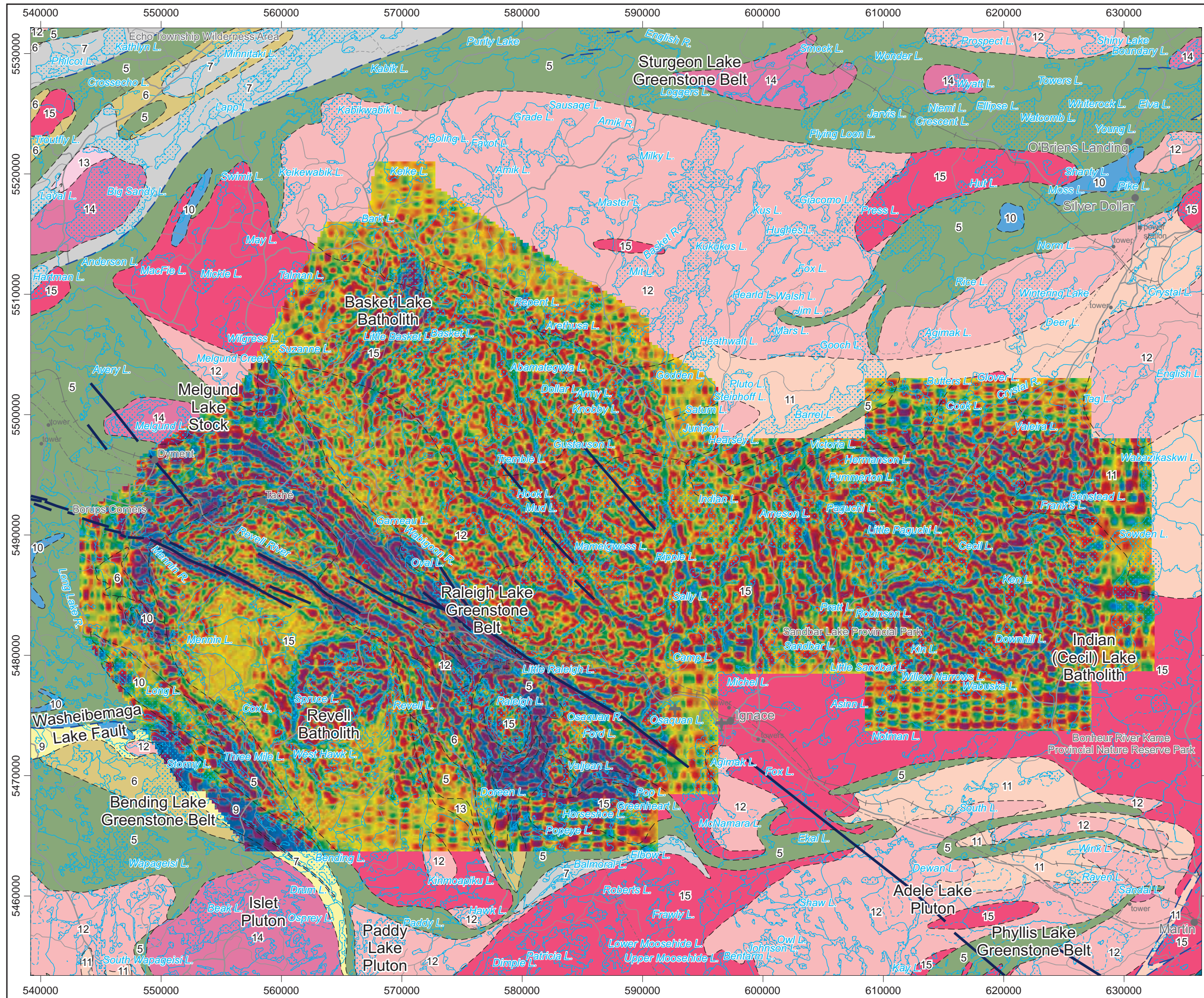
km 5 0 5 10 km

**Airborne Geophysics  
 Acquisition and Interpretation**

**Ignace Area, Ontario 2014**

**Second Vertical Derivative of the  
 Reduction to the Pole of the Total Magnetic Intensity  
 (25 m cell)**

	DESIGN	JK	29/01/2015	REV. 1.1
	GIS	YC, AP	06/02/2015	<b>FIGURE: 4.15</b>
	DATA	MM, DK	06/02/2015	
	QC	MB	06/02/2015	



**Legend**

Hydrography .....

Road .....

Railway .....

**Geology**

Fault .....

Dyke .....

3: Mafic metavolcanic and metasedimentary rocks

5: Mafic to intermediate metavolcanic rocks

6: Felsic to intermediate metavolcanic rocks

7: Metasedimentary rocks

9: Coarse clastic metasedimentary rocks

10: Mafic and ultramafic rocks

11: Gneissic tonalite suite

12: Foliated tonalite suite

13: Muscovite-bearing granite rock

14: Diorite-monzodiorite-granodiorite suite

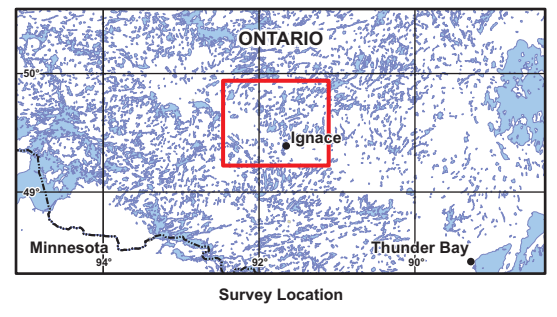
15: Massive granodiorite suite

16: Hornblende - nepheline syenite suite

**Map Parameters**

Illumination: inclination 50°, declination 270°

nT/km2



BASE DATA: National Topographic Database - NRCAN  
 GEOLOGY DATA: OGS Dataset MRD 126-Rev 1  
 DATUM: NAD83  
 PROJECTION: Universal Transverse Mercator (UTM Zone 15N)

Scale 1 : 310 000

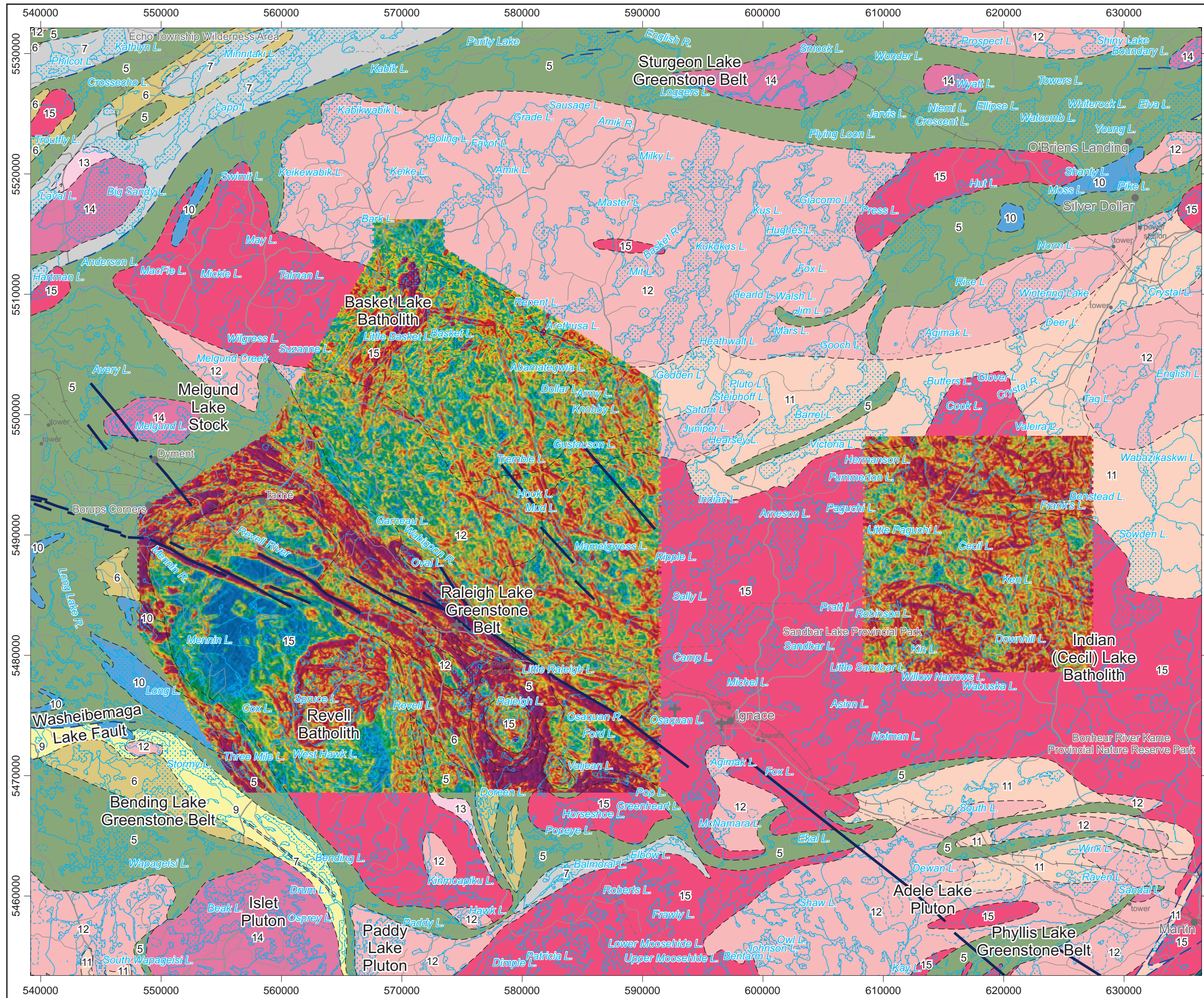
km 5 0 5 10 km

**Airborne Geophysics  
 Acquisition and Interpretation**

Ignace Area, Ontario 2014

**Second Vertical Derivative of the  
 Reduction to the Pole of the Total Magnetic Intensity  
 (250 m cell)**

	DESIGN	JK	29/01/2015	REV. 1.1
	GIS	YC, AP	06/02/2015	<b>FIGURE: 4.16</b>
	DATA	MM, DK	06/02/2015	
	QC	MB	06/02/2015	



**Legend**

Hydrography .....

Road .....

Railway .....

**Geology**

Fault .....

Dyke .....

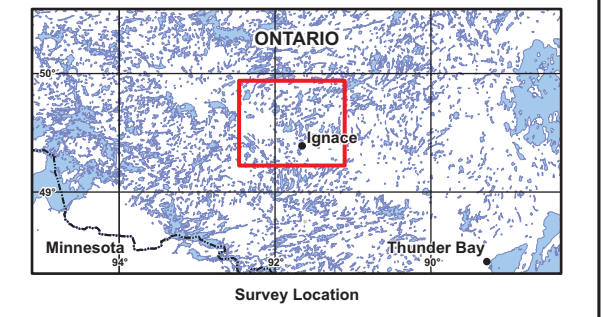
- 3: Mafic metavolcanic and metasedimentary rocks
- 5: Mafic to intermediate metavolcanic rocks
- 6: Felsic to intermediate metavolcanic rocks
- 7: Metasedimentary rocks
- 9: Coarse clastic metasedimentary rocks
- 10: Mafic and ultramafic rocks
- 11: Gneissic tonalite suite
- 12: Foliated tonalite suite
- 13: Muscovite-bearing granite rock
- 14: Diorite-monzodiorite-granodiorite suite
- 15: Massive granodiorite suite
- 16: Hornblende - nepheline syenite suite

**Map Parameters**

Illumination: inclination 50°, declination 270°

nT/km

22890.9  
653.7  
427.8  
337.4  
286.6  
252.0  
226.5  
206.9  
191.0  
177.7  
166.3  
156.2  
147.3  
139.2  
131.9  
125.1  
118.7  
113.1  
107.7  
102.8  
98.0  
93.6  
89.3  
85.3  
81.5  
77.8  
74.4  
71.0  
67.8  
64.6  
61.6  
58.7  
55.8  
53.0  
50.3  
47.6  
44.9  
42.3  
39.7  
37.1  
34.6  
31.9  
29.4  
26.7  
24.1  
21.3  
18.3  
15.2  
11.8  
7.7  
0.0



BASE DATA: National Topographic Database - NRCAN  
 GEOLOGY DATA: OGS Dataset MRD 126-Rev 1  
 DATUM: NAD83  
 PROJECTION: Universal Transverse Mercator (UTM Zone 15N)

Scale 1 : 310 000

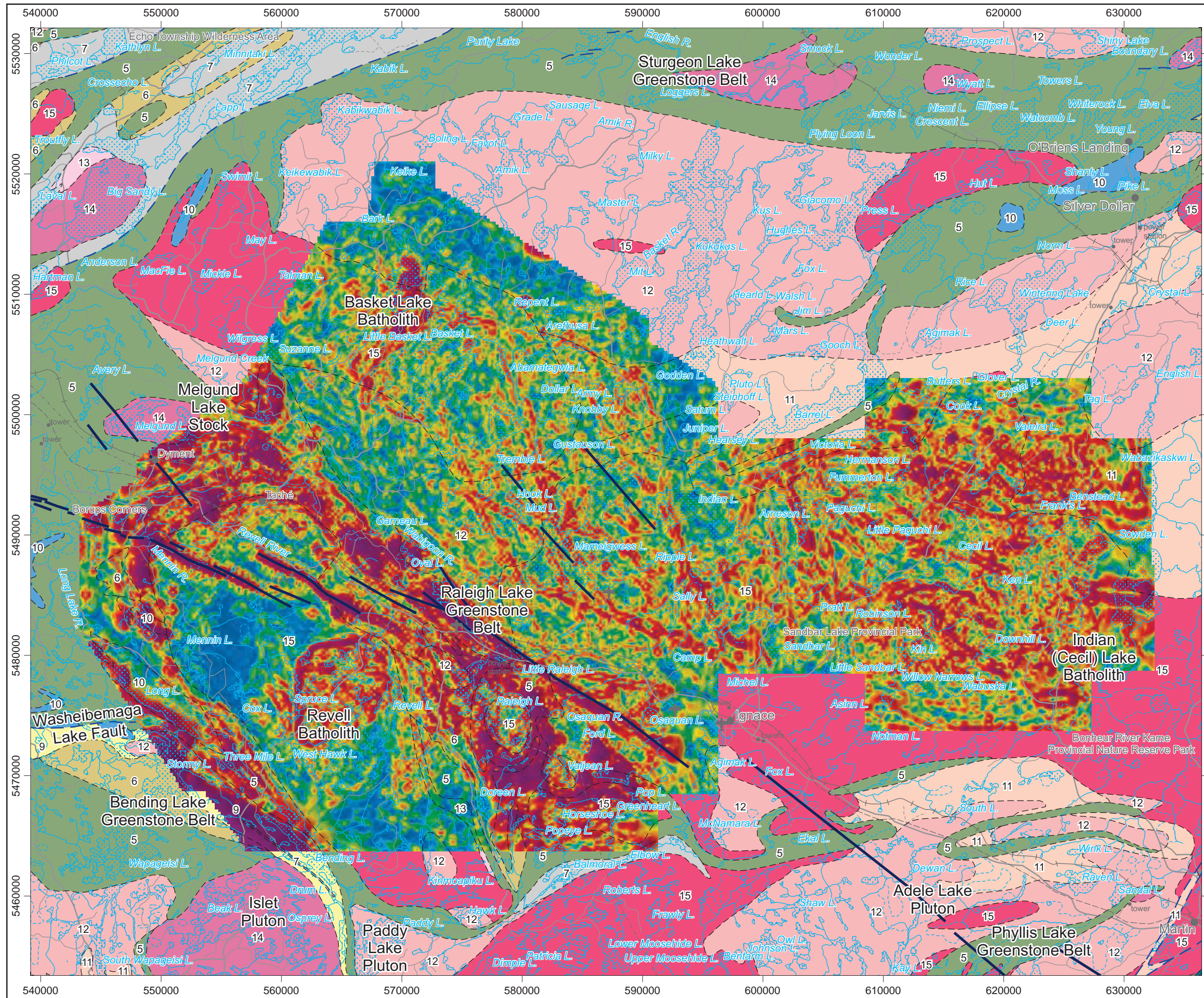
km 5 0 5 10 km

**Airborne Geophysics  
 Acquisition and Interpretation**

**Ignace Area, Ontario 2014**

**Total Horizontal Derivative of the  
 Reduction to the Pole of the Total Magnetic Intensity  
 (25 m cell)**

	DESIGN	JK	29/01/2015	REV. 1.1
	GIS	YC, AP	06/02/2015	<b>FIGURE: 4.17</b>
	DATA	MM, DK	06/02/2015	
	QC	MB	06/02/2015	



**Legend**

Hydrography .....

Road .....

Railway .....

**Geology**

Fault .....

Dyke .....

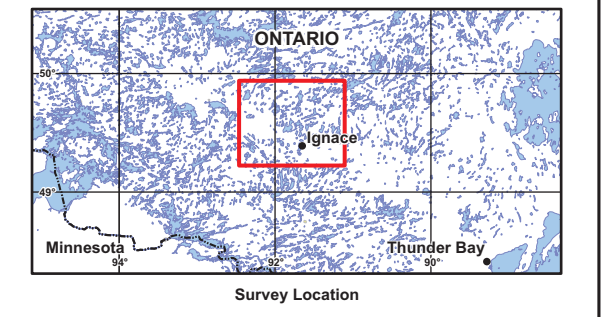
- 3: Mafic metavolcanic and metasedimentary rocks
- 5: Mafic to intermediate metavolcanic rocks
- 6: Felsic to intermediate metavolcanic rocks
- 7: Metasedimentary rocks
- 9: Coarse clastic metasedimentary rocks
- 10: Mafic and ultramafic rocks
- 11: Gneissic tonalite suite
- 12: Foliated tonalite suite
- 13: Muscovite-bearing granite rock
- 14: Diorite-monzodiorite-granodiorite suite
- 15: Massive granodiorite suite
- 16: Hornblende - nepheline syenite suite

**Map Parameters**

Illumination: inclination 50°, declination 270°

nT/km

46262.5  
510.4  
330.1  
261.9  
221.6  
194.6  
175.3  
160.5  
148.5  
138.5  
130.0  
122.6  
116.1  
110.1  
104.7  
99.7  
95.2  
90.9  
86.8  
83.1  
79.5  
76.2  
73.0  
70.1  
67.3  
64.6  
61.9  
59.3  
56.9  
54.5  
52.2  
50.0  
47.8  
45.7  
43.6  
41.6  
39.6  
37.6  
35.6  
33.6  
31.7  
29.8  
27.8  
25.7  
23.6  
21.4  
19.0  
16.5  
13.5  
10.0  
-23.9



BASE DATA: National Topographic Database - NRCAN  
 GEOLOGY DATA: OGS Dataset MRD 126-Rev 1  
 DATUM: NAD83  
 PROJECTION: Universal Transverse Mercator (UTM Zone 15N)

Scale 1 : 310 000

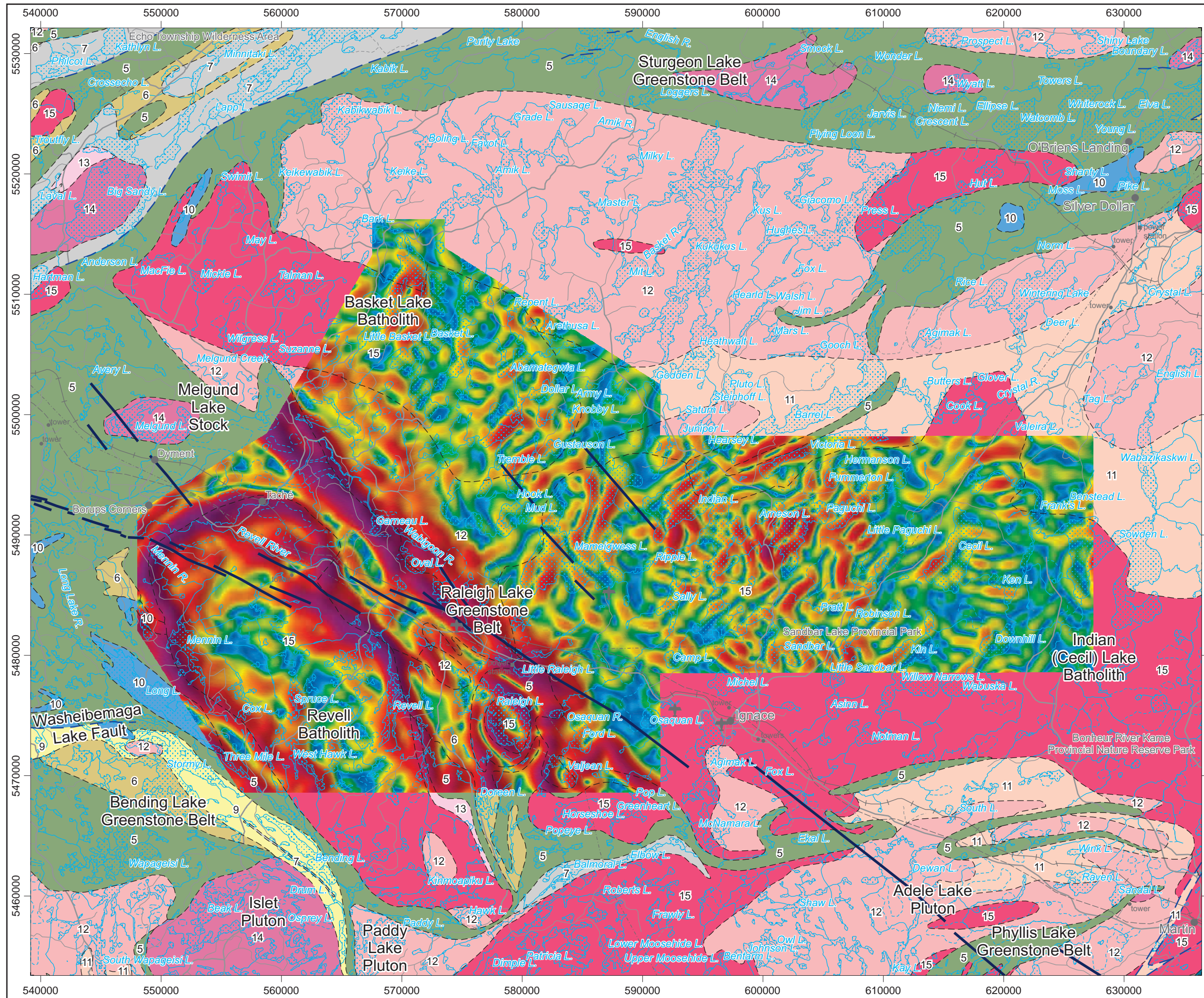
km 5 0 5 10 km

**Airborne Geophysics  
 Acquisition and Interpretation**

Ignace Area, Ontario 2014

**Total Horizontal Derivative of the  
 Reduction to the Pole of the Total Magnetic Intensity  
 (250 m cell)**

	DESIGN	JK	29/01/2015	REV. 1.1
	GIS	YC, AP	06/02/2015	<b>FIGURE: 4.18</b>
	DATA	MM, DK	06/02/2015	
	QC	MB	06/02/2015	



**Legend**

Hydrography .....

Road .....

Railway .....

**Geology**

Fault .....

Dyke .....

3: Mafic metavolcanic and metasedimentary rocks

5: Mafic to intermediate metavolcanic rocks

6: Felsic to intermediate metavolcanic rocks

7: Metasedimentary rocks

9: Coarse clastic metasedimentary rocks

10: Mafic and ultramafic rocks

11: Gneissic tonalite suite

12: Foliated tonalite suite

13: Muscovite-bearing granite rock

14: Diorite-monzodiorite-granodiorite suite

15: Massive granodiorite suite

16: Hornblende - nepheline syenite suite

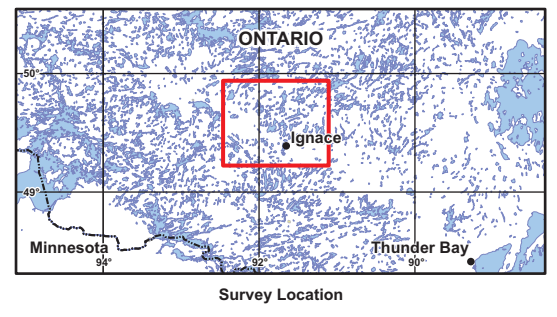
**Map Parameters**

Illumination: inclination 50°, declination 270°

Spatial Filter (half-wavelength): 1000 m

Bouguer Density: 2.67 g/cm<sup>3</sup>

mGal/km



BASE DATA: National Topographic Database - NRCAN

GEOLOGY DATA: OGS Dataset MRD 126-Rev 1

DATUM: NAD83

PROJECTION: Universal Transverse Mercator (UTM Zone 15N)

Scale 1 : 310 000

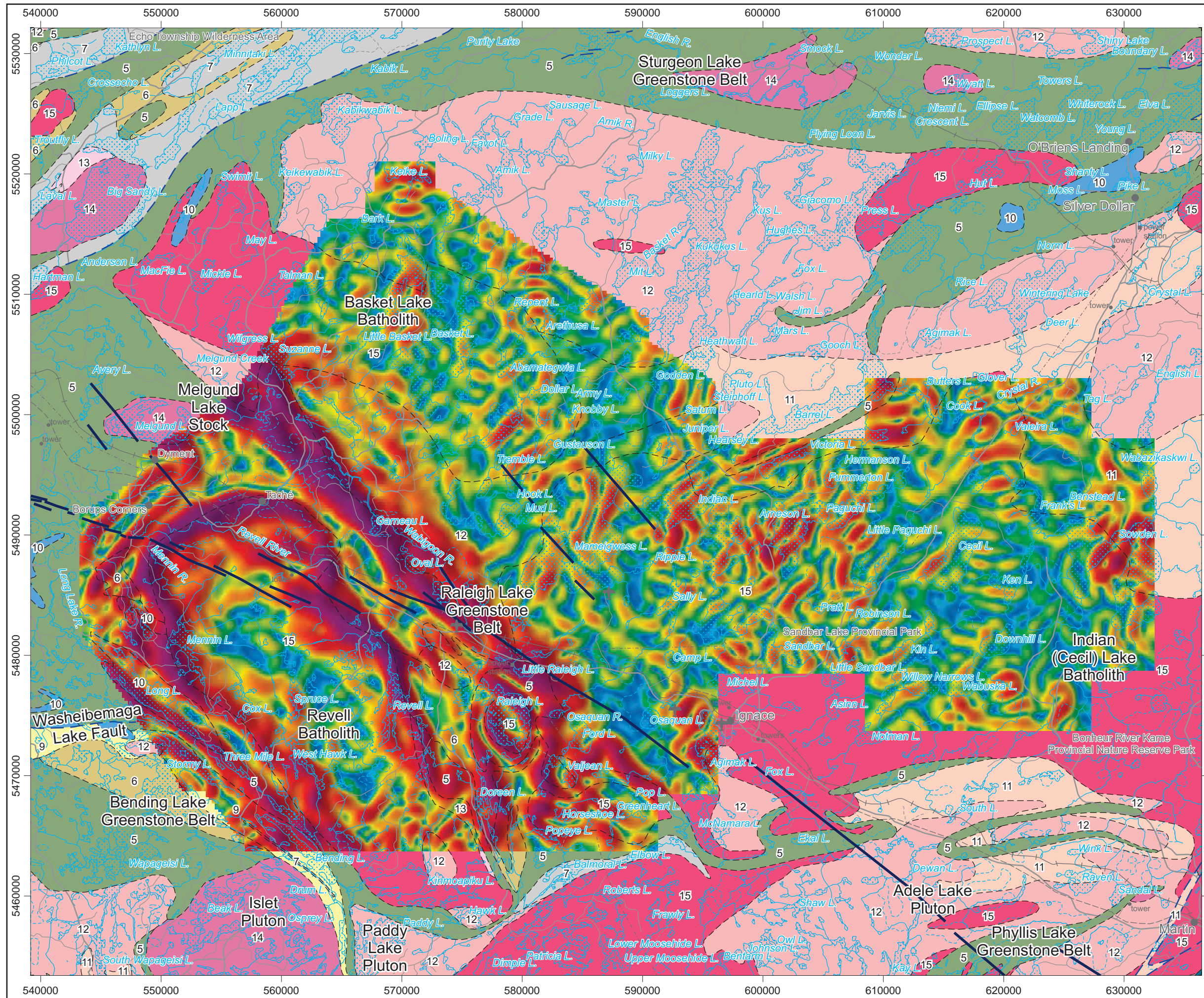
km 5 0 5 10 km

**Airborne Geophysics  
Acquisition and Interpretation**

**Ignace Area, Ontario 2014**

**Total Horizontal Derivative of the Bouguer Gravity  
(Density: 2.67 g/cm<sup>3</sup>) (25 m cell)**

	DESIGN	JK	29/01/2015	REV. 1.1
	GIS	YC, AP	06/02/2015	<b>FIGURE: 4.19</b>
	DATA	MM, DK	06/02/2015	
	QC	MB	06/02/2015	



**Legend**

Hydrography .....

Road .....

Railway .....

**Geology**

Fault .....

Dyke .....

3: Mafic metavolcanic and metasedimentary rocks

5: Mafic to intermediate metavolcanic rocks

6: Felsic to intermediate metavolcanic rocks

7: Metasedimentary rocks

9: Coarse clastic metasedimentary rocks

10: Mafic and ultramafic rocks

11: Gneissic tonalite suite

12: Foliated tonalite suite

13: Muscovite-bearing granite rock

14: Diorite-monzodiorite-granodiorite suite

15: Massive granodiorite suite

16: Hornblende - nepheline syenite suite

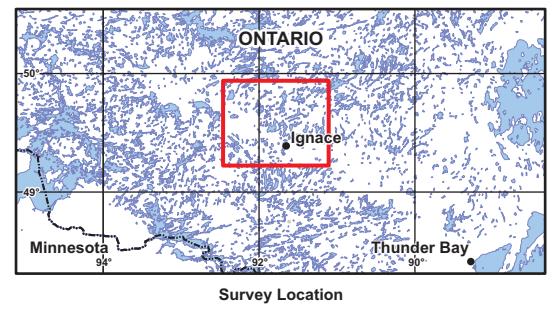
**Map Parameters**

Illumination: inclination 50°, declination 270°

Spatial Filter (half-wavelength): 1000 m

Bouguer Density: 2.67 g/cm<sup>3</sup>

mGal/km



BASE DATA: National Topographic Database - NRCAN

GEOLOGY DATA: OGS Dataset MRD 126-Rev 1

DATUM: NAD83

PROJECTION: Universal Transverse Mercator (UTM Zone 15N)

Scale 1 : 310 000

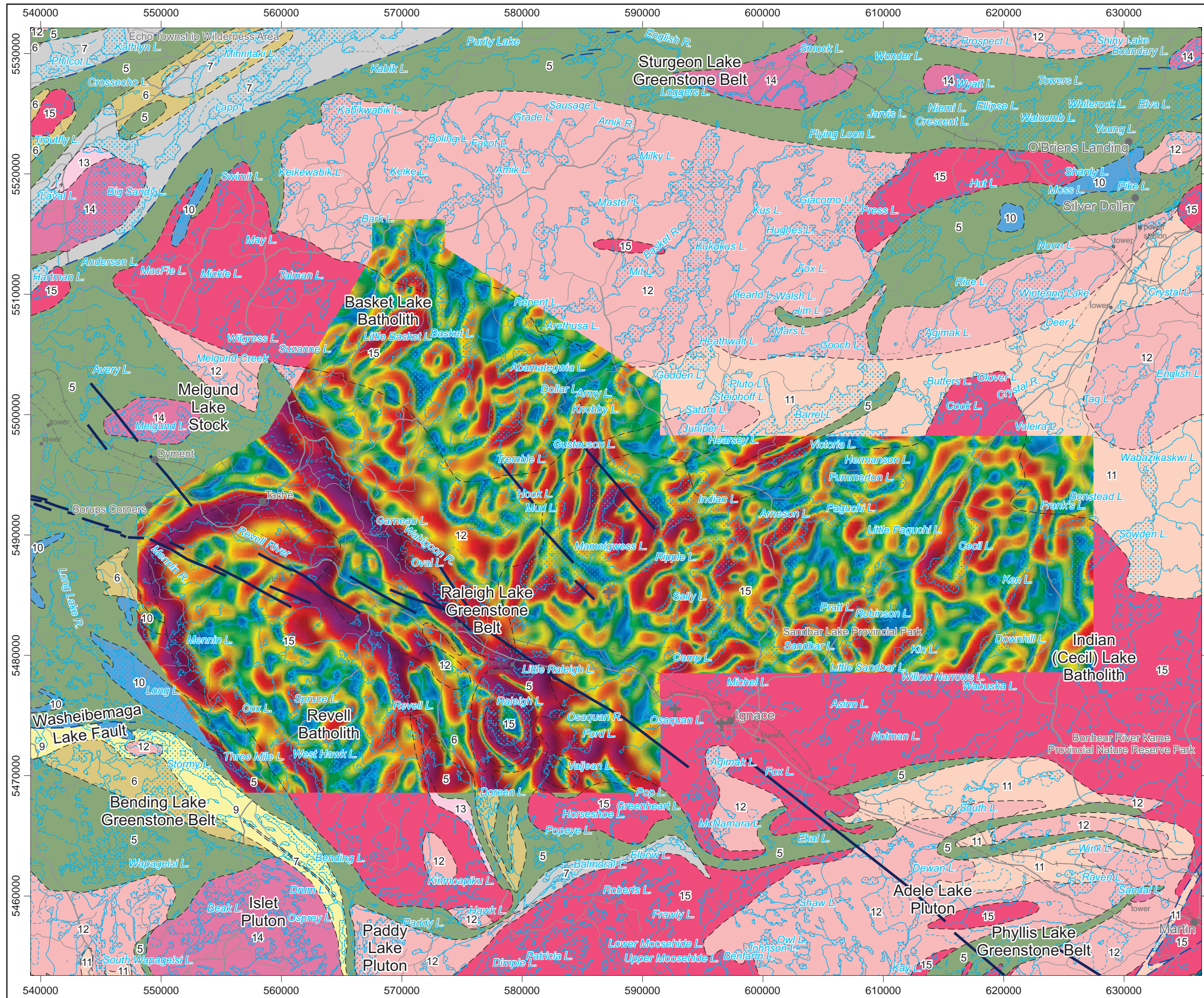
km 5 0 5 10 km

**Airborne Geophysics  
Acquisition and Interpretation**

**Ignace Area, Ontario 2014**

**Total Horizontal Derivative of the Bouguer Gravity  
(Density: 2.67 g/cm<sup>3</sup>) (250 m cell)**

	DESIGN	JK	29/01/2015	REV. 1.1
	GIS	YC, AP	06/02/2015	<b>FIGURE: 4.20</b>
	DATA	MM, DK	06/02/2015	
	QC	MB	06/02/2015	



**Legend**

Hydrography .....

Road .....

Railway .....

**Geology**

Fault .....

Dyke .....

3: Mafic metavolcanic and metasedimentary rocks

5: Mafic to intermediate metavolcanic rocks

6: Felsic to intermediate metavolcanic rocks

7: Metasedimentary rocks

9: Coarse clastic metasedimentary rocks

10: Mafic and ultramafic rocks

11: Gneissic tonalite suite

12: Foliated tonalite suite

13: Muscovite-bearing granite rock

14: Diorite-monzodiorite-granodiorite suite

15: Massive granodiorite suite

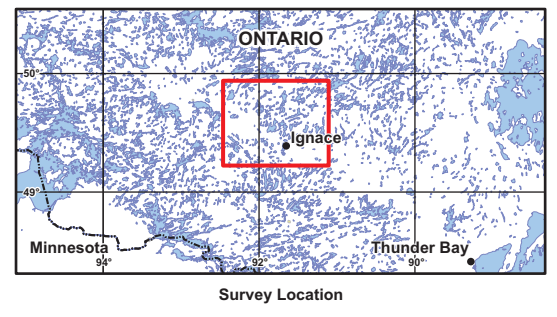
16: Hornblende - nepheline syenite suite

**Map Parameters**

Illumination: inclination 50°, declination 270°

Spatial Filter (half-wavelength): 1000 m

mGal/km



BASE DATA: National Topographic Database - NRCAN  
 GEOLOGY DATA: OGS Dataset MRD 126-Rev 1  
 DATUM: NAD83  
 PROJECTION: Universal Transverse Mercator (UTM Zone 15N)

Scale 1 : 310 000

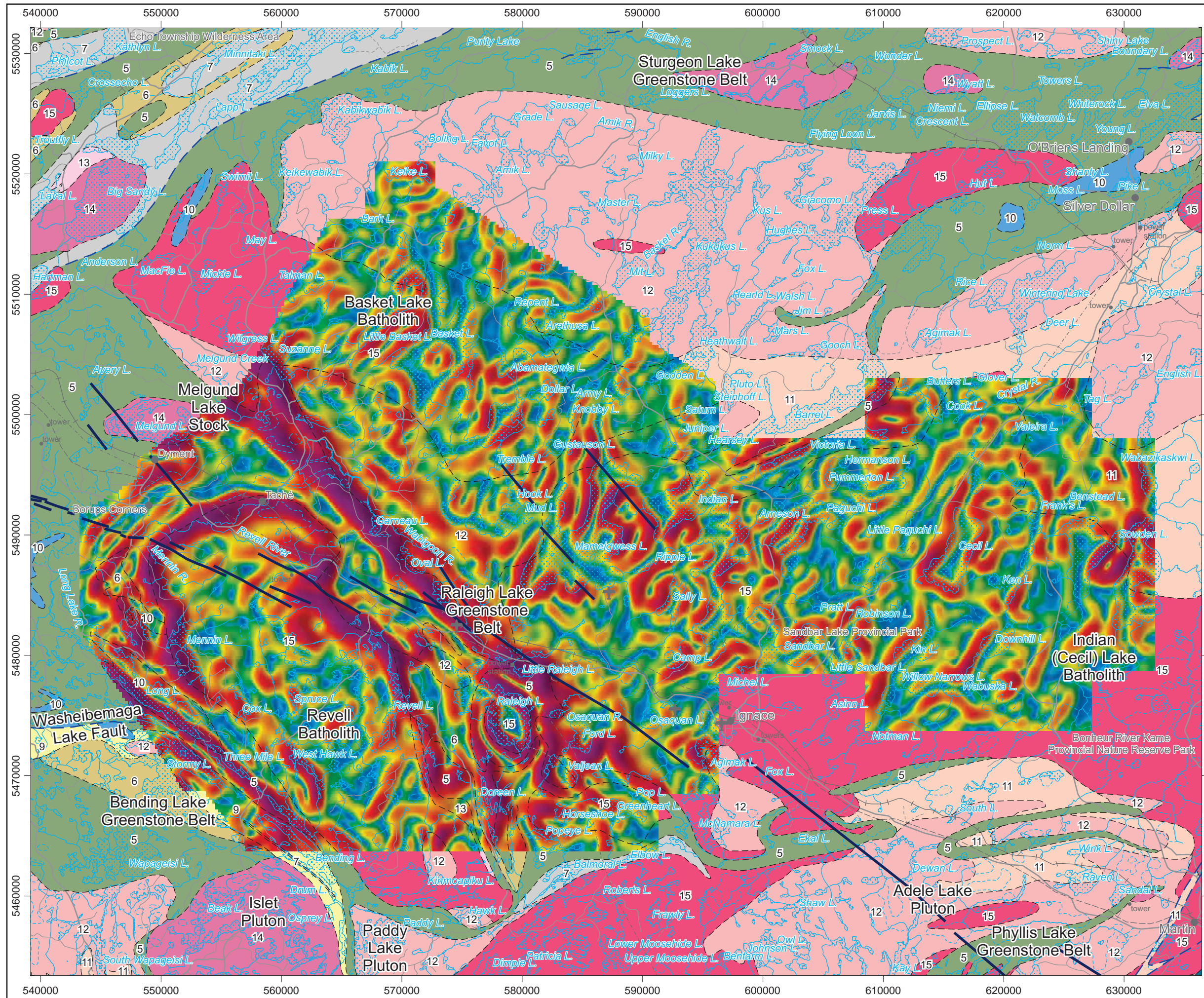
km 5 0 5 10 km

**Airborne Geophysics  
 Acquisition and Interpretation**

**Ignace Area, Ontario 2014**

**Total Horizontal Derivative  
 of the Free Air Gravity (25 m cell)**

	DESIGN	JK	29/01/2015	REV. 1.1
	GIS	YC, AP	06/02/2015	<b>FIGURE: 4.21</b>
	DATA	MM, DK	06/02/2015	
	QC	MB	06/02/2015	



**Legend**

Hydrography .....

Road .....

Railway .....

**Geology**

Fault .....

Dyke .....

**Map Parameters**

Illumination: inclination 50°, declination 270°

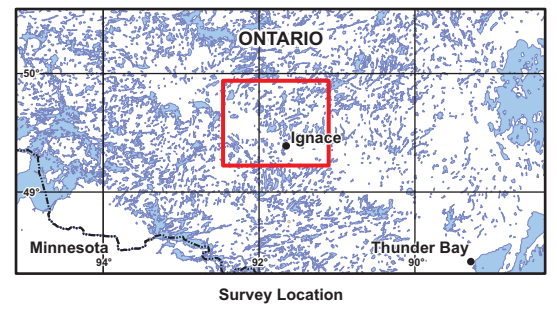
Spatial Filter (half-wavelength): 1000 m

**Color Scale (mGal/km)**

10.78  
7.21  
6.11  
5.37  
4.85  
4.45  
4.13  
3.86  
3.63  
3.43  
3.26  
3.11  
2.98  
2.86  
2.75  
2.65  
2.56  
2.47  
2.39  
2.31  
2.24  
2.17  
2.10  
2.03  
1.97  
1.90  
1.84  
1.78  
1.72  
1.66  
1.60  
1.54  
1.49  
1.43  
1.37  
1.31  
1.26  
1.20  
1.14  
1.08  
1.02  
0.96  
0.90  
0.84  
0.77  
0.70  
0.62  
0.54  
0.44  
0.32  
-0.04

**Geology Legend**

- 3: Mafic metavolcanic and metasedimentary rocks
- 5: Mafic to intermediate metavolcanic rocks
- 6: Felsic to intermediate metavolcanic rocks
- 7: Metasedimentary rocks
- 9: Coarse clastic metasedimentary rocks
- 10: Mafic and ultramafic rocks
- 11: Gneissic tonalite suite
- 12: Foliated tonalite suite
- 13: Muscovite-bearing granite rock
- 14: Diorite-monzodiorite-granodiorite suite
- 15: Massive granodiorite suite
- 16: Hornblende - nepheline syenite suite



BASE DATA: National Topographic Database - NRCAN  
 GEOLOGY DATA: OGS Dataset MRD 126-Rev 1  
 DATUM: NAD83  
 PROJECTION: Universal Transverse Mercator (UTM Zone 15N)

Scale 1 : 310 000

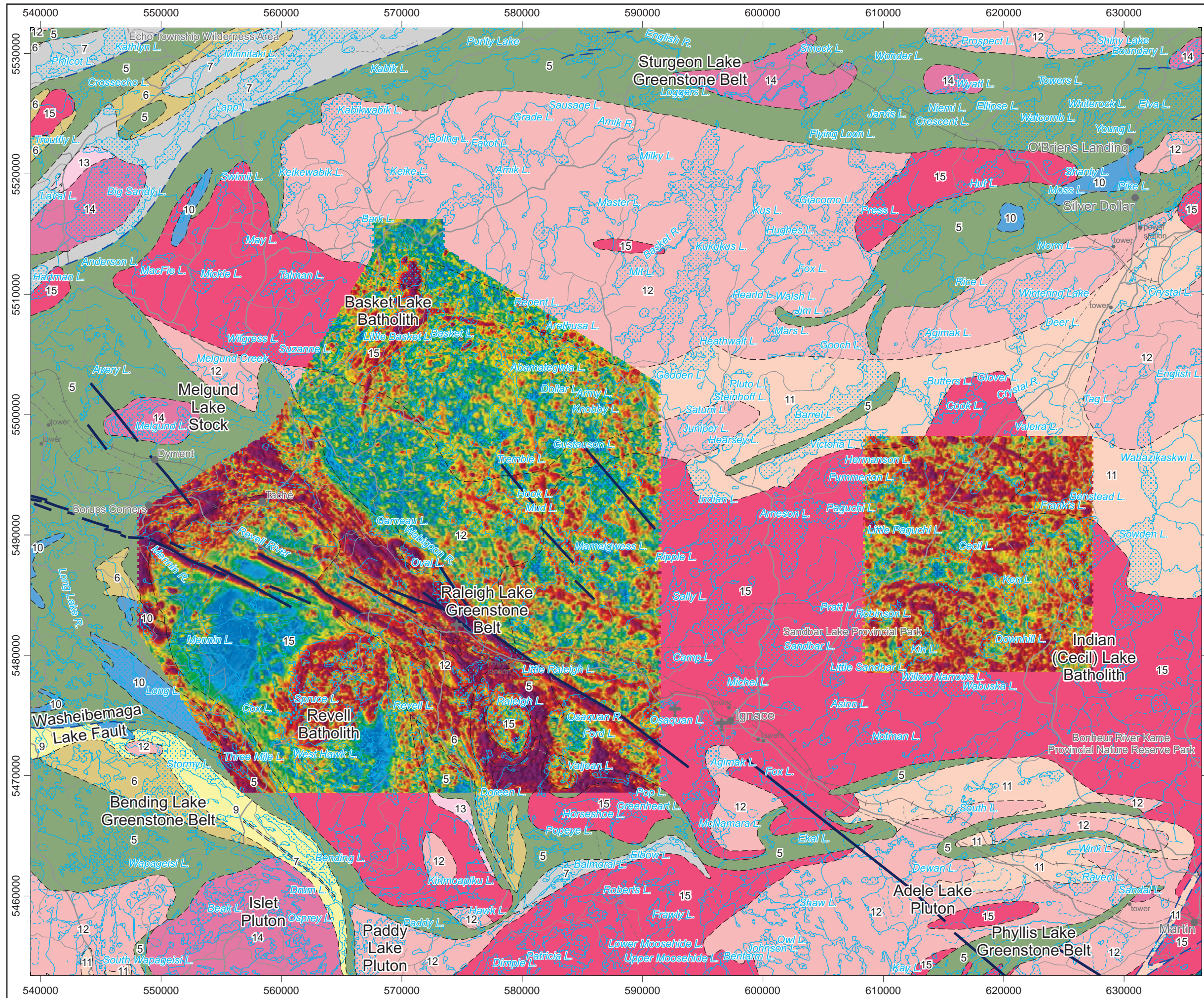
km 5 0 5 10 km

**Airborne Geophysics  
 Acquisition and Interpretation**

**Ignace Area, Ontario 2014**

**Total Horizontal Derivative  
 of the Free Air Gravity (250 m cell)**

	DESIGN	JK	29/01/2015	REV. 1.1
	GIS	YC, AP	06/02/2015	<b>FIGURE: 4.22</b>
	DATA	MM, DK	06/02/2015	
	QC	MB	06/02/2015	



**Legend**

Hydrography .....

Road .....

Railway .....

**Geology**

Fault .....

Dyke .....

3: Mafic metavolcanic and metasedimentary rocks

5: Mafic to intermediate metavolcanic rocks

6: Felsic to intermediate metavolcanic rocks

7: Metasedimentary rocks

9: Coarse clastic metasedimentary rocks

10: Mafic and ultramafic rocks

11: Gneissic tonalite suite

12: Foliated tonalite suite

13: Muscovite-bearing granite rock

14: Diorite-monzodiorite-granodiorite suite

15: Massive granodiorite suite

16: Hornblende - nepheline syenite suite

**Map Parameters**

Illumination: inclination 50°, declination 270°

nT/km

43.099

0.884

0.581

0.461

0.395

0.352

0.320

0.294

0.274

0.256

0.241

0.227

0.215

0.205

0.195

0.186

0.178

0.170

0.163

0.156

0.149

0.143

0.138

0.132

0.127

0.122

0.117

0.112

0.108

0.104

0.100

0.096

0.092

0.088

0.084

0.081

0.077

0.073

0.070

0.066

0.059

0.055

0.052

0.048

0.044

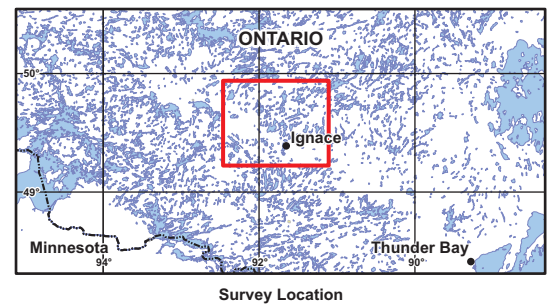
0.040

0.035

0.030

0.024

0.000



BASE DATA: National Topographic Database - NRCAN  
 GEOLOGY DATA: OGS Dataset MRD 126-Rev 1  
 DATUM: NAD83  
 PROJECTION: Universal Transverse Mercator (UTM Zone 15N)

Scale 1 : 310 000

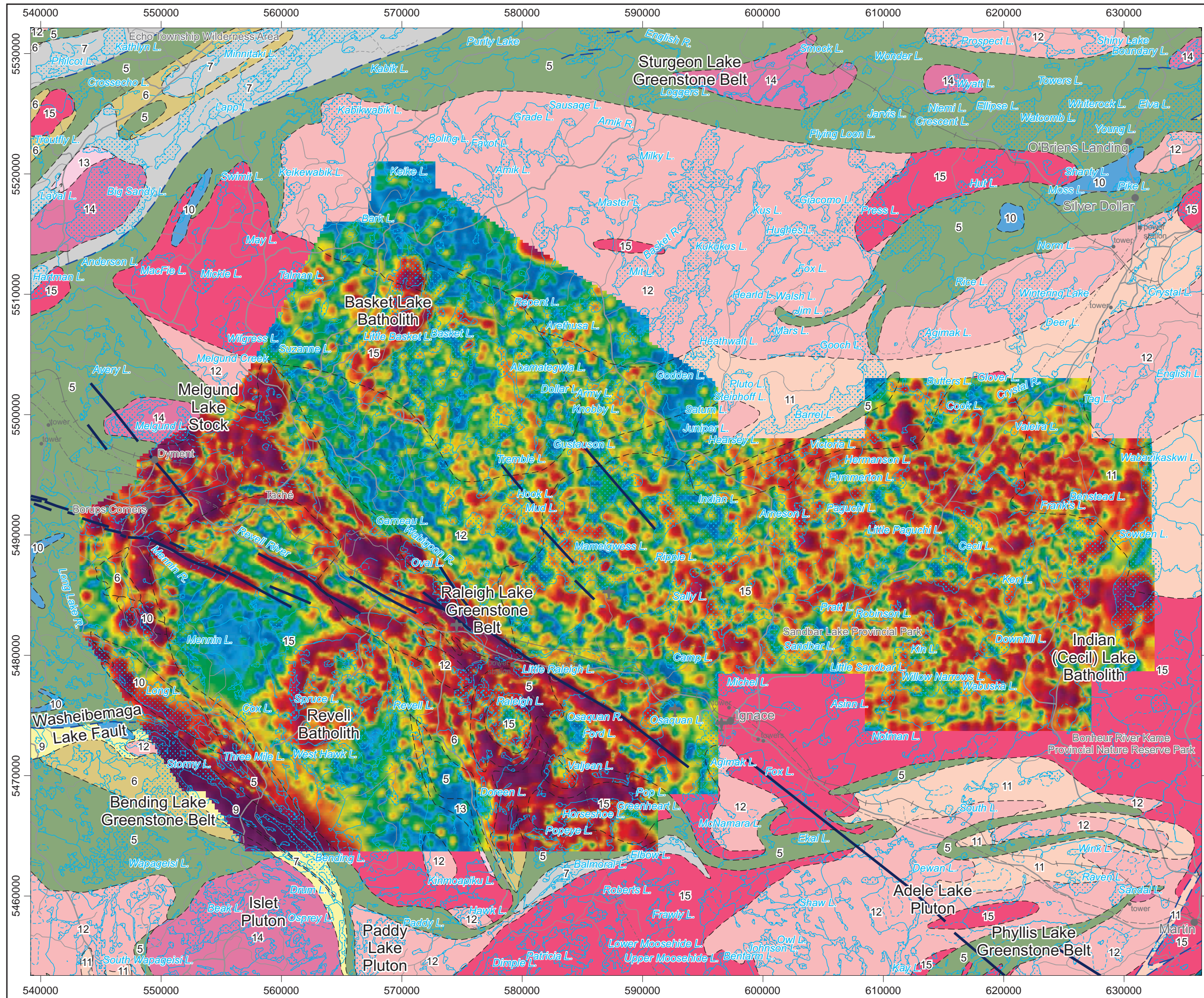
km 5 0 5 10 km

**Airborne Geophysics  
 Acquisition and Interpretation**

**Ignace Area, Ontario 2014**

**Analytic Signal  
 of the Total Magnetic Intensity (25 m cell)**

	DESIGN	JK	29/01/2015	REV. 1.1
	GIS	YC, AP	06/02/2015	<b>FIGURE: 4.23</b>
	DATA	MM, DK	06/02/2015	
	QC	MB	06/02/2015	



**Legend**

Hydrography .....

Road .....

Railway .....

**Geology**

Fault .....

Dyke .....

3: Mafic metavolcanic and metasedimentary rocks

5: Mafic to intermediate metavolcanic rocks

6: Felsic to intermediate metavolcanic rocks

7: Metasedimentary rocks

9: Coarse clastic metasedimentary rocks

10: Mafic and ultramafic rocks

11: Gneissic tonalite suite

12: Foliated tonalite suite

13: Muscovite-bearing granite rock

14: Diorite-monzodiorite-granodiorite suite

15: Massive granodiorite suite

16: Hornblende - nepheline syenite suite

**Map Parameters**

Illumination: inclination 50°, declination 270°

nT/km

66.846

0.574

0.381

0.307

0.265

0.235

0.214

0.197

0.184

0.172

0.163

0.154

0.146

0.139

0.132

0.127

0.121

0.116

0.112

0.107

0.103

0.099

0.095

0.092

0.088

0.085

0.082

0.079

0.076

0.070

0.067

0.065

0.062

0.059

0.057

0.054

0.052

0.049

0.047

0.044

0.042

0.040

0.037

0.035

0.032

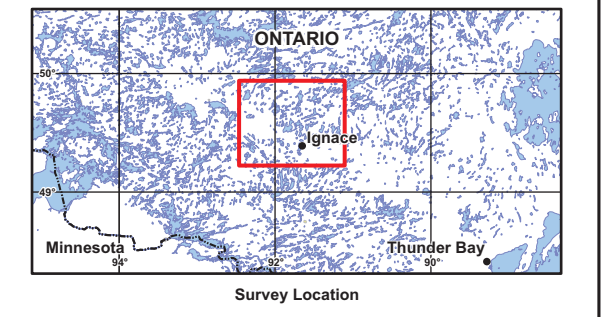
0.029

0.026

0.023

0.018

-0.002



BASE DATA: National Topographic Database - NRCAN  
 GEOLOGY DATA: OGS Dataset MRD 126-Rev 1  
 DATUM: NAD83  
 PROJECTION: Universal Transverse Mercator (UTM Zone 15N)

Scale 1 : 310 000

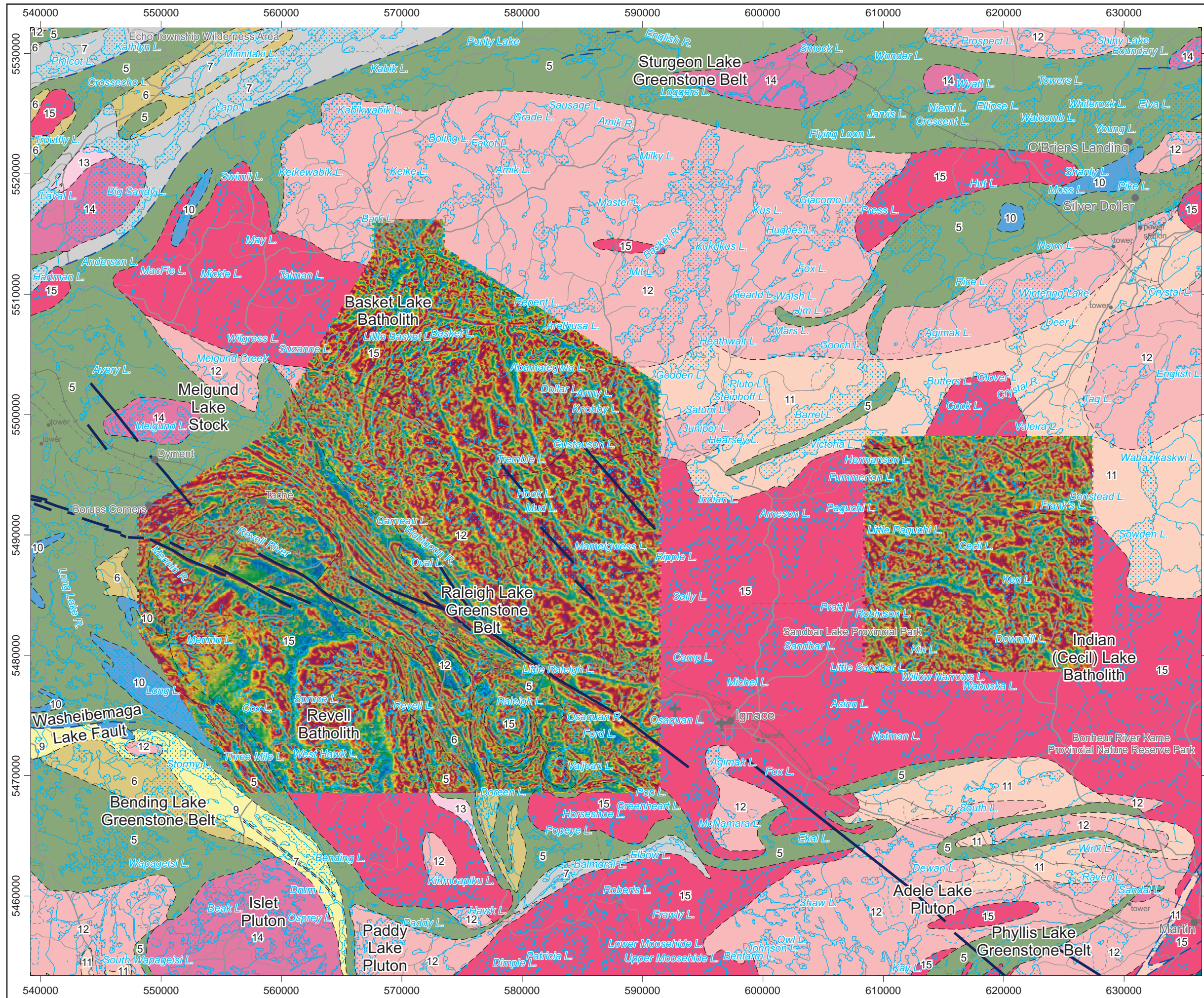
km 5 0 5 10 km

**Airborne Geophysics**  
**Acquisition and Interpretation**

**Ignace Area, Ontario 2014**

**Analytic Signal**  
**of the Total Magnetic Intensity (250 m cell)**

	DESIGN	JK	29/01/2015	REV. 1.1
	GIS	YC, AP	06/02/2015	<b>FIGURE: 4.24</b>
	DATA	MM, DK	06/02/2015	
	QC	MB	06/02/2015	



**Legend**

Hydrography .....

Road .....

Railway .....

**Geology**

Fault .....

Dyke .....

3: Mafic metavolcanic and metasedimentary rocks

5: Mafic to intermediate metavolcanic rocks

6: Felsic to intermediate metavolcanic rocks

7: Metasedimentary rocks

9: Coarse clastic metasedimentary rocks

10: Mafic and ultramafic rocks

11: Gneissic tonalite suite

12: Foliated tonalite suite

13: Muscovite-bearing granite rock

14: Diorite-monzodiorite-granodiorite suite

15: Massive granodiorite suite

16: Hornblende - nepheline syenite suite

**Map Parameters**

Illumination: inclination 50°, declination 270°

degrees

90.0

78.5

73.3

69.1

65.3

61.7

58.2

54.9

51.5

48.2

45.0

41.7

38.3

35.0

31.7

28.3

24.9

21.5

18.1

14.6

11.2

7.8

4.3

-2.5

-5.9

-9.3

-12.7

-16.0

-19.4

-22.6

-25.8

-28.7

-32.0

-35.1

-38.1

-41.0

-44.0

-46.9

-49.7

-52.6

-55.5

-58.3

-61.2

-64.1

-67.1

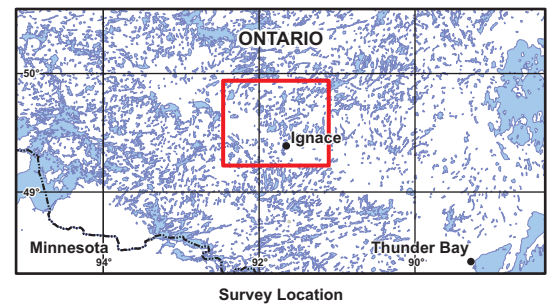
-70.1

-73.3

-76.8

-81.0

-90.0



BASE DATA: National Topographic Database - NRCAN

GEOLOGY DATA: OGS Dataset MRD 126-Rev 1

DATUM: NAD83

PROJECTION: Universal Transverse Mercator (UTM Zone 15N)

Scale 1 : 310 000

km 5 0 5 10 km

**Airborne Geophysics**

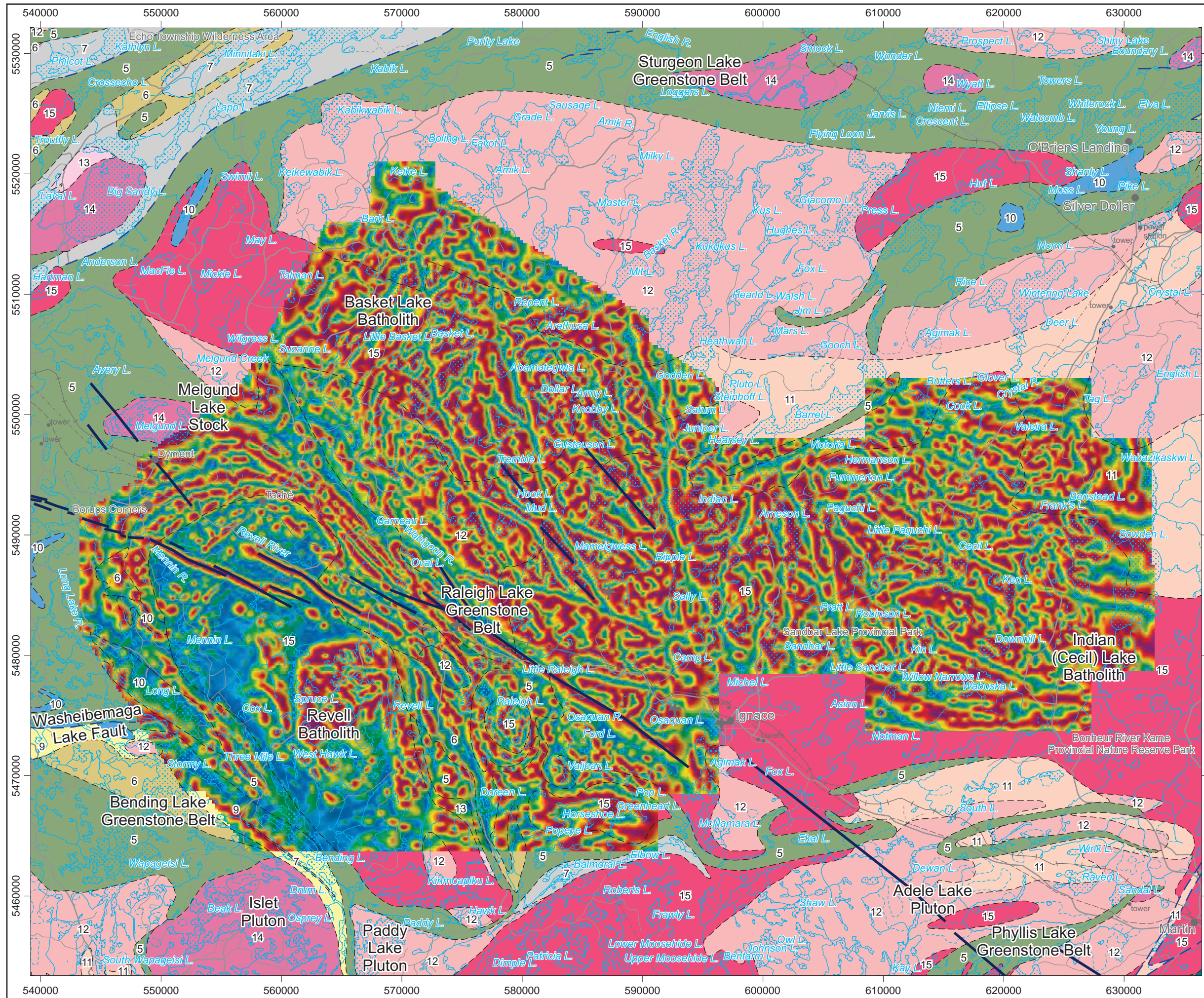
**Acquisition and Interpretation**

**Ignace Area, Ontario 2014**

**Tilt Angle of the Reduction to the Pole**

**of the Total Magnetic Intensity (25 m cell)**

	DESIGN	JK	29/01/2015	REV. 1.1
	GIS	YC, AP	06/02/2015	<b>FIGURE: 4.25</b>
	DATA	MM, DK	06/02/2015	
	QC	MB	06/02/2015	



**Legend**

Hydrography .....

Road .....

Railway .....

**Geology**

Fault .....

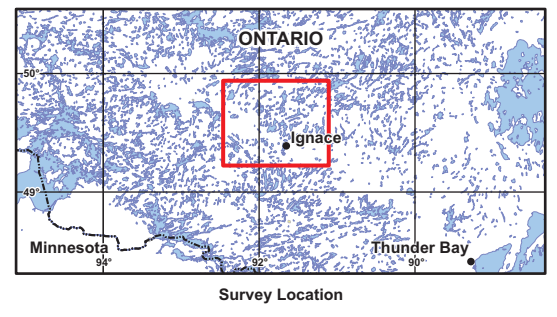
Dyke .....

75.1  
70.1  
65.8  
61.9  
58.2  
54.6  
51.0  
47.5  
44.0  
40.4  
36.9  
33.4  
29.9  
26.4  
22.8  
19.3  
15.7  
12.2  
8.6  
5.0  
1.5  
-2.0  
-5.5  
-8.9  
-12.3  
-15.7  
-19.0  
-22.3  
-25.5  
-28.7  
-31.8  
-34.9  
-37.9  
-40.8  
-43.8  
-46.6  
-49.5  
-52.2  
-54.9  
-57.5  
-60.1  
-62.5  
-64.9  
-67.3  
-69.6  
-71.9  
-74.2  
-76.8  
-80.1

degrees

**Map Parameters**

Illumination: inclination 50°, declination 270°



BASE DATA: National Topographic Database - NRCAN  
 GEOLOGY DATA: OGS Dataset MRD 126-Rev 1  
 DATUM: NAD83  
 PROJECTION: Universal Transverse Mercator (UTM Zone 15N)

Scale 1 : 310 000

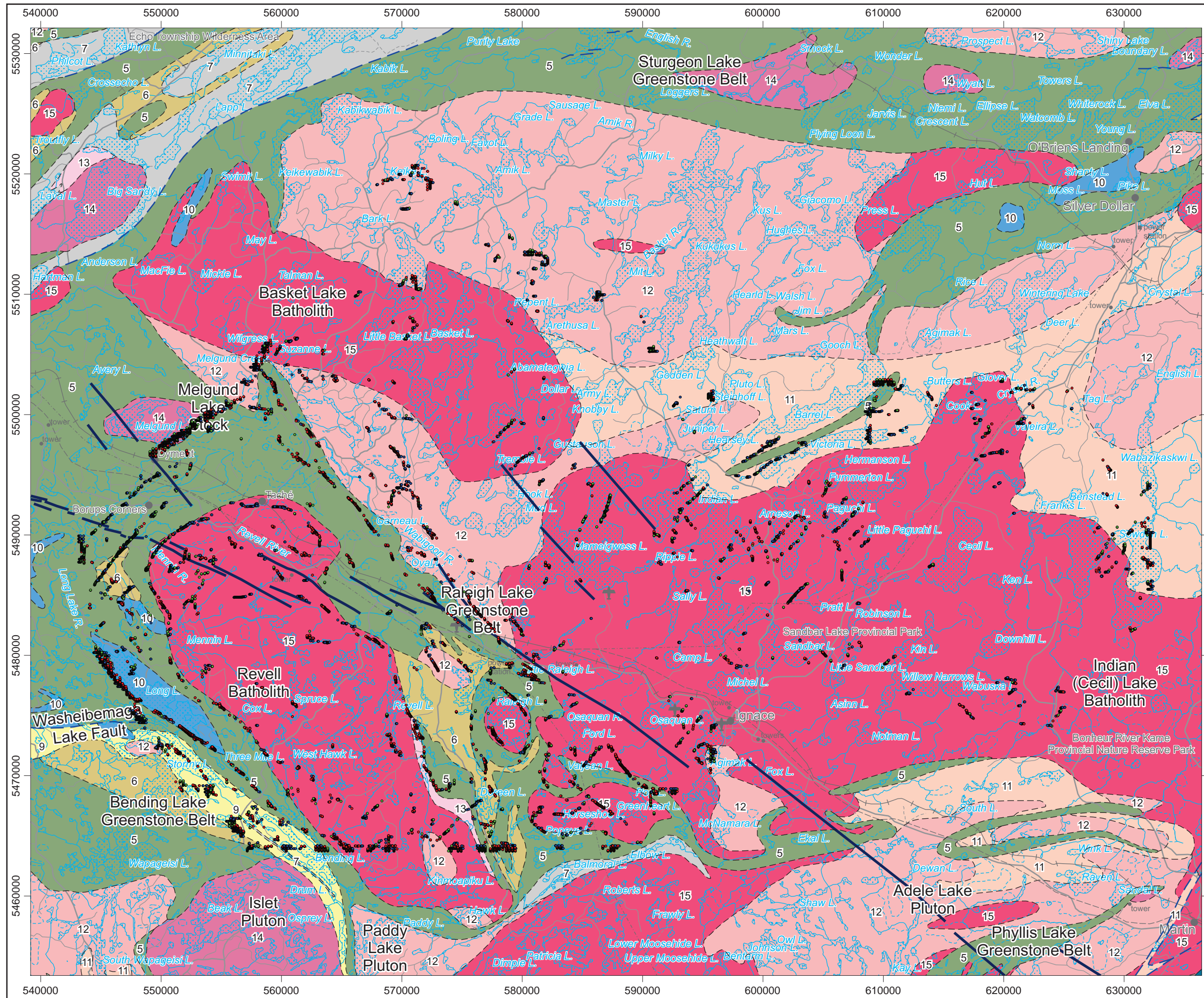
km 5 0 5 10 km

**Airborne Geophysics  
 Acquisition and Interpretation**

Ignace Area, Ontario 2014

**Tilt Angle of the Reduction to the Pole  
 of the Total Magnetic Intensity (250 m cell)**

	DESIGN	JK	29/01/2015	REV. 1.1
	GIS	YC, AP	06/02/2015	<b>FIGURE: 4.26</b>
	DATA	MM, DK	06/02/2015	
	QC	MB	06/02/2015	



**Legend**

Hydrography .....

Road .....

Railway .....

**Geology**

Fault .....

Dyke .....

- 3: Mafic metavolcanic and metasedimentary rocks
- 5: Mafic to intermediate metavolcanic rocks
- 6: Felsic to intermediate metavolcanic rocks
- 7: Metasedimentary rocks
- 9: Coarse clastic metasedimentary rocks
- 10: Mafic and ultramafic rocks
- 11: Gneissic tonalite suite
- 12: Foliated tonalite suite
- 13: Muscovite-bearing granite rock
- 14: Diorite-monzodiorite-granodiorite suite
- 15: Massive granodiorite suite
- 16: Hornblende - nepheline syenite suite

**Interpreted and Mapped Features**

- Surface Geology Mapping - Stone 2011
- OGS Dataset MRD 126-Rev 1 Surface Geology Mapping

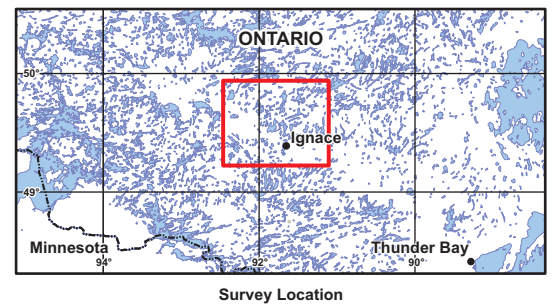
**Trend analysis solutions**

- 0 - 50 m
- 51 - 100 m
- > 100 m trend analysis solution symbol"/> > 100 m

**Map Parameters**

Spatial Filter (half-wavelength): 1000 m

Bouguer Density: 2.67 g/cm<sup>3</sup>



BASE DATA: National Topographic Database - NRCAN  
 GEOLOGY DATA: OGS Dataset MRD 126-Rev 1  
 DATUM: NAD83  
 PROJECTION: Universal Transverse Mercator (UTM Zone 15N)

N  
E  
S  
W

Scale 1 : 310 000

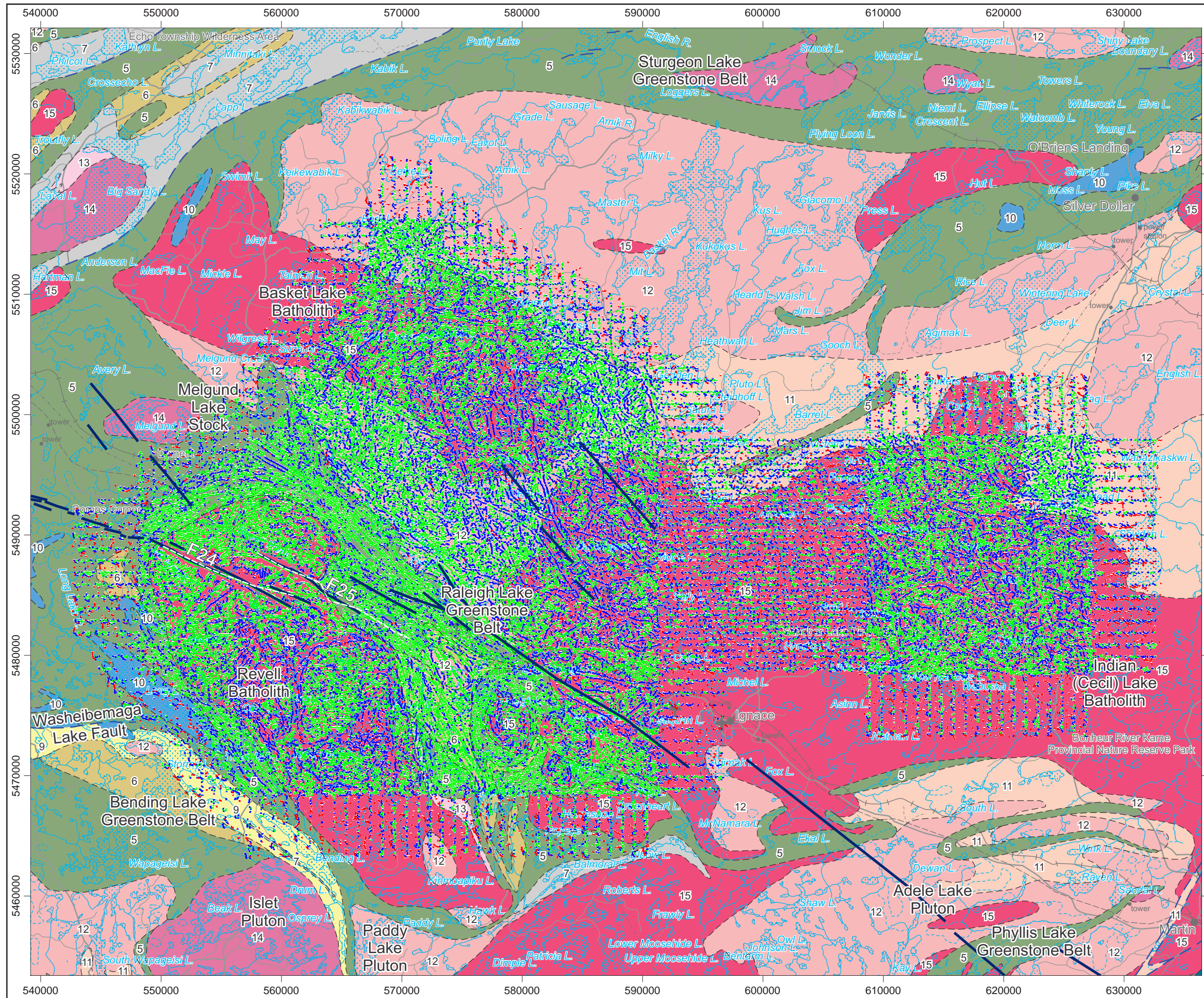
km 5 0 5 10 km

**Airborne Geophysics  
Acquisition and Interpretation**

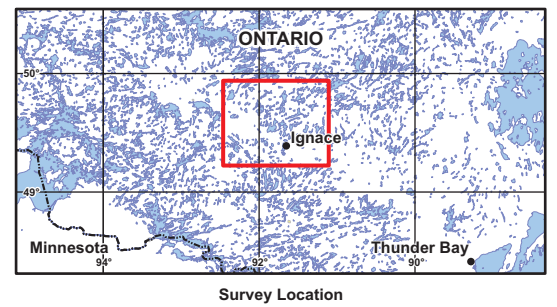
**Ignace Area, Ontario 2014**

**Trend Analysis Solutions of Bouguer Gravity  
(terrain correction density = 2.67 g/cc)**

	DESIGN	JK	29/01/2015	REV. 1.1
	GIS	YC, AP	06/02/2015	<b>FIGURE: 4.27</b>
	DATA	MM, DK	06/02/2015	
	QC	MB	06/02/2015	



- Legend**
- Hydrography
  - Road
  - Railway
- Geology**
- Fault
  - Dyke
- Interpreted and Mapped Features**
- Surface Geology Mapping - Stone 2011
  - OGS Dataset MRD 126-Rev 1 Surface Geology Mapping
  - Trend analysis solutions
    - 0 - 100 m
    - 101 - 200 m
    - > 200 m
- Geology Legend (Detailed)**
- 3: Mafic metavolcanic and metasedimentary rocks
  - 5: Mafic to intermediate metavolcanic rocks
  - 6: Felsic to intermediate metavolcanic rocks
  - 7: Metasedimentary rocks
  - 9: Coarse clastic metasedimentary rocks
  - 10: Mafic and ultramafic rocks
  - 11: Gneissic tonalite suite
  - 12: Foliated tonalite suite
  - 13: Muscovite-bearing granite rock
  - 14: Diorite-monzodiorite-granodiorite suite
  - 15: Massive granodiorite suite
  - 16: Hornblende - nepheline syenite suite



BASE DATA: National Topographic Database - NRCAN  
 GEOLOGY DATA: OGS Dataset MRD 126-Rev 1  
 DATUM: NAD83  
 PROJECTION: Universal Transverse Mercator (UTM Zone 15N)

Scale 1 : 310 000

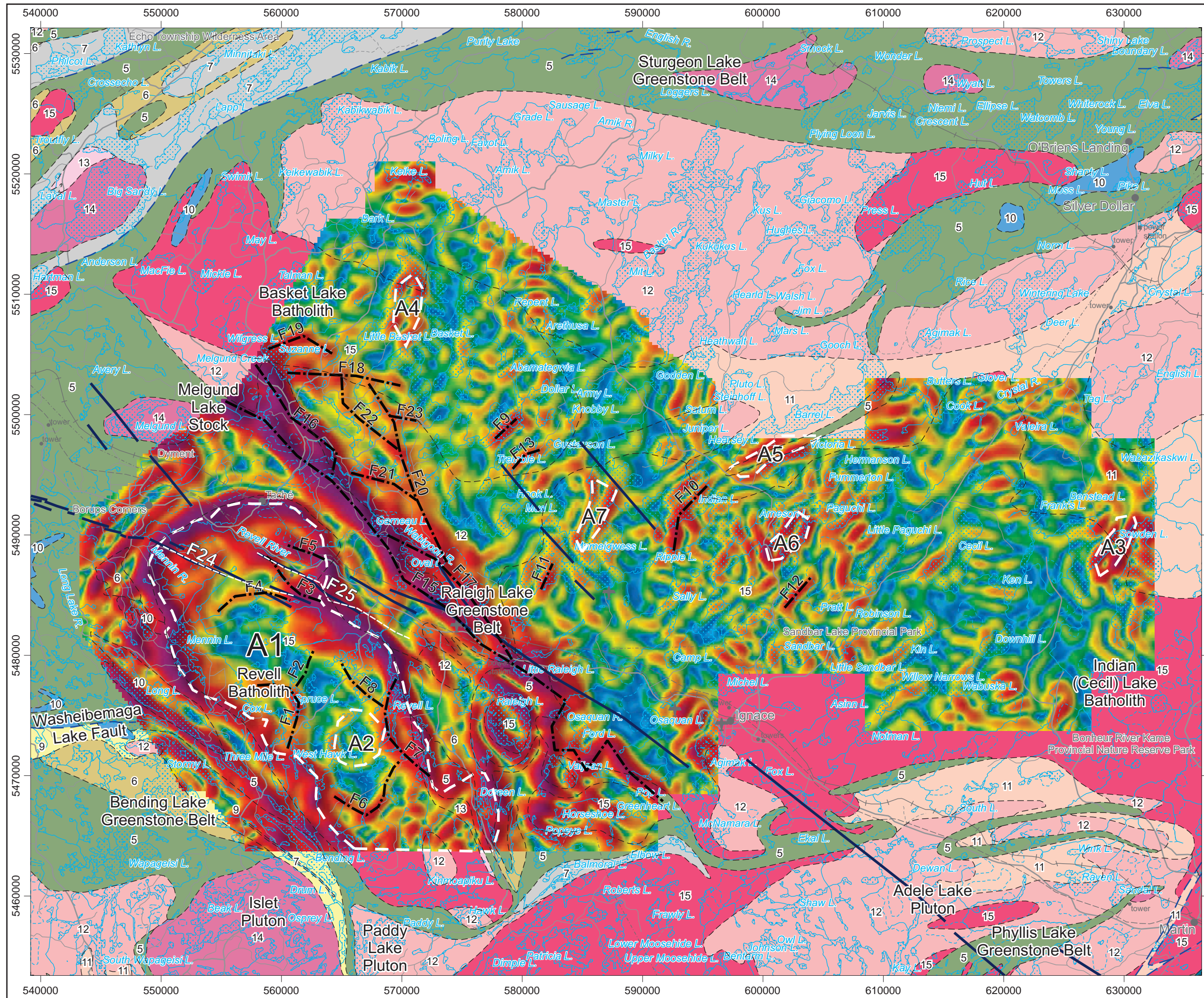
km 5 0 5 10 km

**Airborne Geophysics  
 Acquisition and Interpretation**

**Ignace Area, Ontario 2014**

**Trend Analysis Solutions of Reduction to the Pole  
 of the Total Magnetic Intensity**

	DESIGN	JK	29/01/2015	REV. 1.1
	GIS	YC, AP	06/02/2015	<b>FIGURE: 4.28</b>
	DATA	MM, DK	06/02/2015	
	QC	MB	06/02/2015	



**Legend**

Hydrography .....

Road .....

Railway .....

**Geology**

Fault .....

Dyke .....

3: Mafic metavolcanic and metasedimentary rocks

5: Mafic to intermediate metavolcanic rocks

6: Felsic to intermediate metavolcanic rocks

7: Metasedimentary rocks

9: Coarse clastic metasedimentary rocks

10: Mafic and ultramafic rocks

11: Gneissic tonalite suite

12: Foliated tonalite suite

13: Muscovite-bearing granite rock

14: Diorite-monzodiorite-granodiorite suite

15: Massive granodiorite suite

16: Hornblende - nepheline syenite suite

**Interpreted and Mapped Features**

Surface Geology Mapping - Stone 2011

Feature interpreted from horizontal derivative of Bouguer gravity

Area defined from horizontal derivative of Bouguer gravity

OGS Dataset MRD 126-Rev 1 Surface Geology Mapping

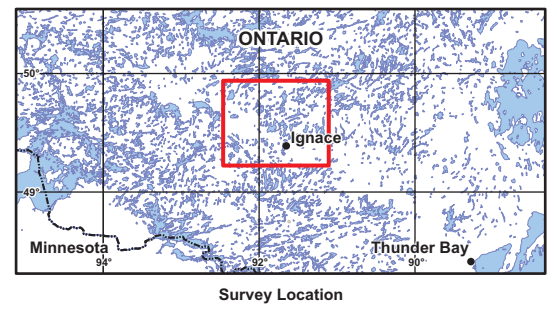
**Map Parameters**

Illumination: inclination 50°, declination 270°

Spatial Filter (half-wavelength): 1000 m

Bouguer Density: 2.67 g/cm<sup>3</sup>

mGal/km



BASE DATA: National Topographic Database - NRCAN  
 GEOLOGY DATA: OGS Dataset MRD 126-Rev 1  
 DATUM: NAD83  
 PROJECTION: Universal Transverse Mercator (UTM Zone 15N)

Scale 1 : 310 000

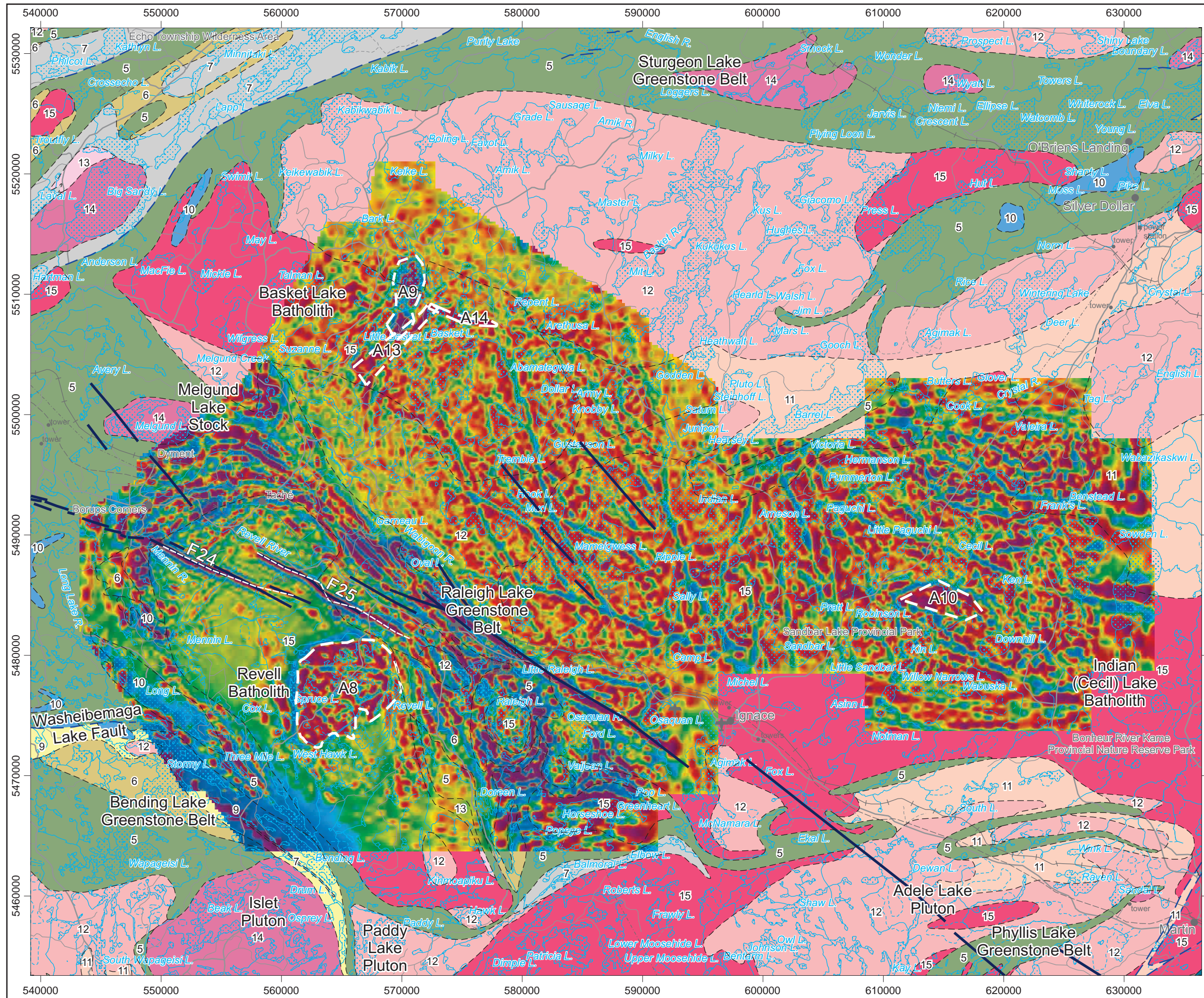
km 5 0 5 10 km

**Airborne Geophysics  
 Acquisition and Interpretation**

Ignace Area, Ontario 2014

**Horizontal Derivative of Bouguer Gravity  
 (terrain correction density = 2.67 g/cc) (250 m cell)  
 with Selected Interpreted Features**

	DESIGN	JK	29/01/2015	REV. 1.1
	GIS	YC, AP	06/02/2015	FIGURE: 5.1
	DATA	MM, DK	06/02/2015	
	QC	MB	06/02/2015	



**Legend**

Hydrography .....

Road .....

Railway .....

**Geology**

Fault .....

Dyke .....

**Interpreted and Mapped Features**

Surface Geology Mapping - Stone 2011

Feature interpreted from Horizontal Derivative of Reduction to the Pole of the Total Magnetic Intensity

Area defined from First Vertical Derivative of the Reduction to the Pole of the Total Magnetic Intensity

OGS Dataset MRD 126-Rev 1 Surface Geology Mapping

**Map Parameters**

Illumination: inclination 50°, declination 270°

nT/km

73681.8  
307.8  
200.0  
155.4  
128.1  
109.2  
94.7  
83.2  
73.4  
64.9  
57.2  
50.4  
44.2  
38.4  
33.0  
27.7  
22.9  
18.2  
13.8  
9.5  
5.4  
1.4  
-2.6  
-6.5  
-10.4  
-14.2  
-18.1  
-22.0  
-25.9  
-29.7  
-33.4  
-37.2  
-41.2  
-45.3  
-49.7  
-54.4  
-59.5  
-65.0  
-71.0  
-77.7  
-85.1  
-93.5  
-103.0  
-113.8  
-126.8  
-142.5  
-161.8  
-188.2  
-230.1  
-338.3  
\*\*\*\*\*

**Geology**

3: Mafic metavolcanic and metasedimentary rocks

5: Mafic to intermediate metavolcanic rocks

6: Felsic to intermediate metavolcanic rocks

7: Metasedimentary rocks

9: Coarse clastic metasedimentary rocks

10: Mafic and ultramafic rocks

11: Gneissic tonalite suite

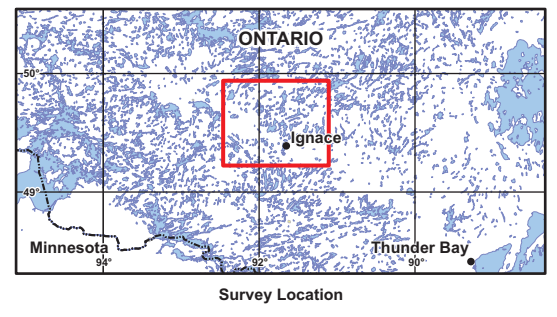
12: Foliated tonalite suite

13: Muscovite-bearing granite rock

14: Diorite-monzodiorite-granodiorite suite

15: Massive granodiorite suite

16: Hornblende - nepheline syenite suite



BASE DATA: National Topographic Database - NRCAN  
 GEOLOGY DATA: OGS Dataset MRD 126-Rev 1  
 DATUM: NAD83  
 PROJECTION: Universal Transverse Mercator (UTM Zone 15N)

Scale 1 : 310 000

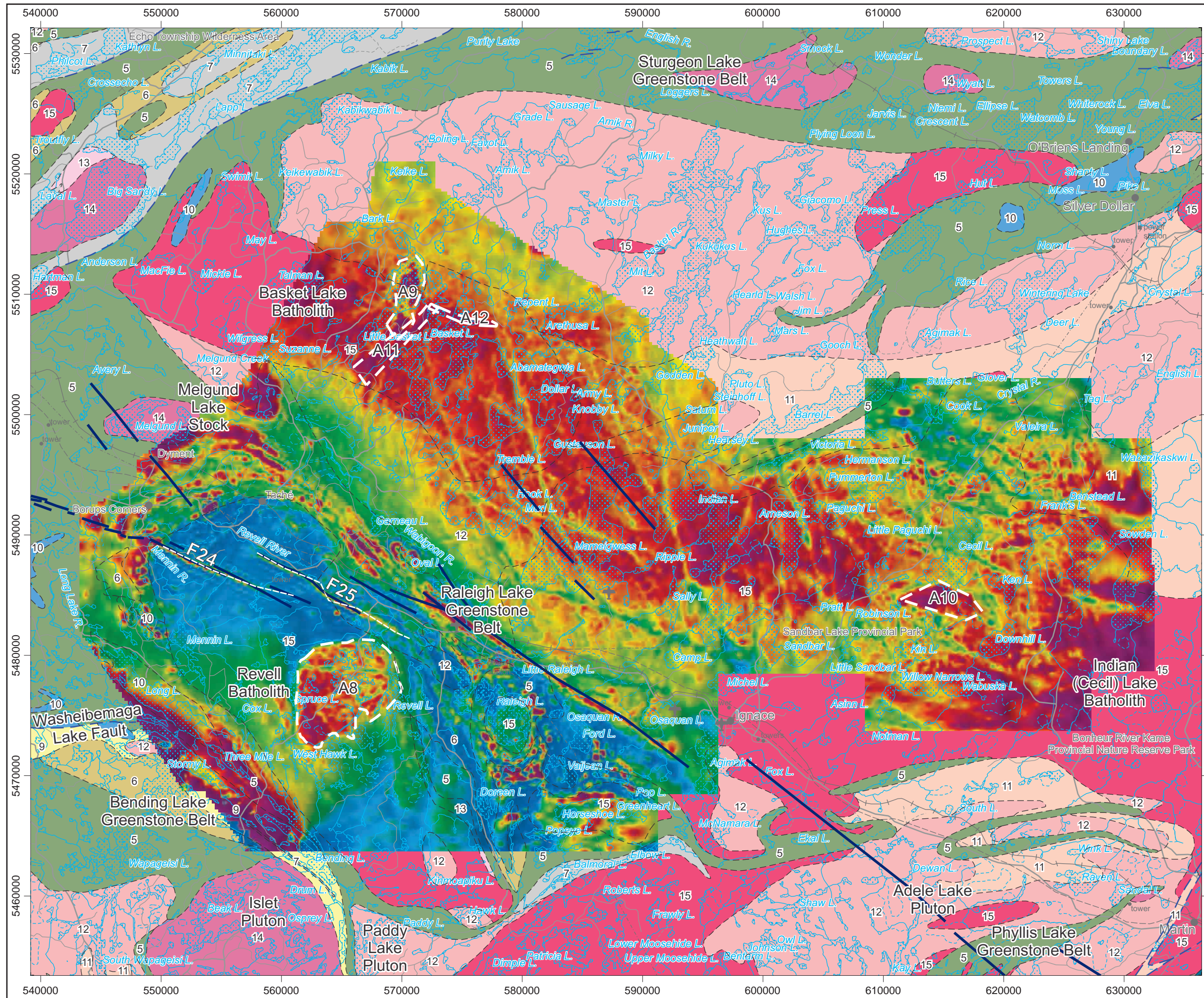
km 5 0 5 10 km

**Airborne Geophysics  
 Acquisition and Interpretation**

Ignace Area, Ontario 2014

First Vertical Derivative of the Reduction to the Pole  
 of the Total Magnetic Intensity (250 m cell)  
 with Selected Interpreted Features

	DESIGN	JK	29/01/2015	REV. 1.1
	GIS	YC, AP	06/02/2015	FIGURE: 5.2
	DATA	MM, DK	06/02/2015	
	QC	MB	06/02/2015	



**Legend**

Hydrography .....

Road .....

Railway .....

**Geology**

Fault .....

Dyke .....

**Interpreted and Mapped Features**

Surface Geology Mapping - Stone 2011

Feature interpreted from Horizontal Derivative of Reduction to the Pole of the Total Magnetic Intensity

Area defined from First Vertical Derivative of the Reduction to the Pole of the Total Magnetic Intensity

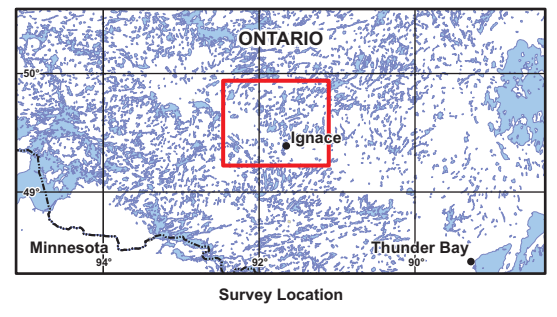
OGS Dataset MRD 126-Rev 1 Surface Geology Mapping

**Map Parameters**

Illumination: inclination 50°, declination 270°

**nT**

25487.0  
171.1  
116.8  
94.8  
82.1  
73.6  
67.1  
61.4  
56.4  
51.7  
47.2  
42.7  
38.2  
33.6  
29.1  
24.8  
20.6  
16.5  
12.5  
8.6  
5.0  
1.4  
-2.2  
-5.7  
-9.2  
-12.8  
-16.2  
-19.8  
-23.5  
-27.5  
-31.8  
-36.5  
-41.4  
-46.7  
-52.5  
-58.3  
-64.2  
-70.5  
-76.9  
-83.9  
-91.1  
-98.8  
-107.5  
-116.8  
-125.8  
-133.9  
-142.0  
-151.6  
-163.4  
-180.3  
-2148.7



BASE DATA: National Topographic Database - NRCAN  
 GEOLOGY DATA: OGS Dataset MRD 126-Rev 1  
 DATUM: NAD83  
 PROJECTION: Universal Transverse Mercator (UTM Zone 15N)

Scale 1 : 310 000

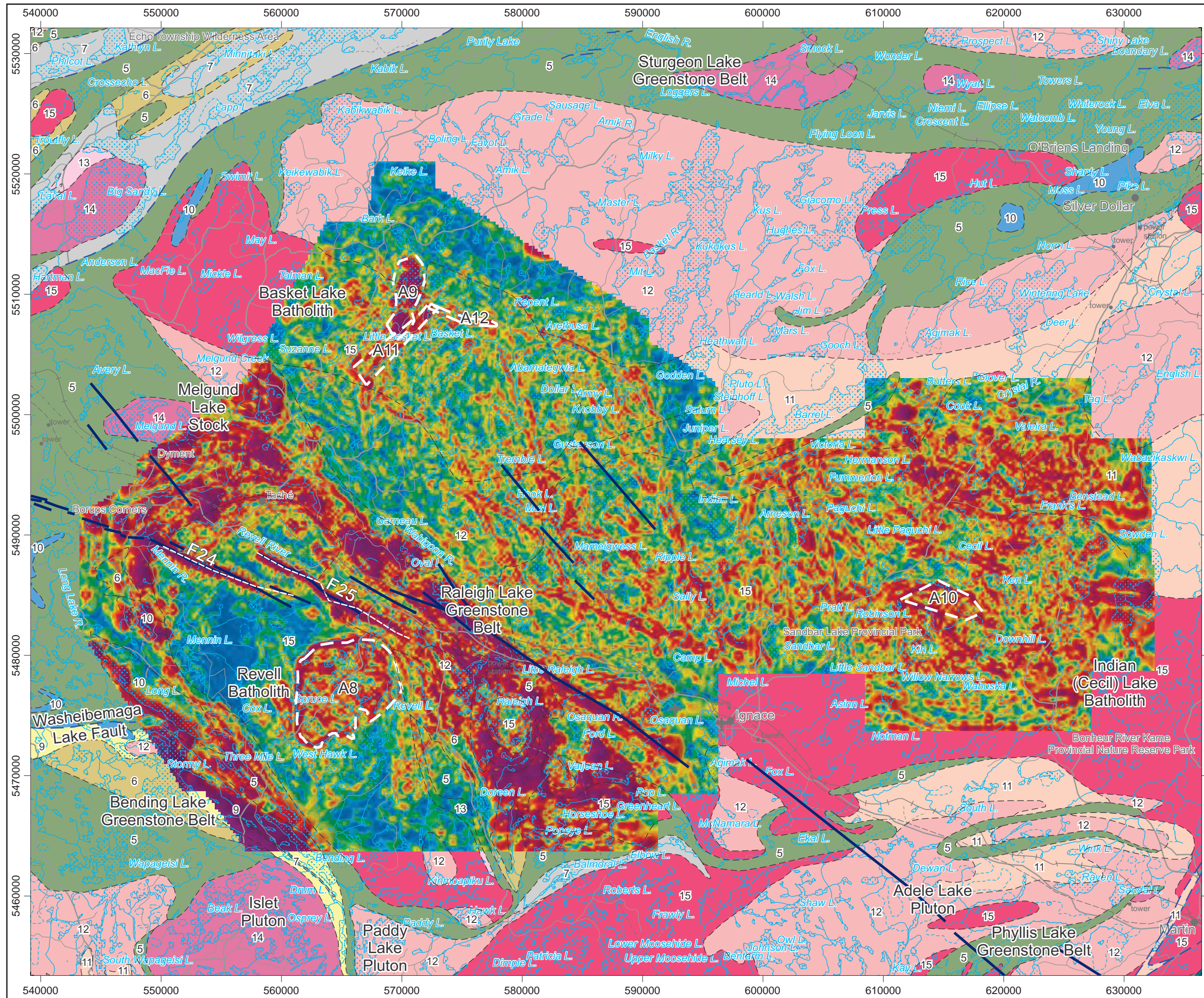
km 5 0 5 10 km

**Airborne Geophysics  
 Acquisition and Interpretation**

**Ignace Area, Ontario 2014**

**Reduction to the Pole  
 of the Total Magnetic Intensity (250 m cell)  
 with Selected Interpreted Features**

	DESIGN	JK	29/01/2015	REV. 1.1
	GIS	YC, AP	06/02/2015	<b>FIGURE: 5.3</b>
	DATA	MM, DK	06/02/2015	
	QC	MB	06/02/2015	



**Legend**

Hydrography .....

Road .....

Railway .....

**Geology**

Fault .....

Dyke .....

**3: Mafic metavolcanic and metasedimentary rocks**

**5: Mafic to intermediate metavolcanic rocks**

**6: Felsic to intermediate metavolcanic rocks**

**7: Metasedimentary rocks**

**9: Coarse clastic metasedimentary rocks**

**10: Mafic and ultramafic rocks**

**11: Gneissic tonalite suite**

**12: Foliated tonalite suite**

**13: Muscovite-bearing granite rock**

**14: Diorite-monzodiorite-granodiorite suite**

**15: Massive granodiorite suite**

**16: Hornblende - nepheline syenite suite**

**Interpreted and Mapped Features**

Surface Geology Mapping - Stone 2011

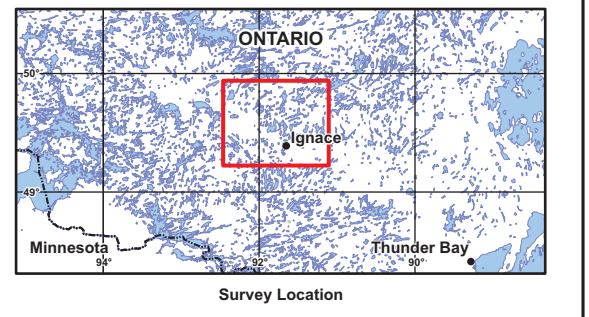
Feature interpreted from Horizontal Derivative of Reduction to the Pole of the Total Magnetic Intensity

Area defined from First Vertical Derivative of the Reduction to the Pole of the Total Magnetic Intensity

OGS Dataset MRD 126-Rev 1 Surface Geology Mapping

**Map Parameters**

Illumination: inclination 50°, declination 270°



BASE DATA: National Topographic Database - NRCAN  
 GEOLOGY DATA: OGS Dataset MRD 126-Rev 1  
 DATUM: NAD83  
 PROJECTION: Universal Transverse Mercator (UTM Zone 15N)

Scale 1 : 310 000

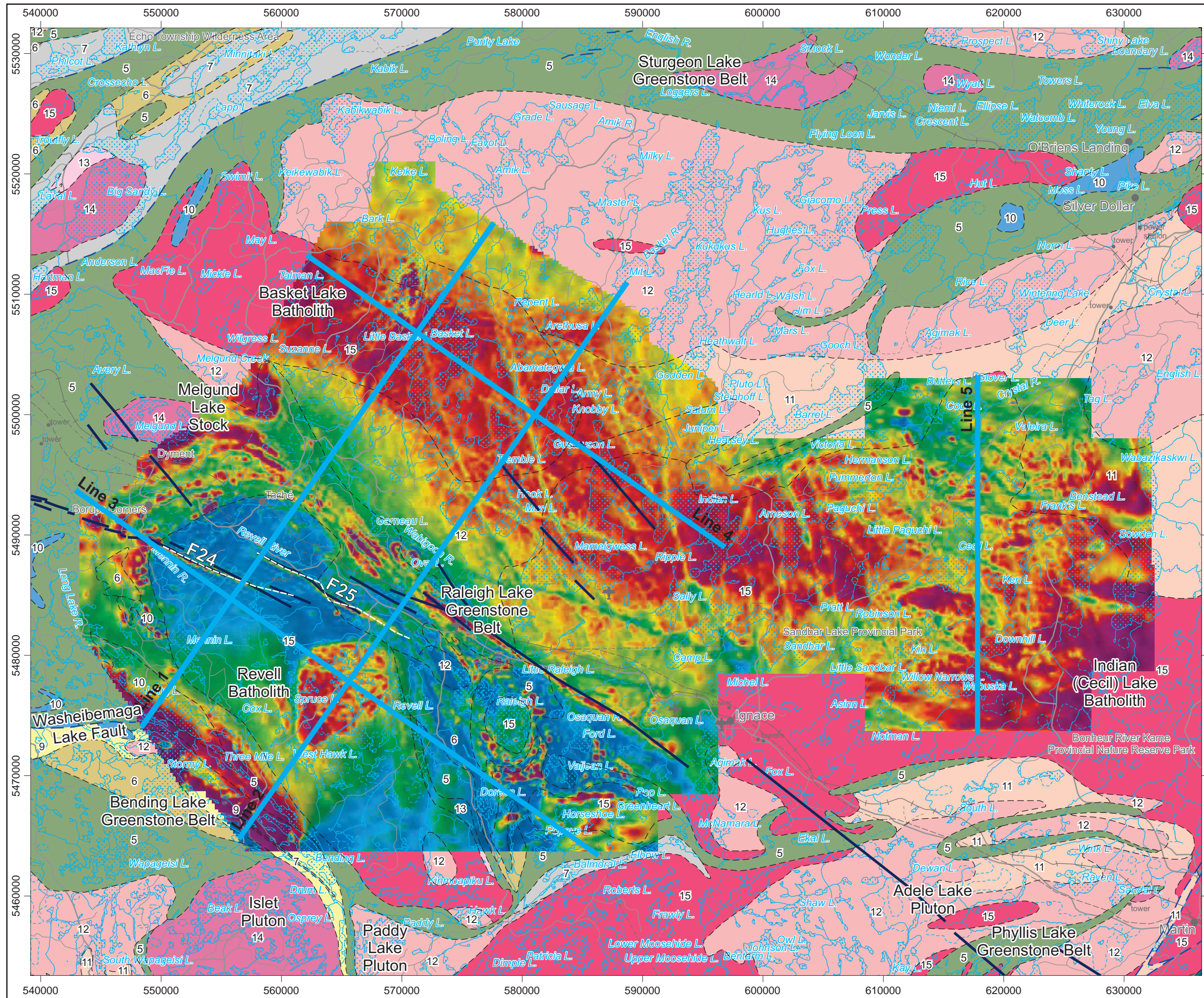
km 5 0 5 10 km

**Airborne Geophysics  
 Acquisition and Interpretation**

**Ignace Area, Ontario 2014**

**Total Horizontal Derivative of the Reduction to the Pole  
 of the Total Magnetic Intensity (250 m cell)  
 with Selected Interpreted Features**

	DESIGN	JK	29/01/2015	REV. 1.1
	GIS	YC, AP	06/02/2015	<b>FIGURE: 5.4</b>
	DATA	MM, DK	06/02/2015	
	QC	MB	06/02/2015	



**Legend**

Hydrography .....

Road .....

Railway .....

**Geology**

Fault .....

Dyke .....

**Interpreted and Mapped Features**

Surface Geology Mapping - Stone 2011

OGS Dataset MRD 126-Rev 1 Surface Geology Mapping

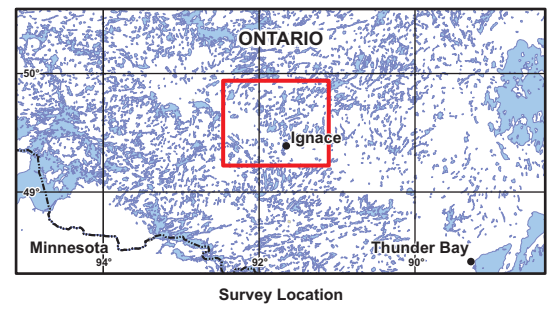
2.5D model line

**Map Parameters**

Illumination: inclination 50°, declination 270°

**Magnetic Intensity Scale (nT)**

25487.0  
171.1  
116.8  
94.8  
82.1  
73.6  
67.1  
61.4  
56.4  
51.7  
47.2  
42.7  
38.2  
33.6  
29.1  
24.8  
20.6  
16.5  
12.5  
8.6  
5.0  
1.4  
-2.2  
-5.7  
-9.2  
-12.8  
-16.2  
-19.8  
-23.5  
-27.5  
-31.8  
-36.5  
-41.4  
-46.7  
-52.5  
-58.3  
-64.2  
-70.5  
-76.9  
-83.9  
-91.1  
-98.8  
-107.5  
-116.8  
-125.8  
-133.9  
-142.0  
-151.6  
-163.4  
-180.3  
-2148.7



BASE DATA: National Topographic Database - NRCAN  
 GEOLOGY DATA: OGS Dataset MRD 126-Rev 1  
 DATUM: NAD83  
 PROJECTION: Universal Transverse Mercator (UTM Zone 15N)

Scale 1 : 310 000

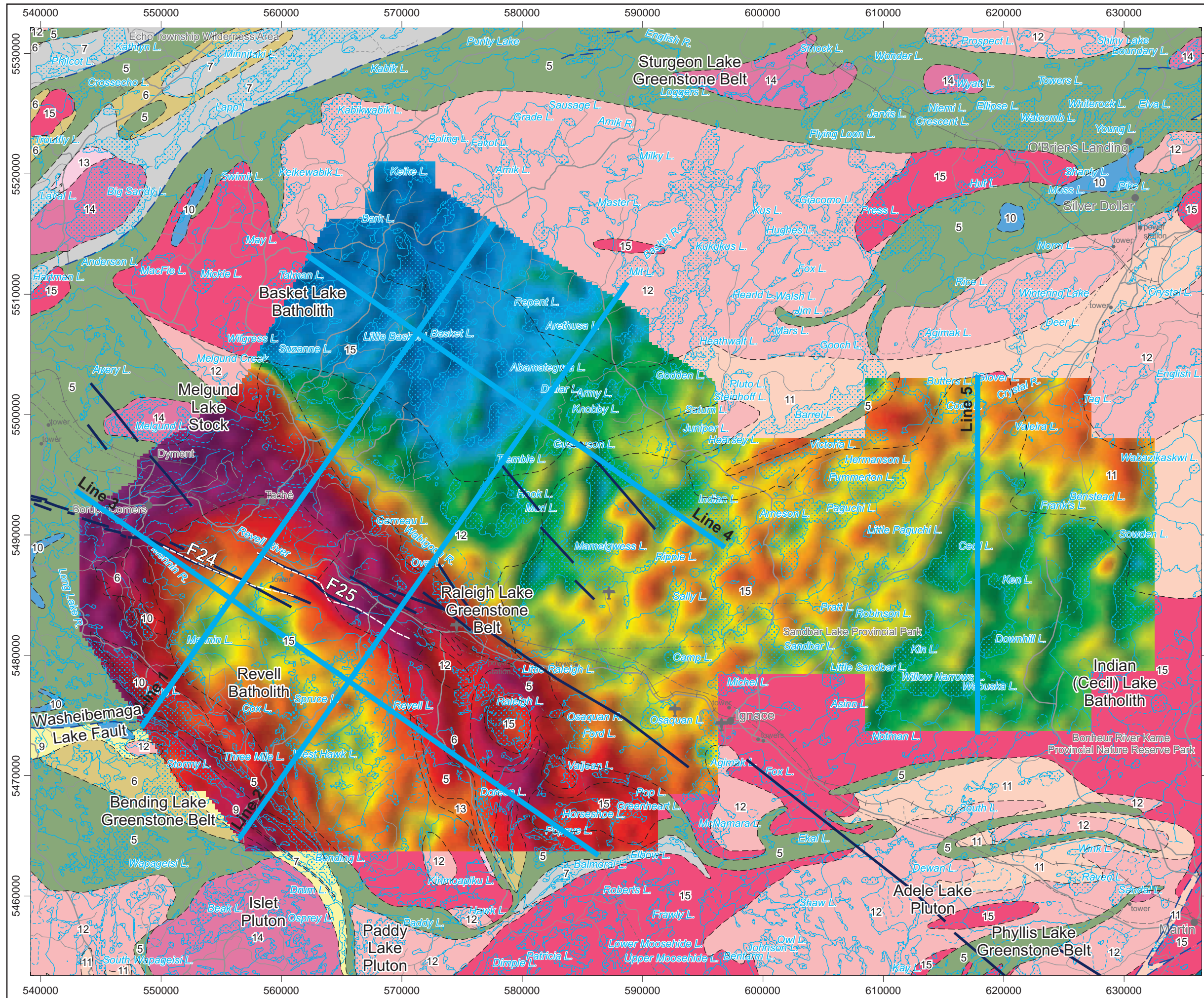
km 5 0 5 10 km

**Airborne Geophysics  
 Acquisition and Interpretation**

**Ignace Area, Ontario 2014**

**Location of 2.5D Model Lines shown with  
 Reduction to the Pole of the  
 Total Magnetic Intensity (250 m cell)**

	DESIGN	JK	29/01/2015	REV. 1.1
	GIS	YC, AP	06/02/2015	<b>FIGURE: 5.5</b>
	DATA	MM, DK	06/02/2015	
	QC	MB	06/02/2015	



**Legend**

Hydrography .....

Road .....

Railway .....

**Geology**

Fault .....

Dyke .....

**Interpreted and Mapped Features**

Surface Geology Mapping - Stone 2011

OGS Dataset MRD 126-Rev 1 Surface Geology Mapping

2.5D model line

**Map Parameters**

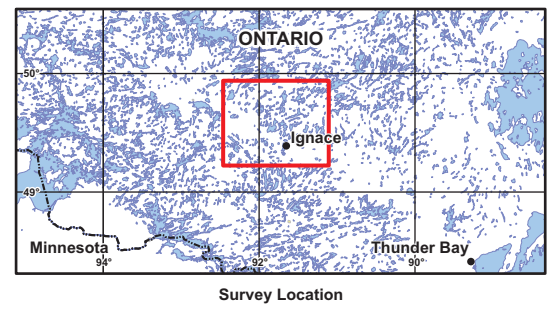
Illumination: inclination 50°, declination 270°

Spatial Filter (half-wavelength): 1000 m

**Color Scale (mGal)**

5.7  
-5.1  
-7.4  
-9.1  
-11.0  
-13.1  
-14.7  
-16.0  
-17.3  
-18.6  
-19.9  
-21.1  
-22.6  
-23.9  
-24.8  
-25.5  
-26.1  
-26.6  
-27.0  
-27.4  
-27.7  
-28.0  
-28.2  
-28.5  
-28.8  
-29.1  
-29.4  
-29.7  
-30.0  
-30.3  
-30.6  
-30.9  
-31.2  
-31.6  
-31.9  
-32.3  
-32.7  
-33.1  
-33.5  
-34.0  
-34.4  
-34.9  
-35.5  
-36.6  
-38.0  
-39.3  
-40.6  
-42.0  
-43.2  
-44.2  
-47.7

mGal



BASE DATA: National Topographic Database - NRCAN  
 GEOLOGY DATA: OGS Dataset MRD 126-Rev 1  
 DATUM: NAD83  
 PROJECTION: Universal Transverse Mercator (UTM Zone 15N)

Scale 1 : 310 000

km 5 0 5 10 km

**Airborne Geophysics  
 Acquisition and Interpretation**

**Ignace Area, Ontario 2014**

**Location of 2.5D Model Lines shown with  
 Free Air Gravity (250 m cell)**

	DESIGN	JK	29/01/2015	REV. 1.1
	GIS	YC, AP	06/02/2015	<b>FIGURE: 5.6</b>
	DATA	MM, DK	06/02/2015	
	QC	MB	06/02/2015	

Figure 5.7 - Forward Modeling Results: Line 1, Model 1.6, Ignace Ontario

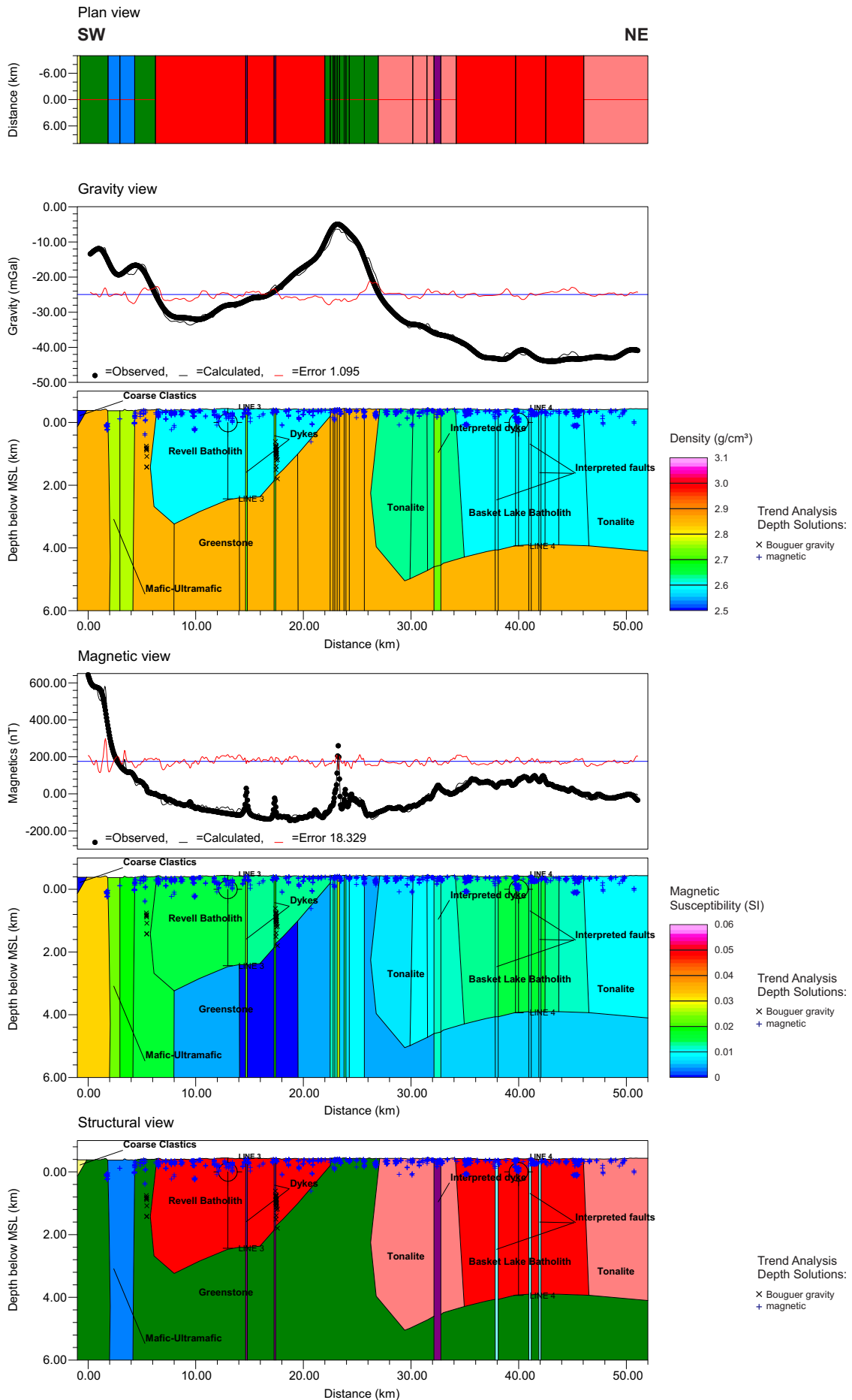


Figure 5.8 - Forward Modeling Results: Line 1, Model 1.5, Ignace Ontario

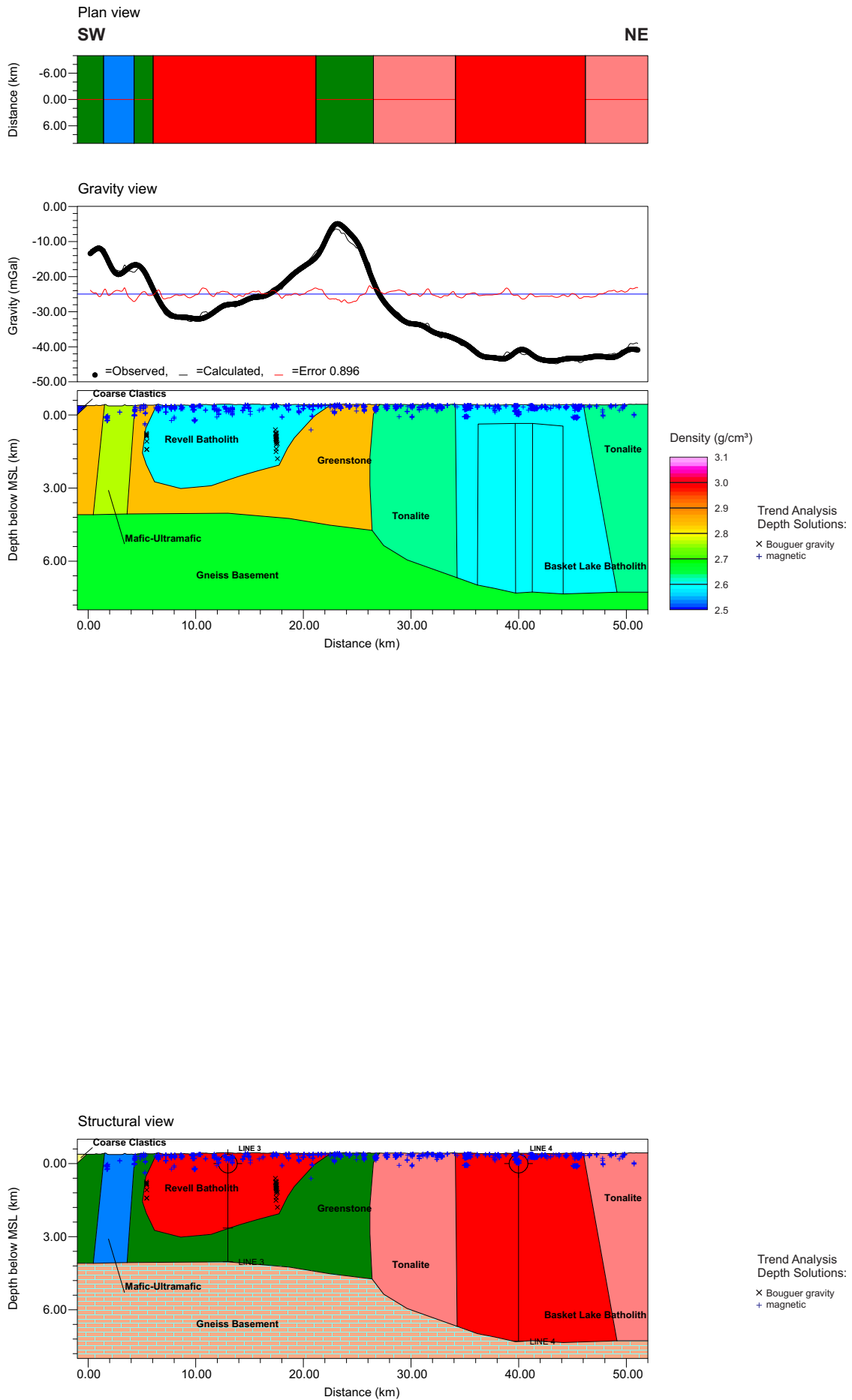


Figure 5.9 - Forward Modeling Results: Line 2, Model 2.3, Ignace Ontario

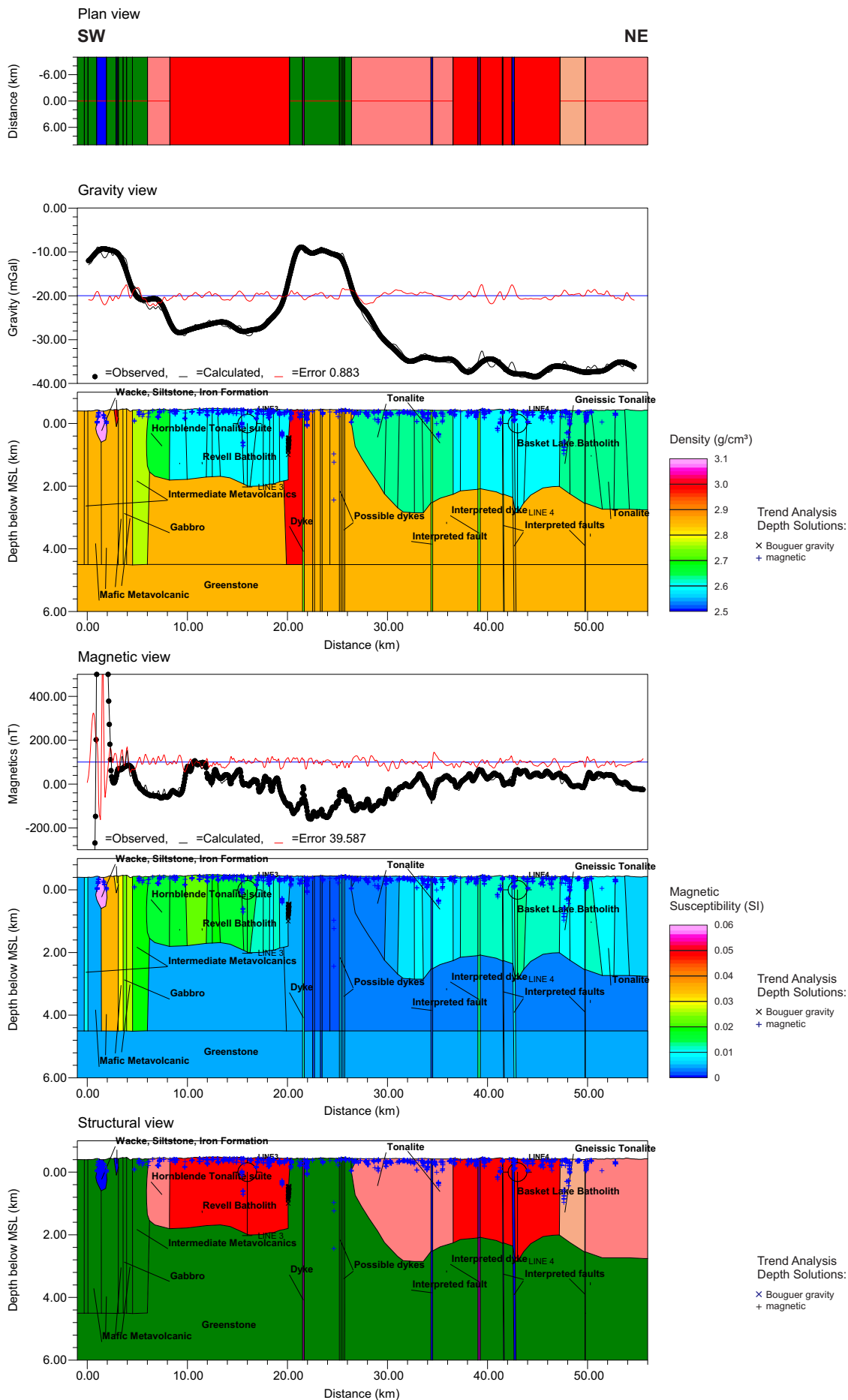


Figure 5.10 - Forward Modeling Results: Line 2, Model 2.5, Ignace Ontario

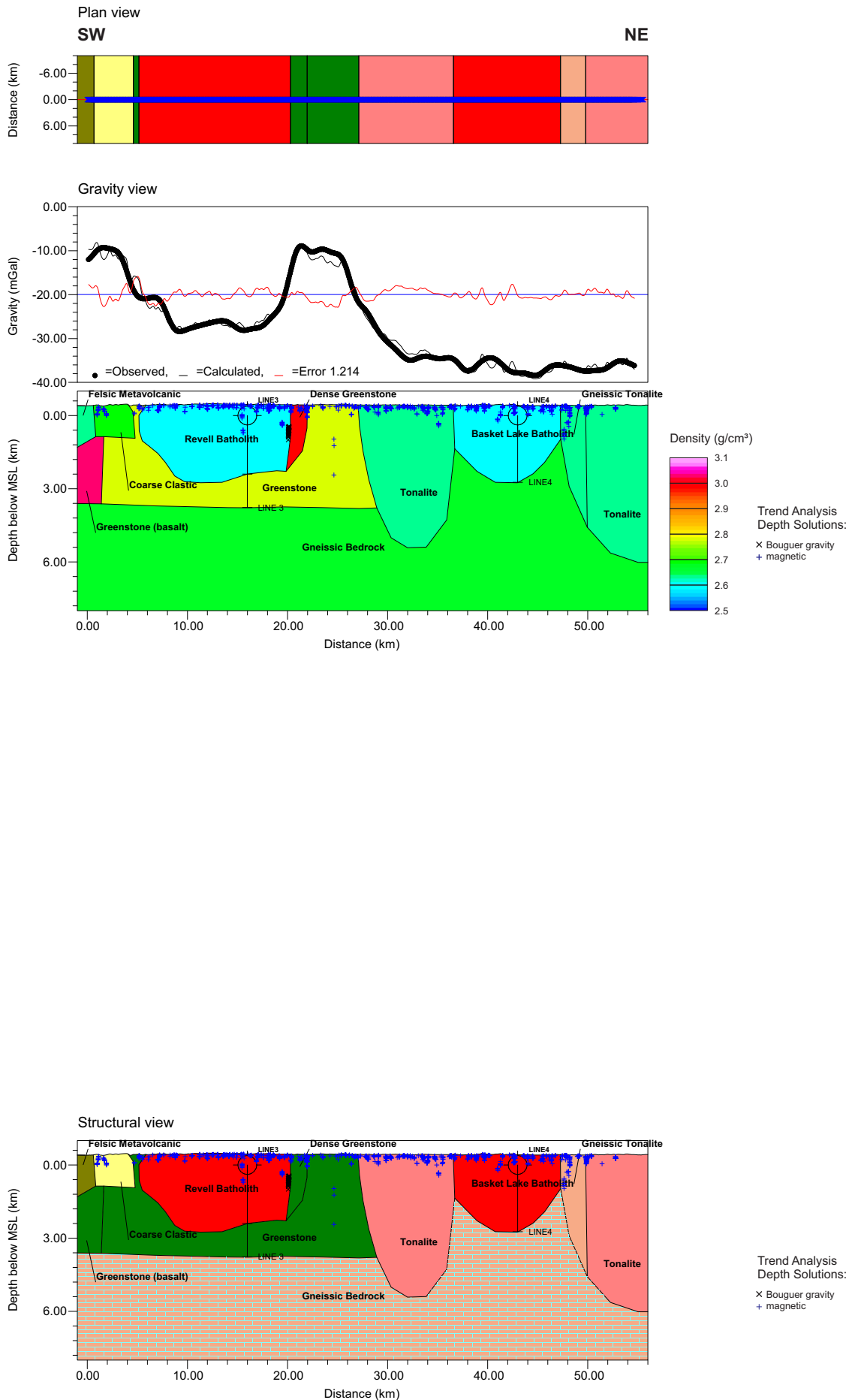


Figure 5.11 - Forward Modeling Results: Line 3, Model 3.3.4, Ignace Ontario

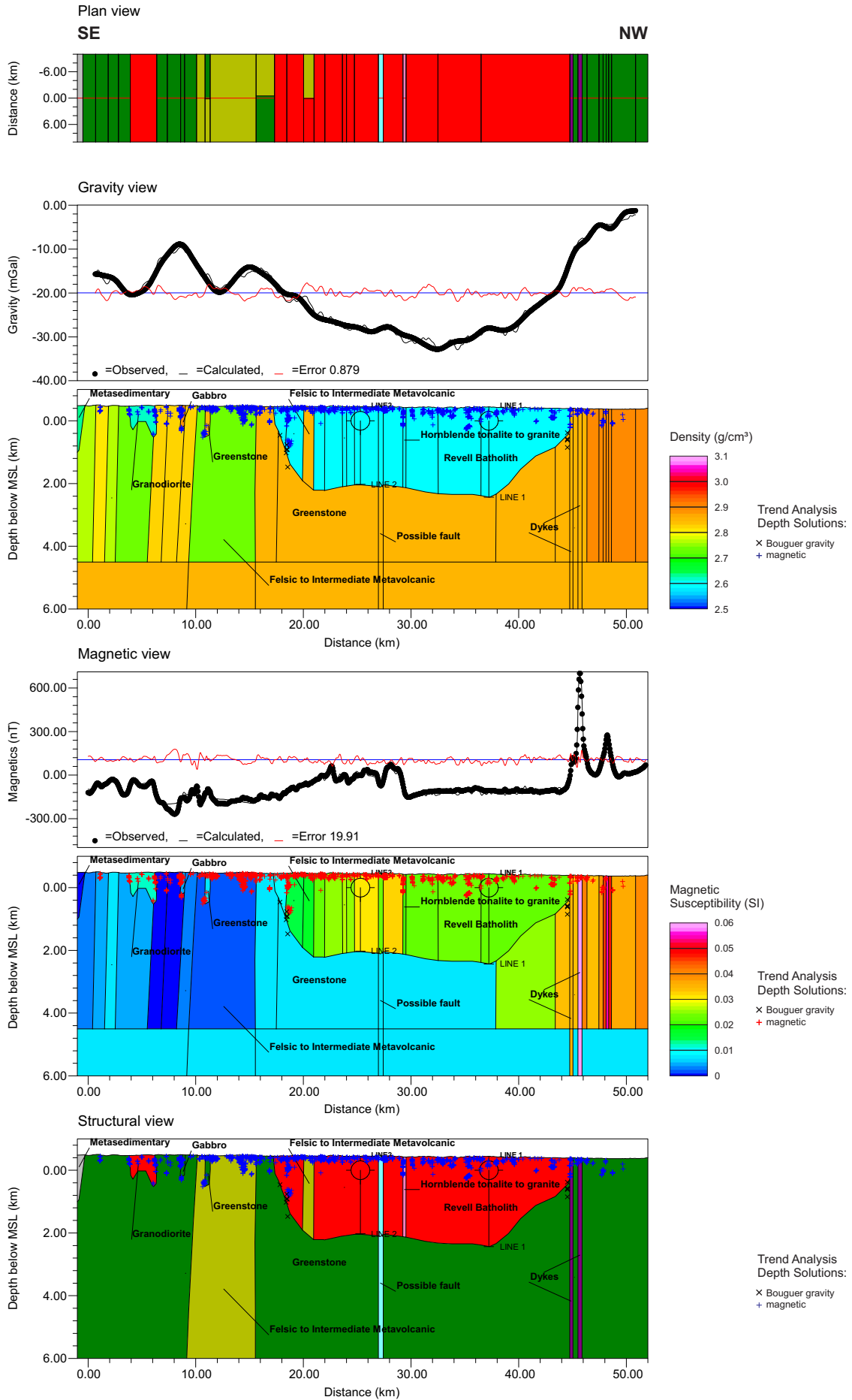


Figure 5.12 - Forward Modeling Results: Line 3, Model 3.5, Ignace Ontario

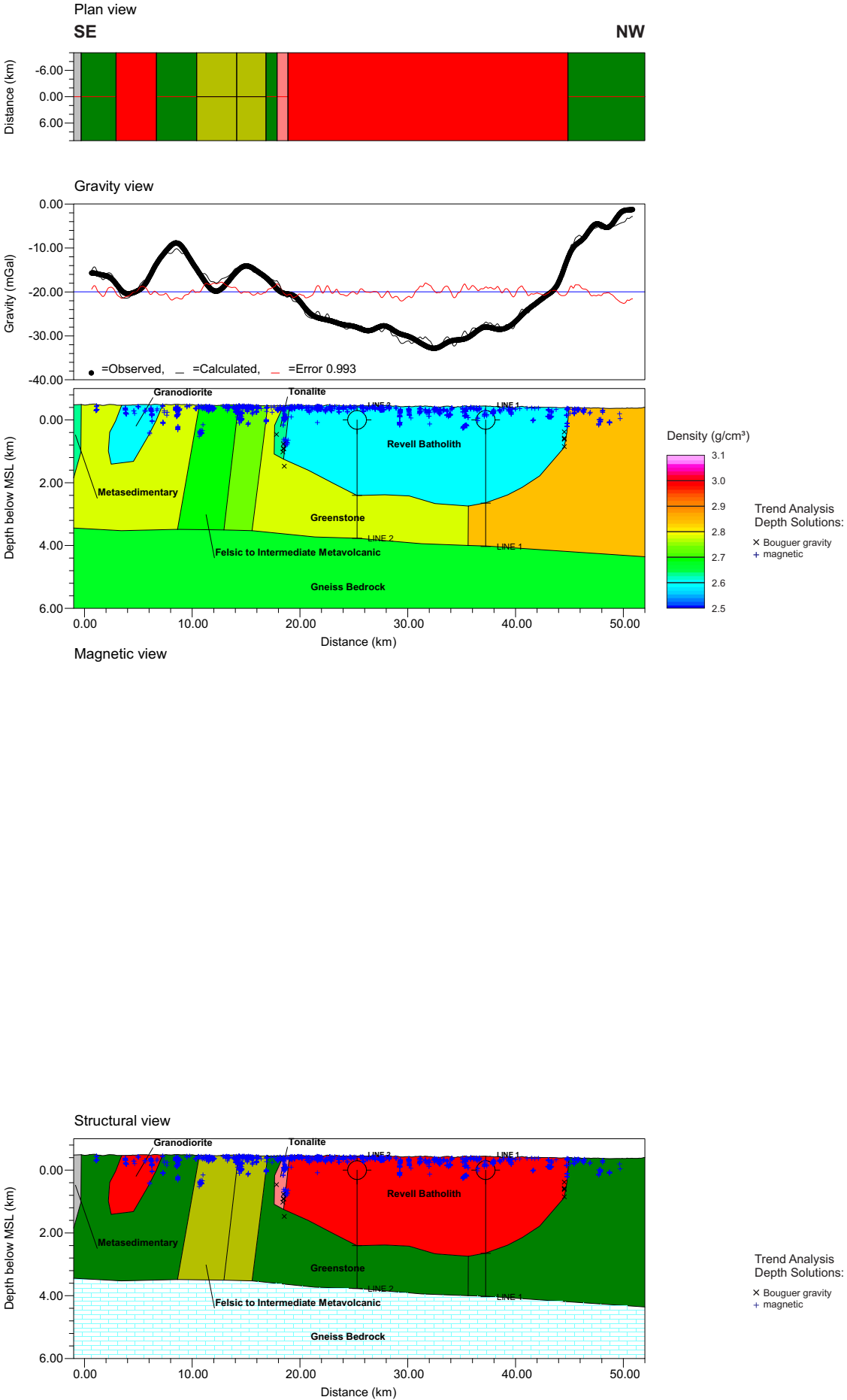


Figure 5.13 - Forward Modeling Results: Line 4, Model 4.3.3, Ignace Ontario

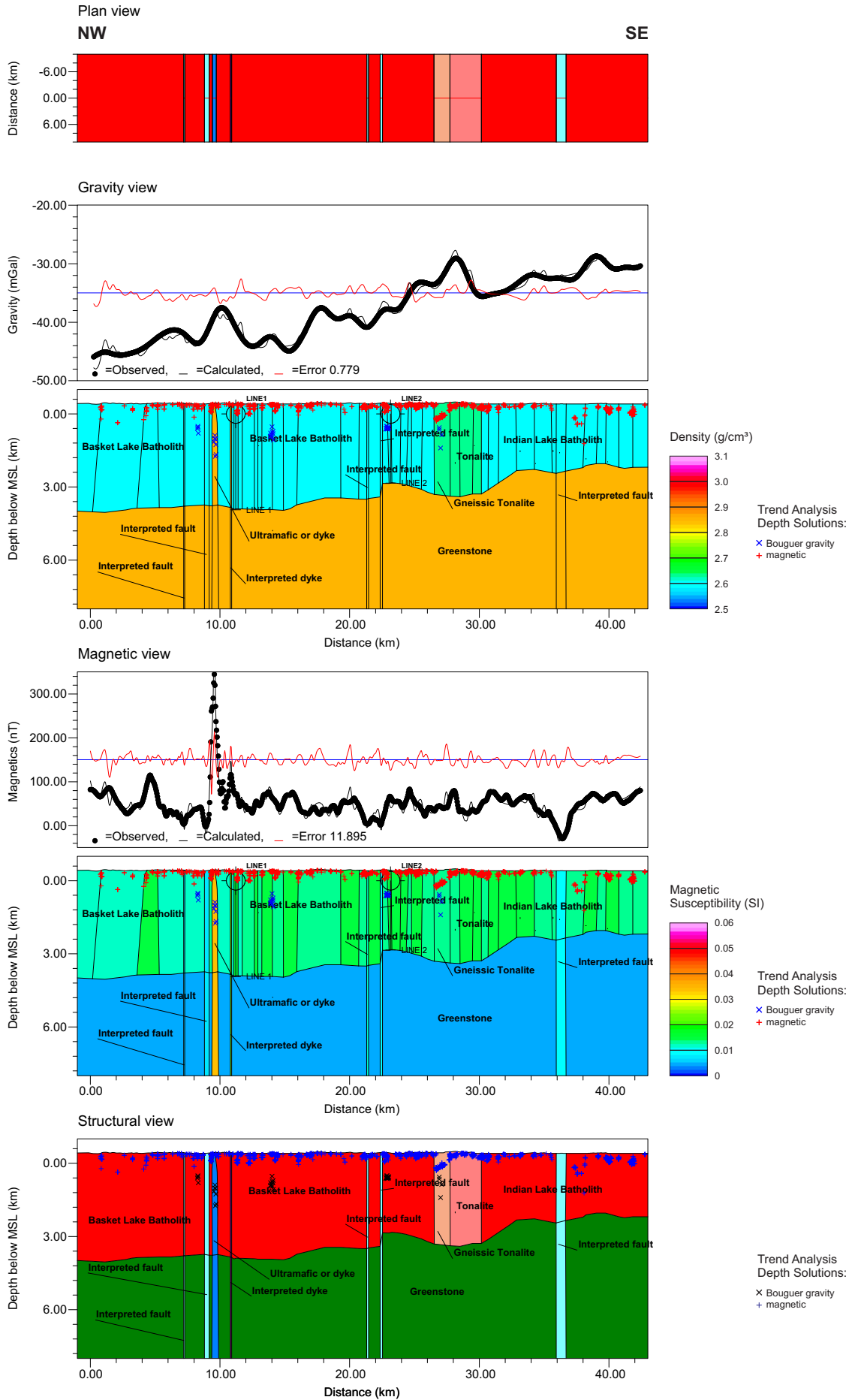


Figure 5.14 - Forward Modeling Results: Line 4, Model 4.5.2, Ignace Ontario

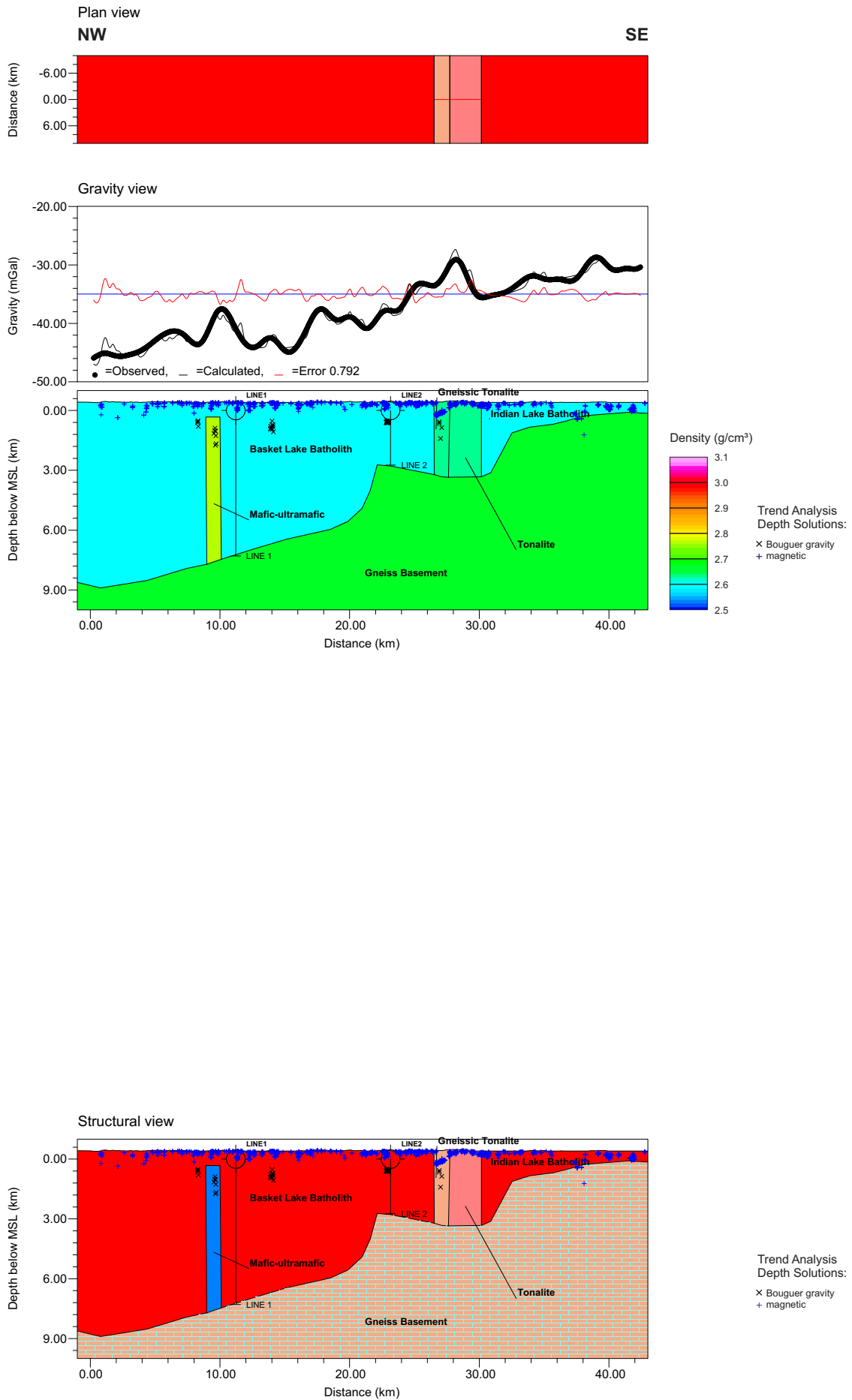


Figure 5.15 - Forward Modeling Results: Line 5, Model 5.2, Ignace Ontario

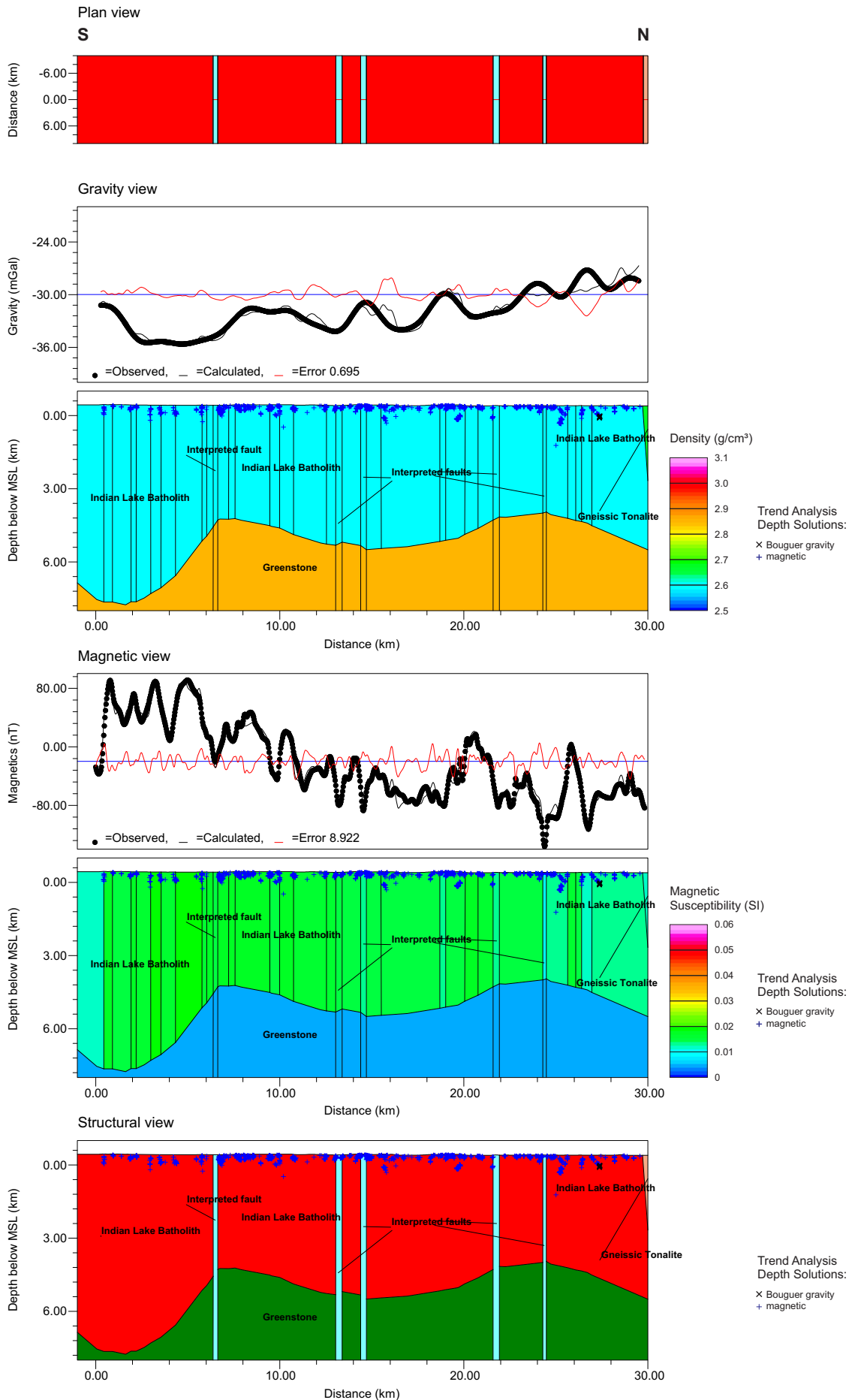


Figure 5.16 - Forward Modeling Results: Line 5, Model 5.3, Ignace Ontario

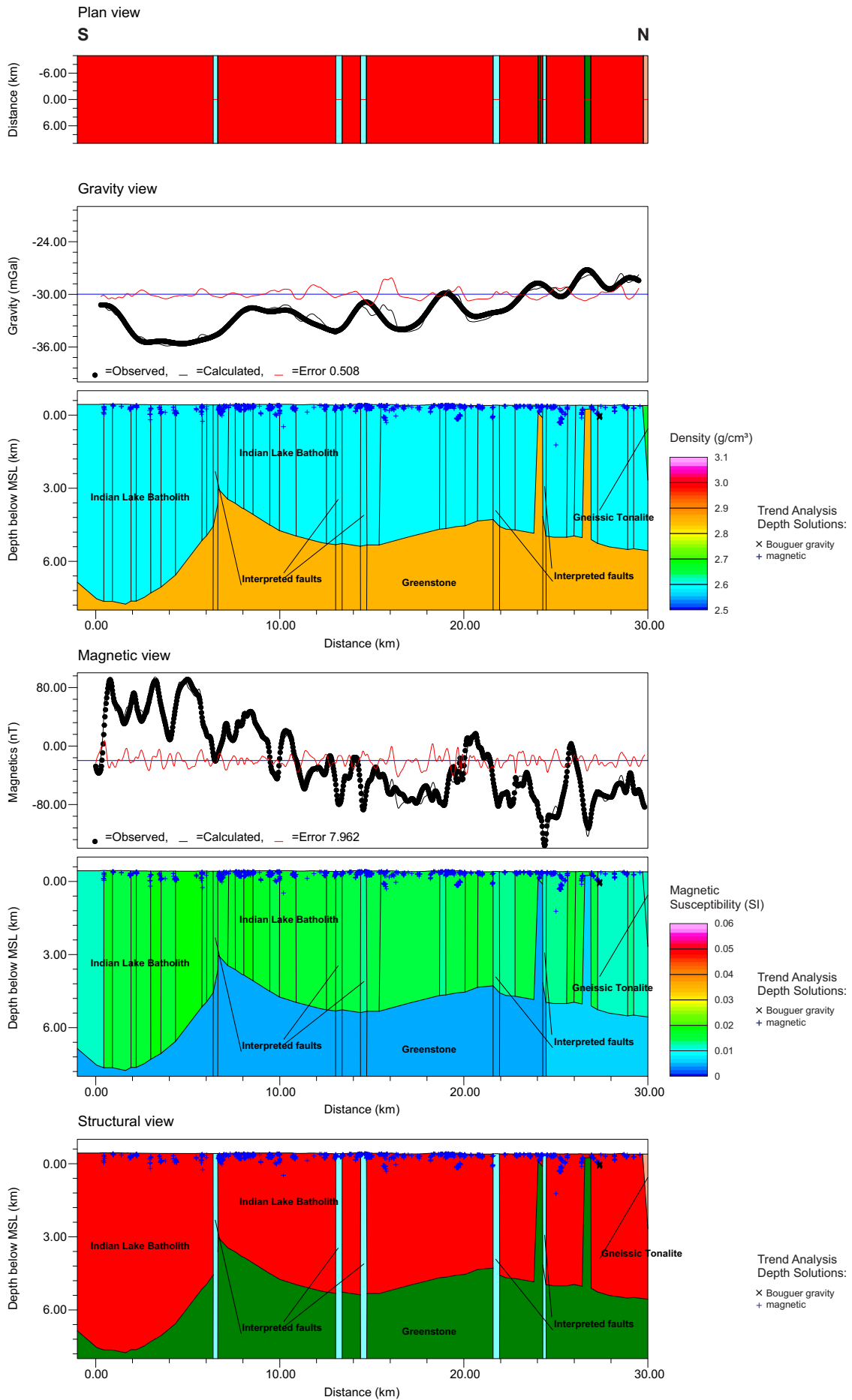


Figure 5.17 - Forward Modeling Results: Line 5, Model 5.5, Ignace Ontario

